Potential benefits and neural correlates of acupuncture treatment and physiotherapy on resting state functional connectivity in ischaemic stroke patients with unilateral limb dysfunction

by

Soné Fouché

DPSSON001

SUBMITTED TO THE UNIVERSITY OF CAPE TOWN

In fulfilment of the requirements for the degree

MSc Biomedical Engineering

Faculty of Health Sciences

UNIVERSITY OF CAPE TOWN

11 February 2024

Supervisor: Dr Jia Fan

Co-supervisors: Prof Ernesta Meintjes, Prof Chunhong Zhang

Department of Human Biology, University of Cape Town

DECLARATION

I, *Soné Fouché*, hereby declare that the work on which this dissertation/thesis is based is my original work (except where acknowledgements indicate otherwise) and that neither the whole work nor any part of it has been, is being, or is to be submitted for another degree in this or any other university.

I empower the university to reproduce for the purpose of research either the whole or any portion of the contents in any manner whatsoever.

Signature: Signed by candidate

Date: 11 February 2024

AKNOWLEDGEMENTS

I would firstly like to thank my Lord and Saviour, Jesus Christ, for every ability He has given me to complete this master's degree. He has sustained me through difficult times and given me the strength to complete this degree.

I want to thank my supervisor, Dr Jia Fan, for all his help and guidance during this degree. He was always ready to help and truly made this degree easier to complete. I would like to thank my co-supervisor, Prof Ernesta Meintjes, and our whole research group in the MRI division for their support and help when I needed it.

I would like to thank Prof Chunhong Zhang for sharing their data with us. Thank you to Drs Hai Lu, Xuesong Ren, and Yu Wang for acquiring the data. Thank you to Drs Paul Taylor and Gang Chen for data processing advice. A big thank you also to Dr Chris Warton from neuroanatomy for helping me identify the different brain regions.

I would like to thank my husband, Whian, and my whole family for their love, prayers, and support during this degree. They were truly an amazing support system that I could rely on every day.

I would lastly like to thank the office of the premier of the Free State for funding my degree and making it possible for me to study what I've always dreamed of.

ABSTRACT:

Introduction: Stroke patients often have lasting physical and cognitive impairments, leading to functional dependence even after discharge from hospital. Acupuncture has been recommended by the World Health Organisation (WHO) as an adjunctive treatment for stroke. Physiotherapy serves as the primary rehabilitation approach in South Africa and numerous other Western nations. Despite their widespread use, the precise mechanisms underlying both acupuncture and physiotherapy remain elusive, and the neurological alterations following extended rehabilitation programs are yet to be defined. Resting-state functional magnetic resonance imaging (rs-fMRI) is a non-invasive technique used to map brain regions that are temporally correlated, indicative of functional connectivity, during periods of rest. In the present study, treatment-related alterations in brain RSFC in ischaemic stroke patients with unilateral limb dysfunction were randomised to receive either 1) True Acupuncture (TA), 2) TA and Physiotherapy (PT), or 3) PT and Sham Acupuncture (SA), representing a placebo or non-acupoint acupuncture.

Methods: Right-handed participants were recruited from the First Teaching Hospital of Tianjin University of Traditional Chinese Medicine, including 23 stroke patients (58.5±8.0 yrs.) and 10 healthy controls (53.9±6.9 yrs.). As part of a stroke rehabilitation programme, stroke patients were assigned to one of the three treatment arms: TA alone (6 participants), TA with PT (7 participants), or SA with PT (10 participants). Each participants received 5 sessions over 3 weeks. Fugl-Meyer Assessment (FMA) data were collected before, after, and during (on day 8) treatment.

MRI scans were performed on a 3T Skyra Scanner (Siemens, Erlangen, Germany) before and after the 3-week rehabilitation programme, including rs-fMRI using a gradient echo EPI sequence and T1-weighted structural images using an MPRAGE sequence. Healthy controls underwent a single scan without treatment.

Rs-fMRI data were pre-processed using AFNI_proc.py. Eleven resting-state networks (RSNs) were identified through group independent component analysis (ICA) using FSL-MELODIC in data from the healthy controls. Dual regression and randomise in FSL were then applied to identify the clusters within the identified resting state networks (RSNs) showing significant differences (at $p<0.01$; cluster size threshold at $\alpha<0.05$). The mean Z-score within each cluster was subsequently correlated to the FMA scores.

Results: Before treatment, lower RSFC in 2 clusters in the precuneus within the Default Mode Network (DMN) and the Ventral Attention Network were found in the TA with PT group compared to the TA only and SA with PT groups. No significant differences in mean Z-scores within these two clusters were seen among the three groups after treatment.

After treatment, differences in RSFC among groups were found in five regions within three networks, including the cingulate gyrus and the precuneus in the DMN, the orbitofrontal cortex in the executive control network, and the inferior and superolateral occipital lobe in the visual network. In all five of these regions, patients receiving TA+PT showed a significantly higher RSFC compared to individuals in the other groups. There were no significant differences in RSFC between groups in these five regions before treatment.

After receiving TA+PT treatment, patients demonstrated higher resting-state functional connectivity (RSFC) compared to themselves before treatment in nine regions spanning four resting-state networks (RSNs), including the bilateral precuneus, right (R) anterior calcarine sulcus, R primary motor cortex, and left (L) angular gyrus in the first DMN; the bilateral precuneus in the second DMN; the R visual cortex, R posterior lingual gyrus and L visual cortex in the visual network; and the R posterior cingulate sulcus in the ventral attention network.

However, after SA+PT treatment, individuals in the group exhibited lower RSFC compared to themselves before treatment in two regions within two networks, including the R postcentral gyrus in the somatosensory network and the L lingual gyrus in the visual network.

All three treatment groups showed a significant increase in FMA scores from before treatment, to after treatment. No significant differences were found when comparing FMA scores between treatment groups. The TA+PT group's results showed a significant positive correlation between RSFC and FMA scores.

Conclusions:

Stroke patients who received one of three treatments demonstrated improved FMA scores, with no significant differences in FMA scores observed among the three treatment arms after treatment. Patients in the TA+PT group showed significant changes in key brain regions associated with cognition, sensorimotor integration, and motor function. Specifically, increases in RSFC within the precuneus, motor cortex, and posterior cingulate sulcus, which are involved in neural recovery and cognitive improvement. In contrast, the SA+PT group exhibited RSFC decreases within somatosensory and visual networks, indicating a different pattern of neural recognition. After treatment, patients in the TA+PT group exhibited higher RSFC in the precuneus in the DMN and executive control network. These findings highlight the potential efficacy of combining TA with PT for stroke rehabilitation, suggesting that this approach may facilitate positive neural adaptations. However, the study also highlights the necessity for further investigation with larger sample sizes and extended treatment durations to comprehensively grasp the efficacy and underlying mechanisms of this integrated approach.

Table of Contents

List of Figures:

List of Tables:

List of Abbreviations:

3T: Three Tesla

A: Anterior

ACF: Autocorrelation function

ANCOVA: Analysis of Covariance

ANOVA: Analysis of Variance.

AT: After Treatment

BL40: Acupoint on the posterior aspect of the knee.

BOLD: Blood Oxygenation Level-Dependent.

BT: Before treatment

CAT: Contralateral Acupuncture Treatment.

CT: Healthy Controls

DICOM: Digital Imaging and Communications in Medicine.

DMN: Default Mode Network

EC: Effective Connectivity.

EPI: Echo-planar imaging

FC: Functional Connectivity

FCP: Functional Connectome Project

FMA: Fugl-Meyer Assessment.

fMRI: Functional Magnetic Resonance Imaging.

FOV: Field of View.

FSL: FMRIB Software Library.

GB34: Acupoint on the fibular aspect of the leg, in the depression anterior and distal to the head of the fibula.

GB40: Acupoint on the anterolateral aspect of the ankle.

GBD: Global Burden of Disease.

GLM: General Linear Model.

GM: Grey Matter

GV26: Acupoint on the face, at the junction of the upper 1/3 and lower 2/3 of the philtrum midline.

IC: Independent Component

ICA: Independent Component Analysis

L: Left

LPNN: Limbic-Paralimbic Neocortical Network

M: Medial

MELODIC: Multivariate Exploratory Linear Optimized Decomposition into Independent Components.

MPRAGE: Magnetization-Prepared Rapid Acquisition Gradient Echo

MRI: Magnetic Resonance Imaging.

NifTi: Neuroimaging Informatics Technology Initiative

NIHSS: National Institutes of Health Stroke Scale.

P: Posterior

PC6: Acupoint on the anterior aspect of the forearm.

PT: Physiotherapy.

R: Right

ROIs: Regions of Interest.

RSFC: Resting State Functional Connectivity.

rs-fMRI: Resting-State Functional Magnetic Resonance Imaging.

RSNs: Resting State Networks.

SA: Sham Acupuncture.

SCA: Seed-Based Correlation Analysis.

SD: Standard Deviation

SLF: Superior Longitudinal Fasciculus

SP6: Acupoint on the tibial aspect of the leg, posterior to the medial border of the tibia.

SPSS: Statistical Package for the Social Sciences.

TA: True Acupuncture.

TE: Echo Time.

TR: Repetition Time.

TT: Talairach-Tournoux.

TUTCM: Tianjin University of Traditional Chinese Medicine

WHO: World Health Organization.

XNKQ: Xing Nao Kai Qiao (acupuncture treatment).

1. Introduction

Stroke stands as the main cause behind disability, dementia, and mortality worldwide (Akinyemi et al., 2021). Globally, an average of 1 out of every 4 adults will experience a stroke during their lifetime (Global Burden of Disease (GBD) Lifetime Risk of Stroke Collaborators et al., 2018). In Africa, the incidence rate of stroke reaches up to 316 per 100 000 individuals annually, underscoring the urgent requirement for effective post-stroke treatments on the continent, to limit the enduring consequences of the condition.

In South Africa, physiotherapy is utilised as the main post-stroke rehabilitation treatment, while others include occupational and speech therapies, which are only intermittently available at specific community health centres (Rhoda, 2014). An intensive 30–60-minute physiotherapy session conducted 5 to 7 days a week yields optimal results in stroke recovery while tailoring to address patient-specific tasks (Pollock et al., 2014).

Acupuncture, a traditional Chinese medicine, is well-know and socially accepted by most of the East Asian countries (Du et al., 2020). It has served as a prominent stroke rehabilitation treatment for an extended period (Cao et al., 2021). Additionally, the World Health Organization (WHO) endorses acupuncture as adjunctive therapy for post-stroke treatment (Lv et al., 2021).

Acupuncture could potentially activate the central nervous system, facilitate synapse formation, and consequently restore activation in the brain regions affection by stroke (Huang et al., 2012). Nonetheless, the precise mechanisms and impacts of acupuncture on neuroplasticity remain unknown (Lv et al., 2021). Neuroplasticity denotes the inherent ability of the nervous system to adapt and reorganize both its function and structure, thereby facilitating compensation for damage incurred by stroke (Lv et al., 2021).

Functional magnetic resonance imaging (fMRI) functions as a non-invasive method for evaluating cerebral disorders and mapping the functional interconnections in the brain (Kwong et al., 1992). This non-invasive technique relies on detecting the blood oxygenation level-dependent (BOLD) signals between different brain regions (Kwong et al., 1992). When a particular brain area activates, it experiences a surge in blood flow to that surpasses oxygen extraction (Fox & Raichle, 1986). Consequently, the level of blood oxygenation increases, leading to a corresponding elevation in the MRI signal. By tracking these BOLD signals, the activated brain regions can be identified.

Functional connectivity (FC) quantifies the temporal correlation between different neuronal activations in the brain (Smith, 2012). This metric has been employed to monitor disease burden in the context of rehabilitative strategies (Faivre et al., 2012).

Resting-state fMRI (rs-fMRI) is employed to detect brain regions that demonstrate synchronized activity over time when the subject is not actively engaged in any specific task (Biswal et al., 1995). Rs-fMRI enables the identification of brain regions that anatomically separated but functionally connected (Beckmann et al., 2005). This technique provides insights into the intrinsic functional architecture of the brain and can help elucidate patterns of neural communication and organisation.

Independent component analysis (ICA) is commonly used as a prevalent method for extracting features or components with statistically optimised independent sources from a dataset of measurements (Calhoun et al., 2009). Each component obtained through ICA represents a set of brain regions showing synchronous patterns of activity, such as distinct resting state networks (RSNs).

This project aimed to explore the potential benefits and neural correlates of three treatment arms—true acupuncture (TA), TA with physiotherapy (PT), and sham acupuncture (SA) with PT on resting state functional connectivity (RSFC) in ischaemic stroke patients with unilateral limb dysfunction. The investigation utilised ICA to analyse RSFC and elucidate the effects of these treatments on the brain's intrinsic RSNs.

2. Literature Review

2.1. Stroke

A stroke occurs when blood flow to a specific area of the brain is disrupted due to either occlusion or Haemorrhage. Brain injuries caused by stroke can lead to motor disabilities and cognitive impairments, hence affecting functional performance (Nudo, 2007). Stroke patients often experience prolonged hospitalisation and may endure lasting physical and cognitive impairments of varying degrees of severity (Wu et al., 2022). Stroke survivors commonly experience a decreased quality of life after the event, often grappling with post-stroke disability and depression (Akinyemi et al., 2021). Within 15 months of an ischaemic stroke, nearly 35% of survivors may encounter varying degrees of cognitive impairment, potentially elevating their susceptibility to develop dementia (Peng et al., 2016).

Motor disorder is the leading symptom among stroke survivors, with many individuals remaining functionally dependent even after being discharged from the hospital (Ntsiea, 2019). This adds to the global healthcare burden of extensive rehabilitation and nursing treatment for stroke (Fu et al., 2017). The importance of adequate post-stroke treatment and rehabilitation is underscored by the need to alleviate the burden experienced by both stroke survivors and their caregivers. Family members serving as caregivers of stroke survivors endure psychological and emotional challenges (Akinyemi et al., 2021).

Africa boasts one of the highest stroke occurrence rates globally (Akinyemi et al., 2021). In South Africa specifically, 45% of stroke survivors are under 65 years old, with 27% of these individuals below the age of 55 (Ntsiea, 2019). Therefore, the implementation of effective stroke rehabilitation programmes becomes crucial to facilitate the recovery of both mental and physical abilities among stroke survivors, especially for younger individuals aiming to reintegrate into the work sector.

Figure 1 from Owolabi (2011) illustrates the stroke quadrangle, delineating the four key challenge areas in stroke care across Africa. The current study specifically targets 1) acute care and 2) rehabilitation methods that influence the neuroplasticity of stroke patients, with the aim of offering to bring solutions or recommendations to address these two identified stroke challenge areas.

Neuroplasticity, defined as the brain's capacity to adapt its structure and function to offset damage resulting from a stroke (Graham et al., 2009), plays a critical role in steering and facilitating the recovery and rehabilitation process of stroke patients (Hara, 2015). Studies have shown that functional goal-orientated and increased attention activities can trigger alterations in neuroplasticity (Graham et al., 2009; Arya et al., 2011).

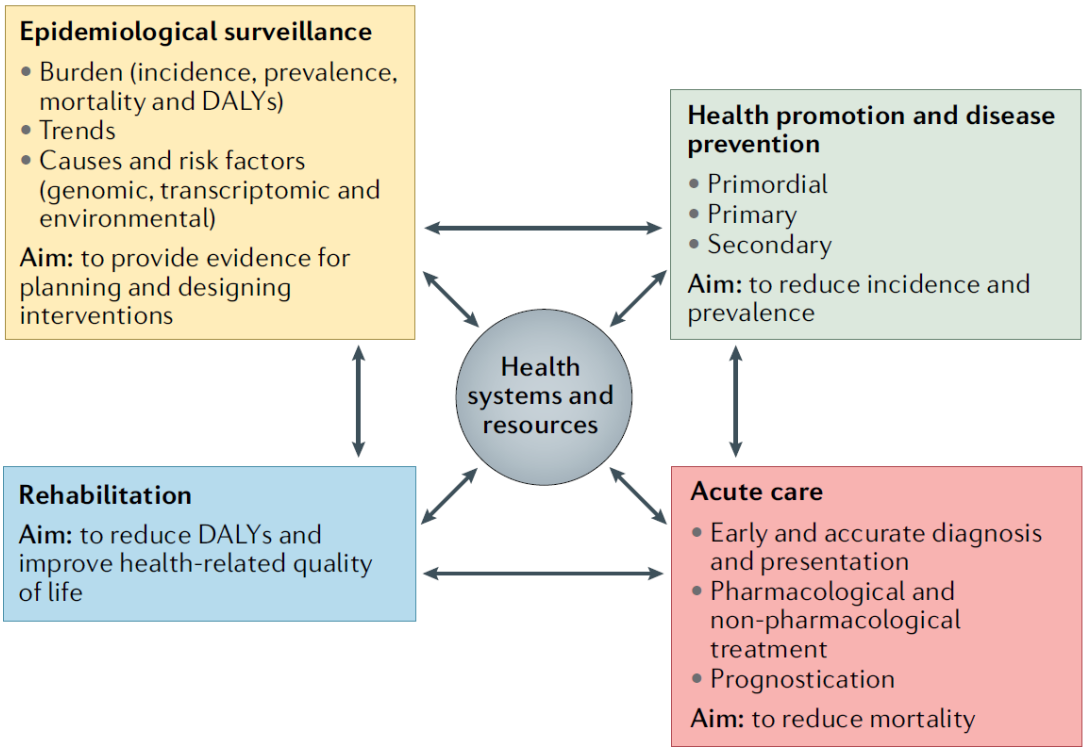

Figure 1: The Stroke Quadrangle (Owolabi, 2011).
DALYs: Disability-adjusted life years.

2.2. fMRI and RSFC

Functional neuroimaging techniques enable the examination of the functional interactions between different brain regions. Functional connectivity (FC) describes the temporal dependence of brain activity patterns among anatomically separate brain regions, indicating functional communication between these regions (Aertsen et al., 1989). FC can be assessed to determine the connectivity between brain regions (Lowe et al., 2000).

Functional magnetic resonance image (fMRI) is a non-invasive technique used to assess cerebral diseases and evaluate functional interconnections in the brain (Kwong et al., 1992). fMRI relies on blood oxygenation level-dependent (BOLD) signals between brain regions (Kwong et al., 1992). When a brain region is activated, oxyhaemoglobin levels increase while deoxyhaemoglobin concentrations decrease due to increased oxygen demand in that region (Ogawa et al., 1998). Oxyhaemoglobin has a diamagnetic effect, while deoxyhaemoglobin has a paramagnetic effect (Kim & Kamil Ugurbil, 1997), leading to increased BOLD signals as the deoxyhaemoglobin concentration decreases (Heeger & Ress, 2002).

Resting-state fMRI (rs-fMRI) measures spontaneous fluctuations in the BOLD signal and can be used to identify resting state networks (RSNs) (Lee et al., 2012). It has been employed to investigate the resting-state FC (RSFC) within RSNs in individuals after a stroke. Previous

studies reported that spontaneous activity exhibited correlations between various brain regions during rest (Buckner, Andrews-Hanna & Schacter, 2008; Buckner & Vincent, 2007).

Task-based fMRI is widely used to assess functional domains in the brain (Smitha et al., 2017). During task-based fMRI, patients are required to perform specific tasks targeting various utilities such as motor, attention, memory, sensory processing, language, or vision (Kesavadas, 2013; Fox, 2010). Rs-fMRI is advantageous as no task is required, making it particularly suitable for research involving children, unconscious patients, and individuals with difficulty understanding the tasks (Smitha et al., 2017).

2.3. Physiotherapy

In South Africa, physiotherapy is one of the primary post-stroke rehabilitation treatments, with occupational and speech therapies being occasionally available at certain community health centres (Rhoda, 2014). Physiotherapy interventions vary based on the therapist preferences and differ across patients and settings (Rahayu et al., 2020). These treatments may include exercise therapy, passive and active mobilization, breathing exercises and changing positions (Rahayu et al., 2020).

Rhoda (2014) conducted a study comparing the quality of life of 73 stroke patients within two- and six-months post-stroke. The study was done at various Community Health Centres in the Western Cape, South Africa, however, only some centres offer rehabilitation services, including physiotherapy, occupational therapies, and speech therapy. Many of these stroke patients experienced pain, discomfort (such as anxiety, and depression), and difficulties with usual activities (such as work and caring for families).

Rehabilitation with a focus on the improving functional ability to enhance the quality of life after a stroke is crucial for stroke patients in South Africa (Rhoda, 2014). Disability, stroke severity and depression contribute a poorer quality of life for stroke survivors compared to stroke-free controls (Akinyemi et al.,2021). The disability following a stroke imposes a significant psychological and emotional burden on stroke survivors and caregivers (Akinyemi et al., 2021).

Physiotherapy has been found to significantly improve balance and the ability to perform activities of daily living (Mayo et al., 2002; Darekar et al., 2015). Both conventional and standard physiotherapy protocols have shown benefits in improving the conditions of stroke patients (Hatem et al., 2016; Veerbeek et al., 2014). A notable advantage of physiotherapy is its inclusivity, as it can be applied to patients of any age and severity of functional ability (Vaughan-Graham, Cott & Wright, 2014; Graham et al., 2009).

Combining physiotherapy methods have been recommended for improved patient outcomes (Rahayu et al., 2020), as well as combining physiotherapy with other rehabilitation methods (McGrath et al., 2018). While most available studies focus on the physical rehabilitation and performance of stroke patients due to physiotherapy, few report its effects on neuroplasticity.

Studies assessing the effect of physiotherapy using MRI are limited, as most studies concentrate solely on the physical outcomes rather than cognitive effects. Stroke-related fMRI studies applying physiotherapy treatment to healthy participants have observed slight effects on cortical brain areas (Seitz, Matyas & Carey, 2008; Butler & Page, 2006; Weiss et al., 1994). Increased activity in the precentral and postcentral areas of the brain have also been observed following imagined or executed movements by patients (Hanakawa, Dimyan & Hallett, 2008; Lacourse et al., 2005).

2.4. Acupuncture

For millennia, acupuncture has been a cornerstone of Traditional Chinese Medicine (TCM) in China (Zhu et al., 2021). Its primary aim is to stimulate specific acupoints on the body. The attainment of *De qi* is essential for fully activation of these acupoints. *De qi* is characterised by sensations such as numbness, heaviness, soreness, or fullness, which can be felt by either the patient or the practitioner (Chen et al., 2020).

During acupuncture practice, both needles as well as needle manipulations are used to stimulate acupoints (Zhu et al., 2021). According to the theory of Traditional Chinese Medicine, *Qi* represents the inner energy essential for healthy humans. Imbalances in *Qi* can predispose individuals to disease or illness (Chon & Lee, 2013). Acupuncture serves to regulate *Qi* flow, balance blood circulation, harmonise *Yin* and *Yang* energies, and establish connections between meridians (Zhu et al., 2021). The meridians of the human body, as well as acupoints are indicated in Figure 2.

During the 1950s, acupuncture gained traction in Western hospitals, with the practice of electroacupuncture becoming popular (Zhang et al., 2020). By 2013, the WHO reported that 183 out of 202 regions or countries worldwide had implemented some form of acupuncture treatment (World Health Organization, 2013).

Acupuncture is recommended by the WHO as an alternative or complementary treatment for stroke rehabilitation (Chavez et al., 2017). Xu and colleagues (2020) suggested that earlier intervention with acupuncture can enhance the long-term effects of acupuncture intervention for stroke patients, leading to improvements in motor dysfunction and inflammation. Xing Nao Kai Qiao (XNKQ) acupuncture, first proposed by Prof Xuemin Shi in 1992 to treat encephalopathy, has gradually been improved and is now widely accepted in stroke rehabilitation (Shi et al., 1992).

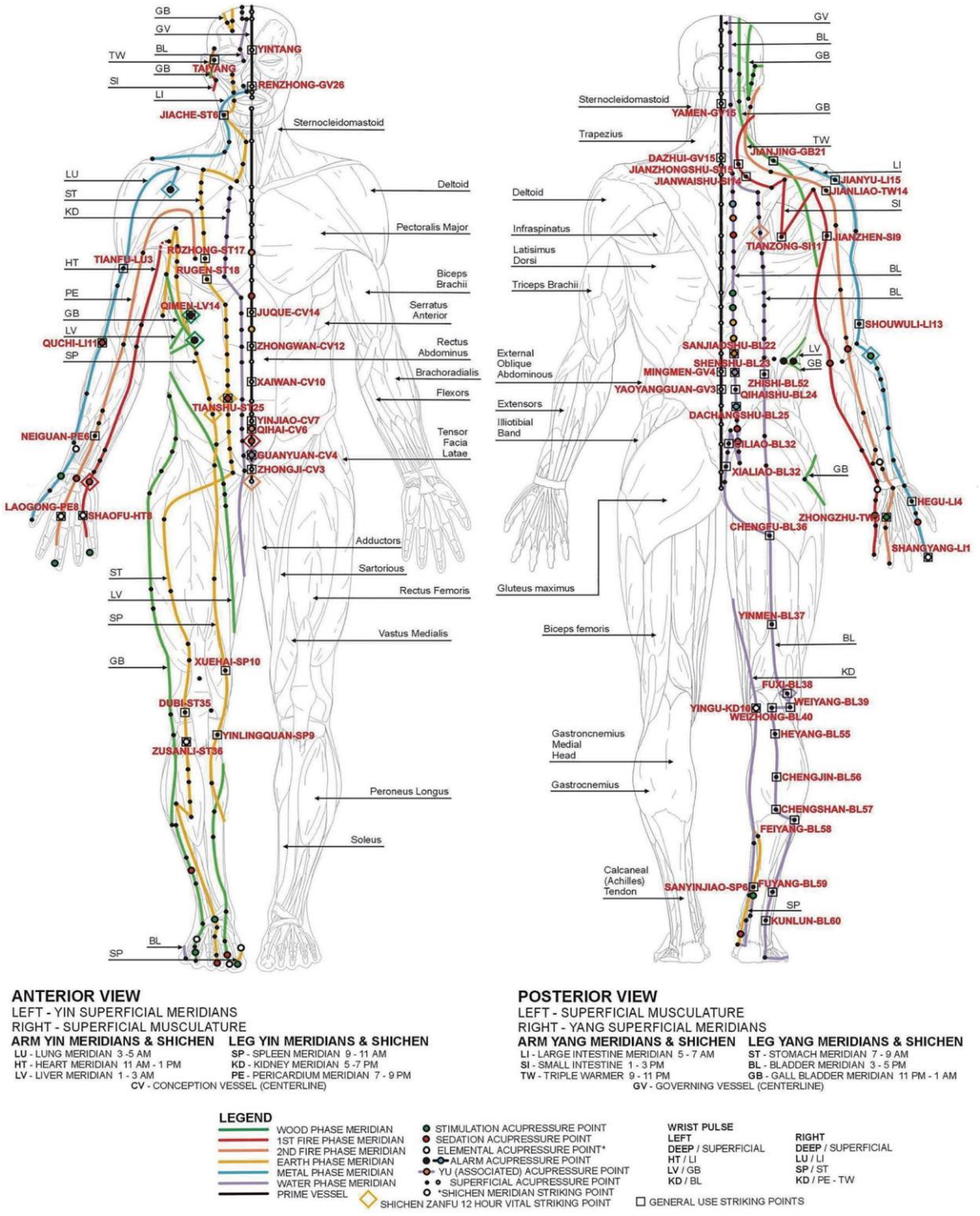

Figure 2: Meridians of the human body, as well as acupoints used in acupuncture practice (Zhang, 2021).

Huang and colleagues (2015) conducted a study involving 12 ischaemic stroke patients aged between 47-65 years. The fMRI scans were acquired while acupuncture was administered at the “Waiguan” acupoint. Participants were divided into two groups according to the sensations experienced during the acupuncture treatment. Five patients reported experiencing *De qi*, characterised by sensations of soreness, numbness, and heaviness, while five others reported feeling no sensation, or “non-*De qi*”. Two subjects were excluded from the study due to experiencing twinge, which was not associated with *De qi*. The study revealed that acupuncture treatment activated different regions in the *De qi* and “non-*De qi*” groups. The areas of brain activation of the *De qi* group were found to correlate with brain tissue remodelling.

Chen and colleagues (2019) discovered that administering acupuncture after a 15-minute contralateral acupuncture treatment (CAT) could stimulate bilateral brain regions. Their findings indicated that combining acupoints could activate more extensive and diverse brain areas compared to stimulating a single acupoint, as suggested by previous research.

Han and colleagues (2019) observed that following acupuncture treatment, there was an augmentation in FC between the premotor cortex/supplementary motor area and the supramarginal gyrus. Additionally, they noted an enhanced communication between various cortices despite the presence of white matter tract injuries. Their findings suggested that acupuncture exerted an immediate neural effect irrespective of structural integrity. However, it is important to mention that their study solely investigated the immediate effects of acupuncture and did not explore the cumulative benefits over time.

Previous studies indicated that extending the observation period following acupuncture treatment could yield significant benefits (Huang et al., 2015; Chen et al., 2019; Fu et al., 2017). Such an approach has the potential to facilitate the exploration of acupuncture’s cumulative impacts beyond its immediate response in brain activity.

2.5. fMRI Analysis

Three commonly used analysis methods for analysing rs-fMRI data are independent component analysis (ICA), seed-based correlation analysis (SCA), and graph theory. In SCA, regions of interest (ROIs) are pre-selected based on existing literature. The average BOLD signal time course of the voxels within this ROI is then correlated with each other, as well as the time courses of other voxels throughout the brain (Biswal et al., 1995; Lee et al., 2012). This process allows us to identify the voxels that show significant correlations with the pre-selected ROI, providing insights into RSFC patterns in the brain.

Graph theory is an analytical approach that conceptualises RSNs as networks composed of nodes and edges. The ROIs are depicted as nodes within the network. The edges between these nodes represent the functional connectivity or correlation between the activity of different ROIs (Lee et al., 2012). By quantifying the connectivity patterns of the edges, various graph measures can be computed to find different measures of interest and investigate different aspects of network organization and dynamics. These measures offer valuable insights into the functional architecture of the brain and how different brain regions interact within RSNs.

ICA is a powerful tool used to extract statistically independent features or components from a set of data, as shown in Figure 3 (Calhoun et al., 2009). ICA can identify distinct patterns of brain activity known as RSNs without the need for predefined ROIs, as required in seed-based analysis (Lee et al., 2012). Each identified component provides a collection of brain regions showing similar patterns of activity, allowing us to characterise the RSNs. This approach offers the advantage of unbiased exploration of the data, enabling the discovery of both well-known and previously unidentified RSNs.

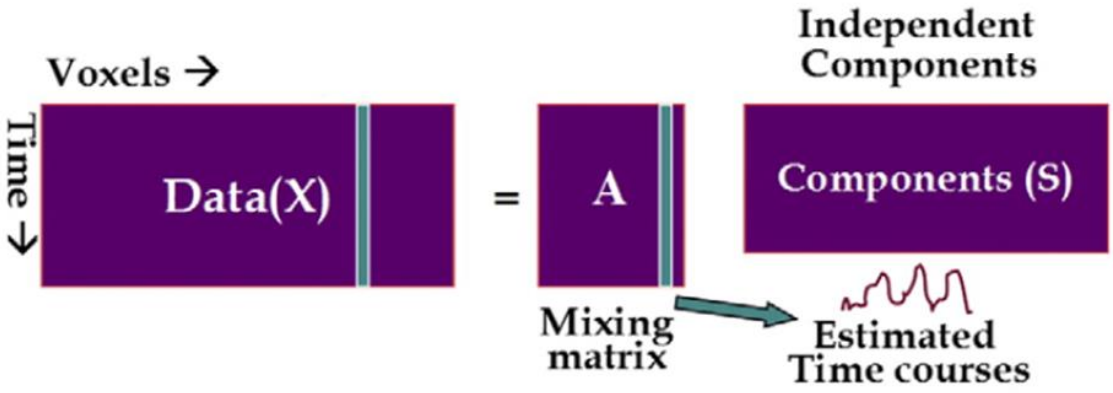

Figure 3: Illustration of how ICA works to estimate time courses from data by maximising the independence between component images (Calhoun, Liu & Adalı, 2009).

ICA has been widely employed in various studies, including more demanding approaches such as standard regression type (Calhoun & Adali, 2006; McKeown 2003). Group ICA can be conducted when analysing data from multiple subjects simultaneously. An advantage of group ICA is that a single ICA analysis can be conducted, and the outcomes can then be separated into subject-specific components (Calhoun, Liu & Adali, 2009). Therefore, ICA facilitates the comparison of individual differences within each component.

There are two commonly used approaches in ICA: (1) temporal concatenation, which allows for unique time courses within each subject while assuming common group maps (Calhoun,

`Liu & Adali, 2009), and (2) spatial concatenation, where time courses are assumed to be common while maps are unique. Given that temporal variations in fMRI data tend to be larger than spatial variations, the temporal concatenation approach is often recommended and widely utilised for rs-fMRI data analysis (Schmithorst & Holland, 2004).

By detecting brain areas with simultaneous activation time courses, ICA allows us to identify distinct RSNs, as illustrated in Figure 4. Calhoun and colleagues (2009) stated that MELODIC software can be employed for the temporal concatenation approach, which was indeed utilised in this study.

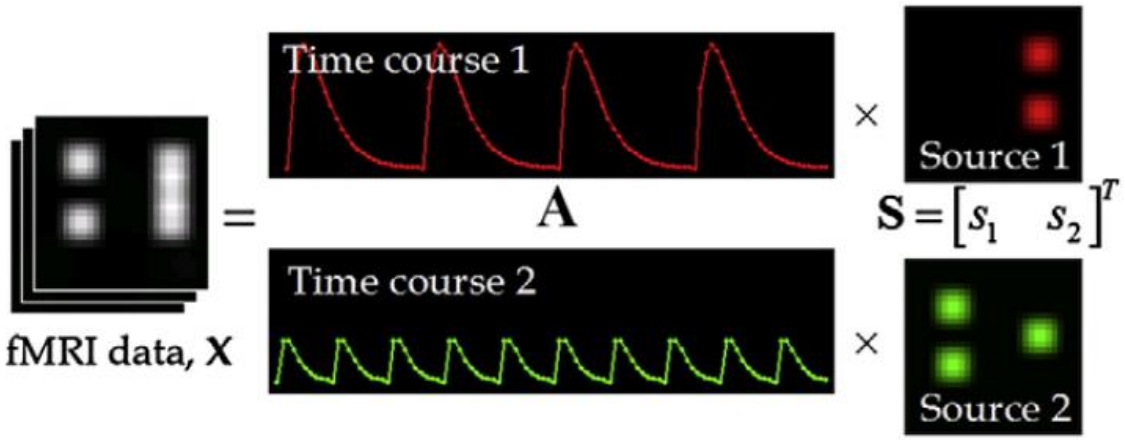

Figure 4: Illustration of how ICA extracts linearly mixed sources and their corresponding time courses from fMRI data (Calhoun, Liu & Adalı, 2009).

Fu and colleagues (2017) investigated the functional connectivity between various brain regions in 19 stroke patients with left hemiplegia aged between 35-75 years compared to 17 control subjects. After acupuncture treatment, stroke patients demonstrated more complex functional connections among various brain regions compared to healthy controls.

Over the last two decades, research has extensively explored the neural mechanisms involved in acupuncture through neuroimaging techniques. fMRI studies have revealed that acupuncture can modulate activity in specific brain regions, such as the somatosensory cortices, insula, thalamus, and anterior cingulate cortex, which are part of the anti-correlated task-positive network. Conversely, it deactivates regions like the medial prefrontal cortex, medial parietal cortex, and medial temporal lobes, associated with the limbic-paralimbic neocortical network (LPNN) (Hui et al., 2009; Chae et al., 2013). The overlap of acupuncture-responsive regions with the default mode network (DMN) has led to hypotheses regarding acupuncture's effects through DMN modulation (Otti and Noll-Husson, 2012; Zhao et al., 2014;

Zhang et al., 2019). Notably, studies employing tactile stimulation as a sham condition have provided support for this hypothesis, indicating differential activation patterns such as greater activation of sensorimotor regions, but less extensive deactivation of the DMN regions (Hui et al., 2009).

In ischaemic stroke patients, acupuncture-induced brain activity alterations have been observed in contralateral primary sensorimotor and medial frontal cortices, but not in the ipsilateral hemisphere, particularly during twist manipulation, suggesting compensatory mechanisms in the affected hemisphere (Chen et al., 2013, 2014; Huang et al., 2013). However, the expected deactivations in DMN regions were not consistently reported, necessitating further investigation. Additionally, while immediate effects of acupuncture on brain activity have been extensively studied using fMRI, investigations into long-term changes following extended acupuncture interventions are limited.

Studies have demonstrated acupuncture's effects on FC in RSNs, such as the DMN and sensorimotor networks, in both healthy individuals and other patients with pain, stroke or mental conditions (Deng et al., 2016; Liang et al., 2014; Bai et al., 2010; Zhao et al., 2014). Differences in FC alterations between healthy controls and patients with pathology have been noted, suggesting potential therapeutic implications. In healthy controls, resting state fMRI following a short 1-min acupuncture manipulation at GB34 (Yanglinquan, located in a depression anterior and inferior to the head of the fibula), for example, produced significantly increased effective connectivity bilaterally from various subcortical brain regions to sensorimotor cortex, but only from the culmen (located in the anterior vermis) to sensorimotor cortices in patients who had suffered an ischaemic stroke in the anterior circulation (Xie et al, 2014). Han and colleagues (2017) recently reported RSFC increases between regions connected by the stroke-injured frontoparietal part of the superior longitudinal fasciculus (SLF) (i.e. the ipsilateral premotor and supplementary motor cortices and the supramarginal gyrus) following a similar short 1-min acupuncture manipulation at GB34 in stroke patients, which was not evident in healthy controls. Notably, regions linked by the temporal part of the SLF did not show acupuncture related RSFC changes in either group.

In a study employing XNKQ acupuncture, healthy participants experienced alterations in RSFC within subcortical brain areas associated with motor function shortly after treatment initiation, primarily attributed to needle stimulation (Nierhaus et al., 2019). Subsequent post-hoc SCA indicated reduced FC between these subcortical regions and primary sensorimotor cortices, potentially conducive to motor deficit recovery in stroke patients. However, due to uncertainty regarding the duration of acupuncture's effects, the long-term significance of these immediate changes in functional connectivity for stroke treatment remains ambiguous.

Given that stroke commonly affects FC (Rehme and Grefkes, 2013; Xie et al., 2014), and functional brain reorganization is believed to play a crucial role in recovery (Almeida et al., 2016; Schaechter, 2004), acupuncture emerges as a potential aid in functional recovery by promoting such reorganization. Studies in stroke mouse models have indicated that multisensory input can enhance functional recovery and RSFC (Hakon et al., 2018). Acupuncture, considered a multisensory input, has been shown to induce hyperactivation in ipsilesional primary and secondary sensorimotor cortices, akin to somatosensory stimuli on the contralesional side (Li et al., 2006), raising concerns regarding its specificity (Dhond et al., 2007). Notably, both true and sham acupuncture have demonstrated correlated changes in upper limb function and motor cortex activity in stroke-affected individuals (Schaechter et al., 2007). However, a systematic review of 38 clinical trials found no significant differences in physical outcomes favouring true acupuncture over non-acupoint or sham puncture (Moffet, 2009).

While findings on brain responses to true versus sham acupuncture have been inconsistent (Huang et al., 2012), likely due to varying protocols, true acupuncture appears to elicit greater and more specific brain responses. For instance, Siguan acupuncture exhibited greater activity in the somatosensory cortex, the limbic-paralimbic system, visual-related cortex, basal ganglia and cerebellum in healthy controls, compared to needling at nearby sham acupoints (Shan et al., 2014).

In a study by Wu and colleagues (2014), a single-session acupuncture targeting LR3 (the Taichong acupoint) induced alterations in RSFC among healthy volunteers across various brain areas associated with vision, movement, sensation, emotion, and analgesia. In contrast, sham acupuncture using a placebo needle, which only made superficial contact with the skin at the same point, primarily affected psychological processes but did not influence RSFC in brain regions implicated in LR3's mechanisms of action. Furthermore, Nierhaus et al. (2019) demonstrated heightened activation in the insula and secondary somatosensory cortex (S2), along with precuneus deactivation, and increased functional connectivity (FC) between S2 and the precuneus in response to needle stimulation at the acupoint ST36 (located on the lower leg) compared to two control points. Additionally, Napadow and colleagues (2012) utilised fMRI to reveal that brief acupuncture stimuli applied to different acupuncture and control points elicited brain responses in healthy controls that correlated with autonomic nervous system reactions, including changes in heart rate and skin conductance response, likely stemming from distinct sensory experiences.

Despite significant evidence of acupuncture's effects on brain function, its long-term benefits and optimal treatment parameters remain uncertain. Most studies in stroke patients have focused on comparing neural correlates of acupuncture intervention with healthy controls

rather than incorporating sham protocols, reporting brain activity and FC changes during and immediately after treatment. To date, no studies have examined neural changes following extended acupuncture interventions as part of stroke rehabilitation programs. Considering the documented long-term benefits of acupuncture in pain management, similar benefits are expected in the treatment of post-stroke motor deficits, possibly attributed to long-term neuroplasticity changes.

3. Aim and Objectives

3.1. Aim

The aim of the present study was to examine the potential benefits and neural correlates of acupuncture treatment in conjunction with physiotherapy during a standard 3-week stroke rehabilitation programme for adults experiencing unilateral limb dysfunction following ischaemic stroke.

3.2. Objectives

Stroke patients participating in this study were randomly assigned to one of three treatment arms:

(a) true acupuncture (TA): participants in this group received true acupuncture treatment five times per week for a duration of three weeks, totalling 15 sessions.

(b) TA with physiotherapy (PT): participants in this group underwent standard physiotherapy interventions along with the true acupuncture treatment, receiving 15 sessions of both modalities over the three-week period.

(c) PT with sham acupuncture (SA): this group received standard physiotherapy interventions in combination with sham acupuncture. The sham acupuncture involved the application of needles to non-acupoints, serving as a placebo control. Similar to the other groups, participants in this group also received 15 sessions over the course of three weeks.

These treatment arms were designed to evaluate the efficacy of acupuncture in conjunction with physiotherapy for stroke rehabilitation. The inclusion of the sham acupuncture group allowed for a comprehensive assessment of the specific effects of true acupuncture, thereby enhancing the robustness of the study's findings.

The objectives of the study were as follows:

(1) to evaluate improvements in stroke patients' physical outcomes using the Fugl-Meyer Assessment scale (FMA).
(2) to assess effects of acupuncture treatment and physiotherapy on RSFC in these patients using rs-fMRI.
(3) to examine whether improvements in RSFC are associated with alterations in physical outcomes.

4. Hypothesis

I hypothesised that:

(1) Participants were expected to exhibit improved physical outcomes and enhanced RSFC in the brain after completing a 3-week rehabilitation programme compared to their baseline measurements.

(2) Participants receiving TA with PT would demonstrate more significant changes in functional connectivity across various RSNs compared to individuals in TA and/or PT with SA groups.

(3) The degree of alterations in brain functional connectivity following rehabilitation programme would be correlated with the improvements in physical outcomes.

5. Methodology

5.1. Study Cohort

Participants were recruited from the First Teaching Hospital of Tianjin University of Traditional Chinese Medicine (TUTCM) in Tianjin, China. The cohort comprised 23 stroke patients (mean age ± standard deviation: 58.5±8.0 years) and 10 healthy controls (mean age ± standard deviation: 55.0±7.3 years). One healthy control was excluded due to motion artifact (9 healthy controls remaining; mean age ± standard deviation: 53.9±6.9 years). The 23 stroke patients were randomly allocated to one of three distinct treatment arms: 1) TA (7 participants; mean age 56.1±7.9 years), 2) TA with PT (6 participants; mean age 63.8±5.5 years), 3) SA with PT (10 participants; mean age 56.9±8.8 years). There were no significant differences between treatment groups with regards to sex, age, and stroke side.

Participants who experienced a stroke on the left side of the basal ganglia exhibited upper and lower limb paralysis on the right side of the body. Conversely, participants with a stroke on the right side of the basal ganglia demonstrated upper and lower limb paralysis on the left side of the body.

5.1.1. Inclusion Criteria

The inclusion criteria of participants included: Male or female 1st stroke patients aged 40-75 years suffering unilateral limb dysfunction following a medium ischaemic stroke in basal ganglia. Patients were enrolled within 2 weeks after stroke onset. WHO criteria were used for stroke diagnoses. The extent of unilateral limb dysfunction was such that patients had to be able to walk with a walking frame and dress with/without assistance.

5.1.2. Exclusion Criteria

The exclusion criteria of participants included that patients with intracerebral haemorrhage were excluded. Patients with any of the following were also excluded from the study: (1) corpus callosum stroke, (2) dependency in activities of daily living before present stroke, (3) inability to complete scheduled treatment course, (4) infection in acupuncture sites, (5) severe aphasia or unconsciousness making it difficult to comprehend the study or cooperate in evaluation, (6) other severe complications or comorbidities such as heart/renal function failure, and (7) HIV positive and diabetic limbs, (8) unwillingness to undergo acupuncture or sensory sensitivity, (9) multiple strokes, (10) previous clinical stroke including small strokes noted in the MRI acquired from the study, (11) undergoing thrombolysis and/or thrombectomy, and (12) have any implants made of metal.

5.2. Acupuncture Treatment

All participants underwent either TA or SA treatments within their designated treatment groups as part of the three-week treatment plan. Participants received five acupuncture sessions per week, resulting in a total of 15 sessions of either TA or SA.

5.2.1. True Acupuncture (TA)

During TA treatment, participants received the "Xing Nao Kai Qiao" (XNKQ) acupuncture treatment. Prior studies have indicated enhanced outcomes on the National Institutes of Health Stroke Scale (NIHSS) for individuals undergoing motor impairment after ischaemic stroke with XNKQ acupuncture, as opposed to SA (Ni & Shi, 2011).

Figure 5 illustrates the anatomical locations of the six XNKQ acupoints. Bilateral stimulation was applied to acupoint PC6, while GV26 was targeted in the midline. Additionally, on the affected side, acupoints SP6, BL40, GB34, and GB40 were stimulated. Descriptions of these specific sites are outlined below:

1. PC6: Pericardium Meridian, on the anterior aspect of the forearm, between the tendons of the palmaris longus and the flexor carpi radialis, 50mm proximal to the palmar wrist crease.

2. GV26: Governor Vessel, on the face, at the junction of the upper 1/3 and lower 2/3 of the philtrum midline.

3. SP6: Spleen Meridian, on the tibial aspect of the leg, posterior to the medial border of the tibia, 75mm superior to the prominence of the medial malleolus.

4. BL40: Bladder Meridian, on the posterior aspect of the knee, at the midpoint of the popliteal crease.

5. GB34: Gallbladder Meridian, on the fibular aspect of the leg, in the depression anterior and distal to the head of the fibula.

6. GB40: Gallbladder Meridian, on the anterolateral aspect of the ankle, in the depression lateral to the extensor digitorum longus tendon, anterior and distal to the lateral malleolus.

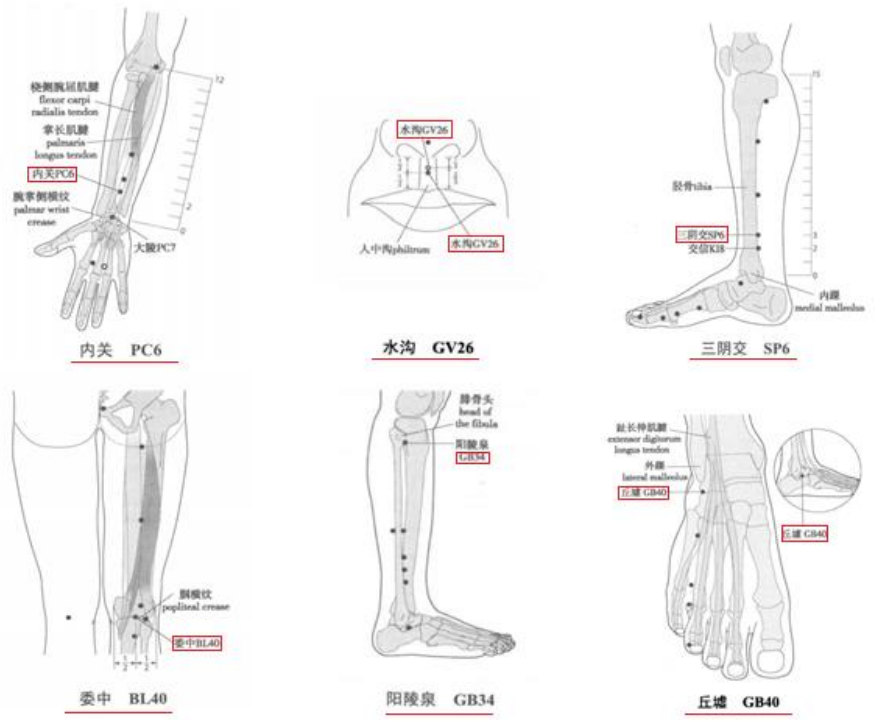

Figure 5: Anatomical locations of XNKQ acupoints.

Cloud Dragon sterile single-use acupuncture needles (1.4-4 cm in length and 0.25 mm in diameter) were utilised, and the disposal of needles followed the designated procedure as per the acupuncture guideline GB/T201709.20. With participants in the supine position and after skin disinfection, acupuncture manipulation was performed without retaining needles, as described below:

1. Bilateral PC6: Acupuncture needles were inserted perpendicularly into the skin to a depth of 13 - 25 mm and stimulated with the reducing method by lifting and thrusting with simultaneous twirling for 1 minute.

2. GV26: The needle was inserted obliquely and upwards towards the nasal septum to a depth of 8 - 13 mm with bird-pecking needling until the patient's eyes moistened or tears flowed.

3. SP6: The needle was inserted obliquely at a 45° angle at the posterior edge of the tibia to a depth of 25 - 40 mm; lifting and thrusting reinforcing manipulation was applied until the affected side lower limb jerked three times.

4. BL40: The needle was inserted perpendicularly on the affected side with the lower limb straight and raised at a 45° angle; reducing by lifting and thrusting was applied until the lower limb jerked three times.

For acupoints GB34 and GB40, electro-acupuncture was applied by connecting the needles to a G6805-2 low-frequency electronic impulse instrument. Electro-acupuncture differs from traditional acupuncture in that the needles are connected to a device providing electric pulses, which can be adjusted to the desired frequency and intensity to optimize the treatment benefits. Electro-acupuncture essentially results in the current delivered by the needle being distributed to a larger area than would be possible by the needle itself. Electro-acupuncture can be applied to several pairs of needles simultaneously, but usually not for more than 30 minutes at a time. The safety of electro-acupuncture is well established.

Sterile adhesive pads were first placed at GB34 and GB40 on the affected side, after which acupuncture needles were inserted perpendicularly through the adhesive pads to a depth of 25 - 40 mm for GB34 and 13 - 20 mm for GB40. Following needle insertion, small, equal manipulations of twirling, lifting, and thrusting were performed on needles to reach *De qi* (a composite of sensations including soreness, numbness, distention, heaviness, and other sensations, mentioned before). A pair of electrodes from the electro-acupuncture apparatus were then attached transversely to the needle handles, and electro-acupuncture stimulation was applied for 30 minutes with a dilatational wave of 2/100Hz and a current intensity of 1 to 3 mA (preferably with the skin around the acupoints shivering mildly without pain).

5.2.2. Sham Acupuncture (SA)

The term sham acupuncture (SA) refers to a sham or placebo acupuncture procedure that stimulates non-acupoints. In the current SA protocol, the non-acupoints were 10 mm lateral to the actual PC6, SP6, BL40, GB34 and GB40 acupoints, and 5 mm lateral to GV26 (usually to the left). The SA protocol involved minimally invasive, shallow (5 - 8 mm) needle insertions with mild reinforcing and reducing manipulations for 1 min, without retaining needles.

The SA electro-acupuncture procedure, electrode placements, and other treatment settings were the same as in the TA group but with no skin penetration, no electricity output, and no needle manipulation for *De qi*.

5.3. Physiotherapy treatment

Participants who underwent physiotherapy treatment received a standardised 3-week post-stroke physiotherapy regiment tailored to each patient's specific needs, as determined by the physiotherapist.

5.4. Physical Examination: Fugl-Meyer Assessment (FMA)

The Fugl-Meyer Assessment (FMA) was developed to establish a standardized measure for evaluating rehabilitation effectiveness. This assessment is tailored to appraise motor function, balance, sensation, and joint function in individuals with post-stroke hemiplegia (Fugl-Meyer et al., 1975). Widely employed in both research and clinical settings, the FMA plays a crucial role in determining disease severity, characterizing motor recovery, and strategizing and evaluating treatment interventions.

The FMA assigns a comprehensive score to each patient, encompassing five domains: motor functioning, sensory functioning, balance, joint range, and joint pain. Regarded as a well-constructed, practical, and effective clinical evaluation, the FMA is strongly recommended as a primary tool for assessing motor recovery post-stroke (Gladstone et al., 2002). It is particularly suitable for comparing improvements in physical outcomes among the three treatment groups.

FMA scores were obtained before treatment started, during treatment on day 8, and after the participant received the rehabilitation treatment.

FMA Scoring:

- Motor function (Maximum score in lower limb = 34)
- Sensory function (Maximum score = 24)
- Balance (Maximum score = 14)
- Range of motion of joints (Maximum score = 44)
- Joint pain (Maximum score = 44)

5.5. MRI Acquisition

Participants were scanned on a 3T Skyra Scanner (Siemens, Erlangen, Germany) at the First Teaching Hospital of the TUTCM both before the initiation of rehabilitation treatment and after the completion of the 3-week programme. The scanning included rs-fMRI data acquisition using a gradient echo EPI sequence (TR=2000 ms, TE=30 ms, flip angle=90˚, FOV=220 mm, voxel size 3.4×3.4×3.0 mm^3) and T1-weighted structural imaging using an MPRAGE sequence (TR=2000 ms, TE=1.97 ms, flip angle=8˚, FOV=256 mm, voxel size 1.0×1.0×1.0 mm^3).

5.6. Image Processing

The preprocessing of rs-fMRI data utilised afni_proc.py in AFNI (Cox, 1996) and included standard procedures including realignment, regression, and blurring. All images were registered to a 3x3x3 mm^3 Talairach-Tournoux (TT) standard space. Group independent component analysis (ICA) and dual regression were performed in FSL (Nickerson et al., 2017). FSL-randomise was employed to find significant clusters ($p<0.01$) within each resting-state network (RSN) identified by the group ICA. Mean Z-scores were obtained in each cluster, and results were reported only for those surviving at a cluster threshold of $\alpha<0.05$ and comprising more than 20 voxels (540 mm^3). Figure 6 illustrates the data processing pipeline adapted from the methodology presented by Fan et al. (2017).

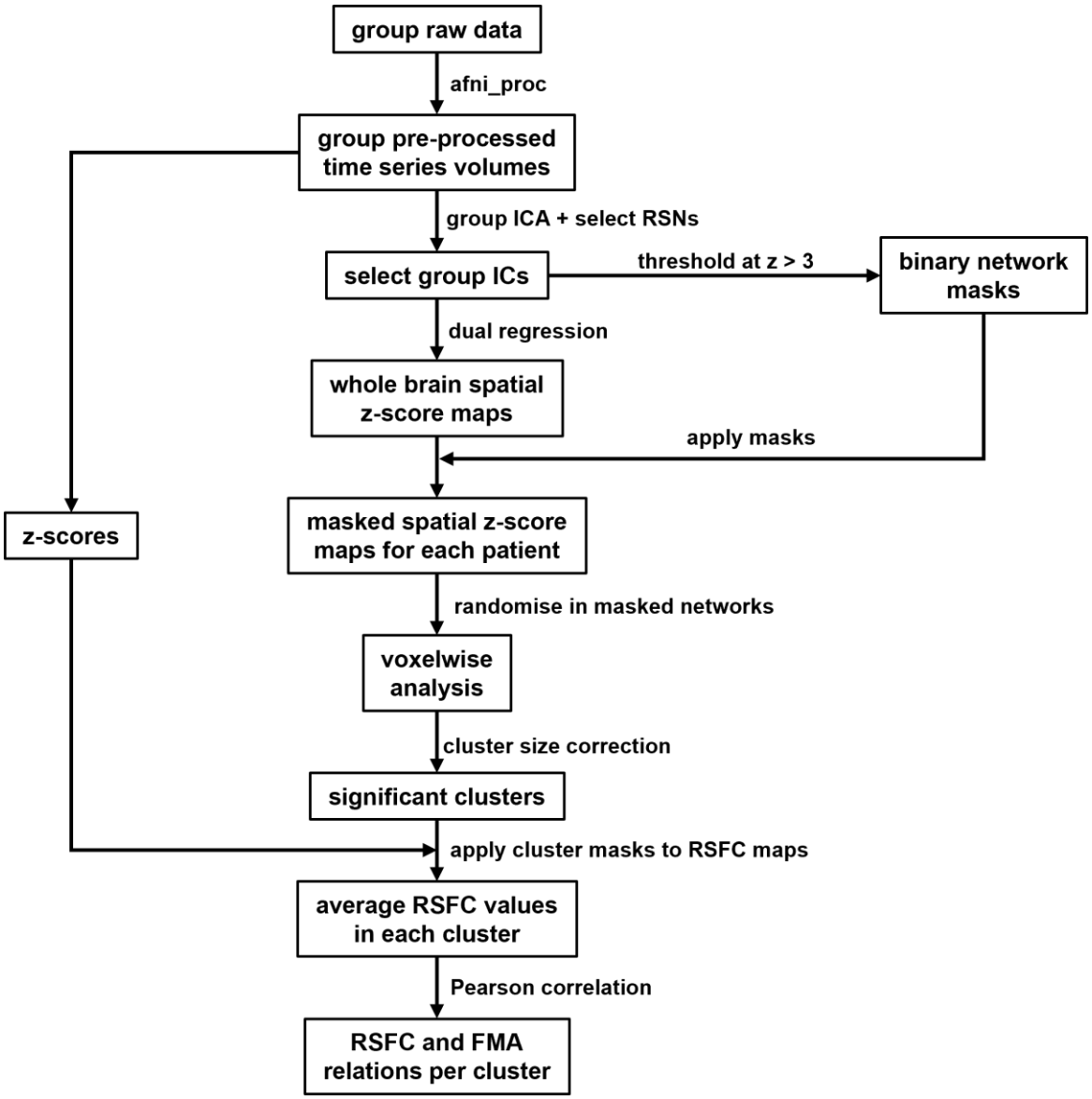

Figure 6: Data processing pipeline.

5.6.1. Preprocessing

Prior to conducting ICA on the rs-fMRI data, a series of preprocessing steps were executed. Firstly, raw MRI data were converted from DICOM format to NifTi files using the *dcm2nii* (Li et al., 2016). The resting state data was then transformed to RPI orientation and resized to dimensions of 3x3x3 mm^3 using AFNI's (version AFNI_21.3.11) 3dresample function (Cox & Hyde, 1997). Additionally, all T1 images underwent a similar conversion to RPI orientation, and their dimensions were adjusted to 1x1x1 mm^3 using 3dresample.

All rs-fMRI data underwent preprocessing through a pipeline of standard procedures, constructed and implemented using afni_proc.py (Pa et al., 2018) as seen in the code in Appendix A. The first 4 volumes were discarded to facilitate signal stabilization. The remaining 176 timepoints underwent despiking and motion correction through rigid body volume registration. For each subject, both linear and nonlinear co-registrations were implemented to align each EPI set first to the subject's anatomical T1-weighted structural image and then to the 3x3x3 mm^3 Talairach–Tournoux (TT) standard space. Each volume was spatially blurred with a full width at half maximum (FWHM) of 6.0 mm. Regression was performed to eliminate signals from white matter (WM) and cerebrospinal fluid (CSF), as well as motion estimates. Time series were subsequently band-pass filtered between 0.01 and 0.1 Hz to mitigate the physiological contributions of respiratory and cardiovascular components.

The motion output from afni-proc.py was utilised to indicate which participant's scans could be used and which participants must be excluded from the study due to motion artifacts. The two codes used for assessing the motion of each participant during the scan are shown in Appendix A. A threshold was set, requiring a minimum of 132 usable volumes (75% of the original 176 timepoints) with a maximum motion of 3 mm or 3 degrees in any direction for a participant to be considered eligible for inclusion in the study. The majority of participants had 176 usable volumes, with the exception of one control and one SA with PT subject. Due to excessive motion, only 86 usable volumes were obtained for one healthy control (Figure 7). This specific participant was thus excluded from the study. In the case of the participant from the SA with PT group, increased motion was observed, and only 125 volumes were deemed usable. The motion code recommended establishing a new reference point at the 16th timepoint from the remaining 176 volumes (Figure 8).

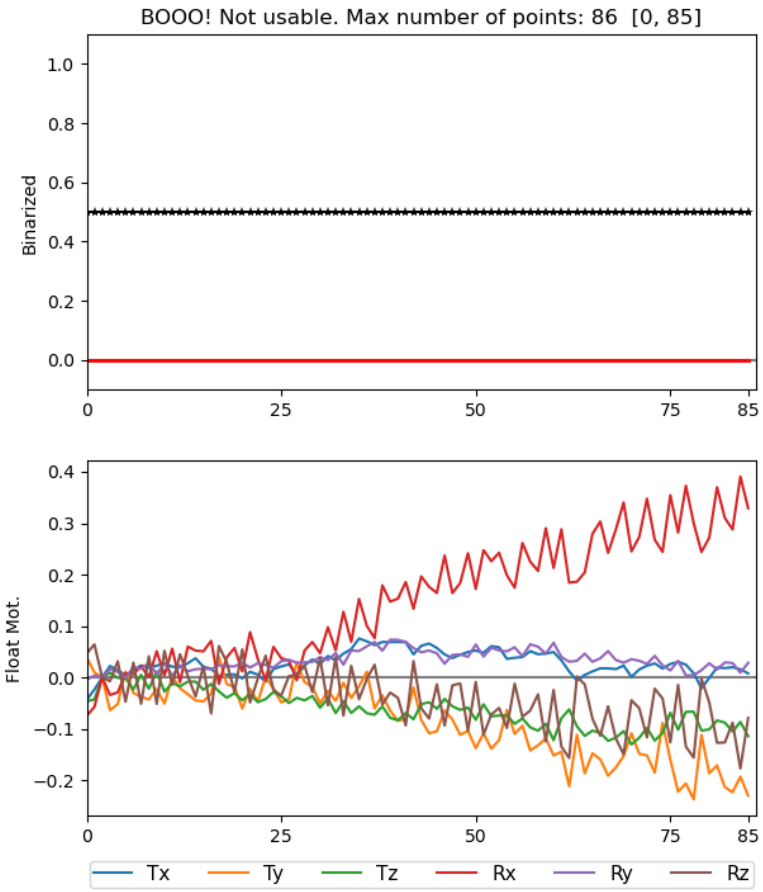

Figure 7: Motion characteristics of the excluded healthy control.

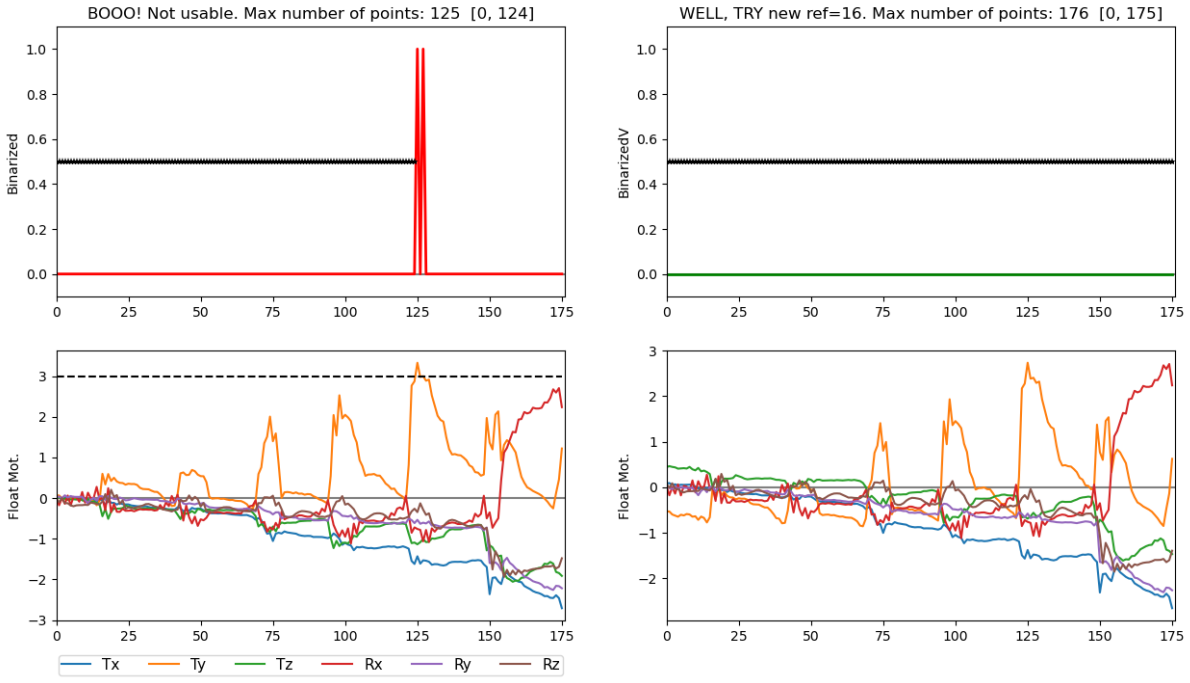

Figure 8: Motion characteristics of the participant in SA+PT group.

To maintain consistency in the number of volumes for all participants, 3dCalc in AFNI was employed. This involved trimming the first 16 volumes of the unprocessed NifTi rs-fMRI data of the above-mentioned SA+PT participant and to trim the last 16 volumes from the data of the remaining participants. Consequently, each participant was left with a total of 164 volumes. Following the volume trimming process, afni-proc.py was once again utilised for data preprocessing. By disregarding the initial four volumes, each participant was left with 160 volumes. The maximum motion displacement during each scan was recorded from the afni-proc.py review outcomes. These displacement values were subsequently used to control for confounders.

5.6.2. Independent Component Analysis (ICA)

MELODIC - FSL

The group ICA was performed using MELODIC in FSL (version 6.0) (Beckmann et al., 2005) to derive independent component (IC) maps of resting-state networks (RSNs) from the nine healthy controls. The ICA code is provided in Appendix B. AFNI's 3dMatch (Taylor & Saad, 2013) was utilised to align with a standard set of 20 RSNs that had been calculated as part of the Functional Connectome Project (FCP) (Biswal et al., 2010). This alignment allowed for obtaining the names of each RSN. Additionally, each network underwent manual verification to ensure consistency with the RSN output from 3dMatch. Following this manual check, eleven RSNs were identified.

Binary masks for the eleven RSNs were generated by applying a threshold to their group ICs at a Z-score > 3.0, employing Brain Extraction Tool (BET) (Smith, 2002), fslsplit (Jenkinson et al., 2012), and fslmaths (Jenkinson et al., 2012) in FSL.

Dual Regression

Dual regression in FSL (Nickerson et al., 2017) was used to derive 4D image files containing spatial Z-score maps of the participants for each group IC. Initially, the dual regression was executed on the after-treatment scans, followed by the before-treatment scans, then for the healthy controls, and finally, for the combined before- and after-treatment scans. The corresponding codes are provided in Appendix B. Outputs from the nine disqualified ICs were excluded from further analysis.

The 4D image files from dual regression were masked by their respective individual RSN binary mask through fslmaths. The fslmaths code is shown in Appendix B.

Voxelwise Analysis

Voxelwise analysis was performed using FSL's Randomise (Winkler et al., 2014) on the masked dual regression Z-score maps to identify clusters exhibiting significant between-group and within-group differences in RSFC.

A. Between group differences

Randomise F-test was employed to detect clusters showing significant differences in RSFC among the three different treatment arms (1) in the after-treatment scans and (2) in the before-treatment scans. A General Lineal Model (GLM) was configured in FSL. Within this GLM, each of the 23 treatment scans (either all after-treatment scans or before treatment) was allocated to its respective treatment groups (TA or TA+PT or SA+PT). The Randomise code is provided in Appendix B.

B. Within-group differences

Randomise T-tests were conducted between the before- and after-treatment scans within each treatment arm to identify significant differences in RSFC. In the GLM, each of the 46 scans was assigned to one of the three treatment arms (TA or TA+PT or SA+PT) and labelled as either before treatment (BT) or after treatment (AT). Six t-tests were then performed to find significant clusters where:

1) BT Z-scores were higher than AT for the TA group,
2) AT Z-scores were higher than BT for the TA group,
3) BT Z-scores were higher than AT for the TA and PT group,
4) AT Z-scores were higher than BT for the TA and PT group,
5) BT Z-scores were higher than AT for the SA and PT group,
6) AT Z-scores were higher than BT for the SA and PT group.

The randomise code used for this analysis is provided in Appendix B.

FSL Cluster

FSL's Cluster (Jenkinson et al., 2012) was used to provide details on the clusters identified as significant at $p < 0.01$, through the voxelwise analysis using randomise. The output included a table listing the cluster index, cluster size and x-, y- and z-coordinates of each cluster. The FSL-Cluster code is provided in Appendix B. AFNI's 3dClustSim with a "mixed ACF" (autocorrelation function) methodology introduced by Cox et al. (2017) was employed to determine the minimum cluster for significance at a voxelwise threshold of $p < 0.01$ and a cluster-level alpha of 0.05. A minimum threshold of 540 mm^3 was applied. A binary mask of

each significant cluster was created and applied to mask the dual regression outcome of each corresponding IC map where the significant cluster was located. A 4D Z-score file of each cluster within the respective network (IC map) was yielded.

5.7. Statistical Analysis

Extracting Z-score values

The Z-score was used to represents the RSFC within the voxel. Fslsplit was used to separate each cluster into the corresponding volumes for each participant. A MATLAB code provided in Appendix C was used to extract the mean Z-score in the cluster for each participant.

5.7.1. Between groups statistical analysis

One-way ANOVA was used to compare the mean Z-scores of each treatment group within each cluster. The F- and p-values were determined using IBM SPSS Statistics Version 28.0.1.1 (15).

5.7.2. Within-group statistical analysis

A repeated measures T-test was conducted to compare the mean Z-scores within groups between before- and after-treatment. The T- and p-values were determined using IBM SPSS Statistics. The 4D image files from dual regression were masked by their respective individual RSN binary masks obtained from the 9 healthy controls, a binary mask for each significant cluster identified through voxel-wise analysis was created. These binary masks were then applied to the dual regression outcomes of each corresponding IC map where the significant clusters were located.

5.7.3. FMA Correlation

Pearson correlation (Freedman, Pisani & Purves, 2007) was utilised to estimate the correlation between brain activity (Z-score) and physical outcomes (FMA scores). The r- and p- values were computed using IBM SPSS.

5.7.4. Confounders

IBM SPSS Statistics Version 28.0.1.1 (15) was used to perform Pearson correlations between Z-scores of each significant cluster and demographic variable, including sex, age, motion displacement during the MRI scan, total grey matter (GM) volume and stroke side (left or right).

Subsequently, an analysis of covariance (ANCOVA) was conducted in IBM SPSS to control for potential confounders and ascertain if the significance persisted.

Total GM Volumes were determined using the recon-all command in FreeSurfer (version 7.4.1) for each fMRI scan.

6. Results

Table 1 displays the sample characteristics and demographic background information of stroke patients and controls, such as age, sex, stroke side, GM volume, motion displacement, and FMA score. Using ANOVA, no significant differences were found among the three treatment groups for any of the characteristics.

Table 1: Sample Characteristics

Group		**TA**	**TA+PT**	**SA+PT**	**F(p)**
N		7	6	10	
Mean Age ± SD (years)		56.1±7.9	63.8±5.5	56.9±8.8	1.930(0.171)
Sex (Male/Female)		5/2	6/0	8/2	0.911(0.418)
Stroke Side (Right/Left)		4/3	1/5	7/3	2.349(0.121)
Motion displacement (mean ± SD) mm	BT	0.94±0.3	0.89±0.4	1.42±1.6	0.500(0.614)
	AT	1.43±0.8	0.97±0.5	1.02±0.7	0.801(0.463)
GM Volume (mean ± SD) $x10^5$ mm^3	BT	6.25±0.7	6.23±0.2	6.45±0.5	0.365(0.698)
	AT	6.32±0.7	6.18±0.2	6.46±0.5	0.511(0.608)
FMA Score (mean ± SD)	BT	18.57±3.7	19.17±4.3	18.40±4.4	0.056(0.946)
	AT	29.29±1.0	30.00±2.6	27.60±5.7	0.662(0.527)

No significant group differences were observed in the FMA scores among all three treatment groups. However, all groups demonstrated a significant increase in FMA scores from before to during and after their respective 3-weeks treatments.

Group ICA was performed on the control subjects. Eleven IC Maps were identified from the healthy control data. These IC maps were used to compare the RSFC of each treatment group across each of these RSNs.

When comparing scans acquired before treatment among the three treatment groups, the TA+PT group exhibited lower RSFC in two regions within two RSNs. No significant differences among the three groups were seen within these two regions after the 3-week treatment. Conversely, post-treatment, the TA+PT group demonstrated five regions within three RSNs with significantly higher RSFC compared to the other two groups, despite no significant differences in RSFC within these regions among the three treatment groups before treatment.

Furthermore, post-treatment, the TA+PT group showed increased RSFC in nine regions within four RSNs compared to pre-treatment RSFC withing these regions. The SA+PT group displayed lower RSFC in two regions within two RSNs after treatment compared to before treatment RSFC. The TA group did not show significant differences in RSFC before versus after treatment.

6.1. FMA examinations

All three treatment groups showed a significant increase in FMA Score after treatment compared to before treatment. Figure 9 indicates the distribution of FMA scores within each group both before and after treatment. There were no significant differences between groups either before or after treatment when comparing group means during a one-way ANOVA test. Figure 10 illustrates the mean group FMA scores before, after and during treatment.

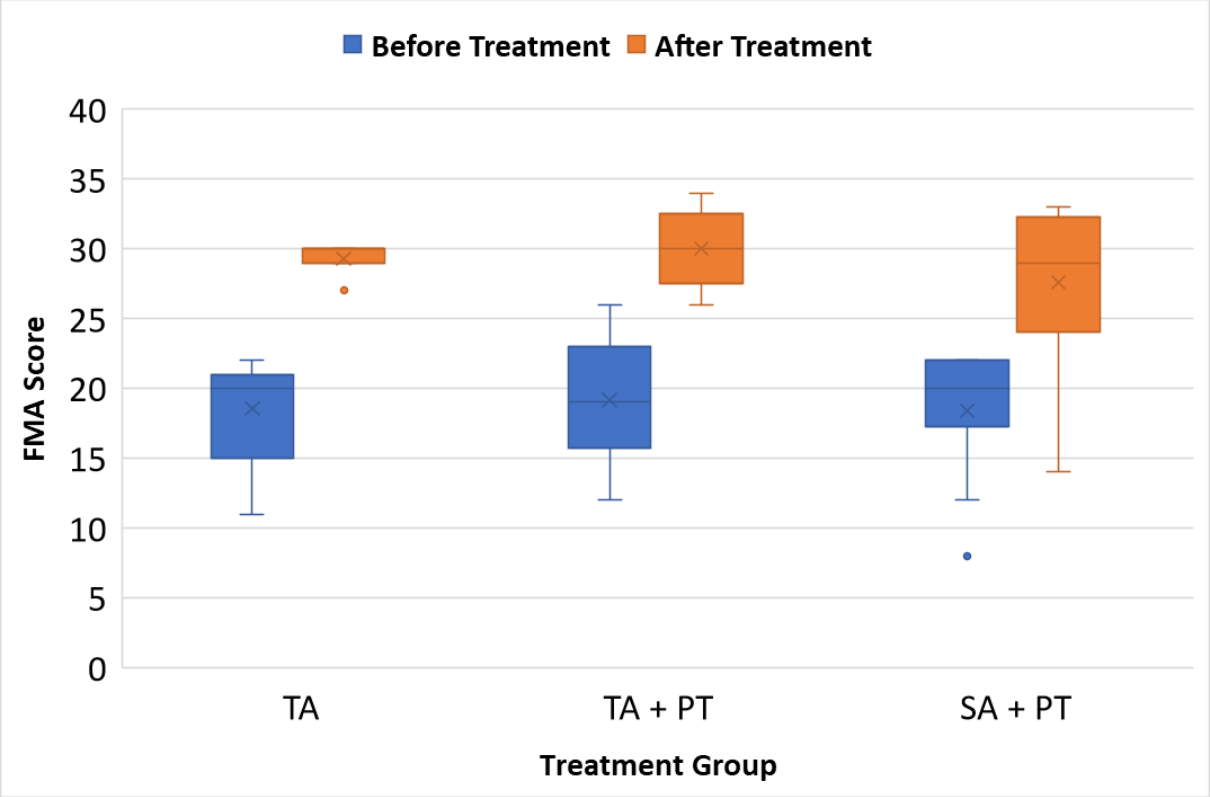

Figure 9: FMA Score distribution of each treatment group before and after treatment (no significant differences between groups).

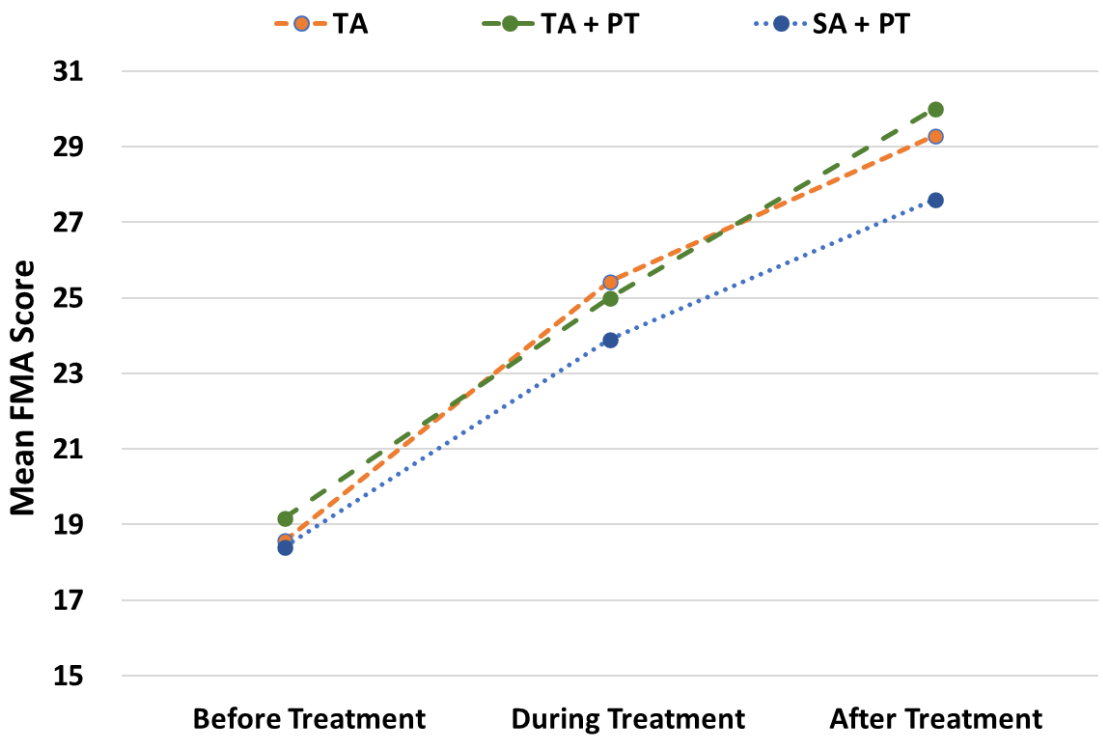

Figure 10: Treatment group average FMA scores before, during and after treatment (no significant differences between groups).

6.2. ICA Maps

Eleven IC Maps (Figure 11) obtained from healthy controls were employed to compare the RSFC of each treatment group across each of these RSNs. The posterior DMN (a) will further be referred to as DMN 1 and the anterior DMN (b) will further be referred to as DMN 2.

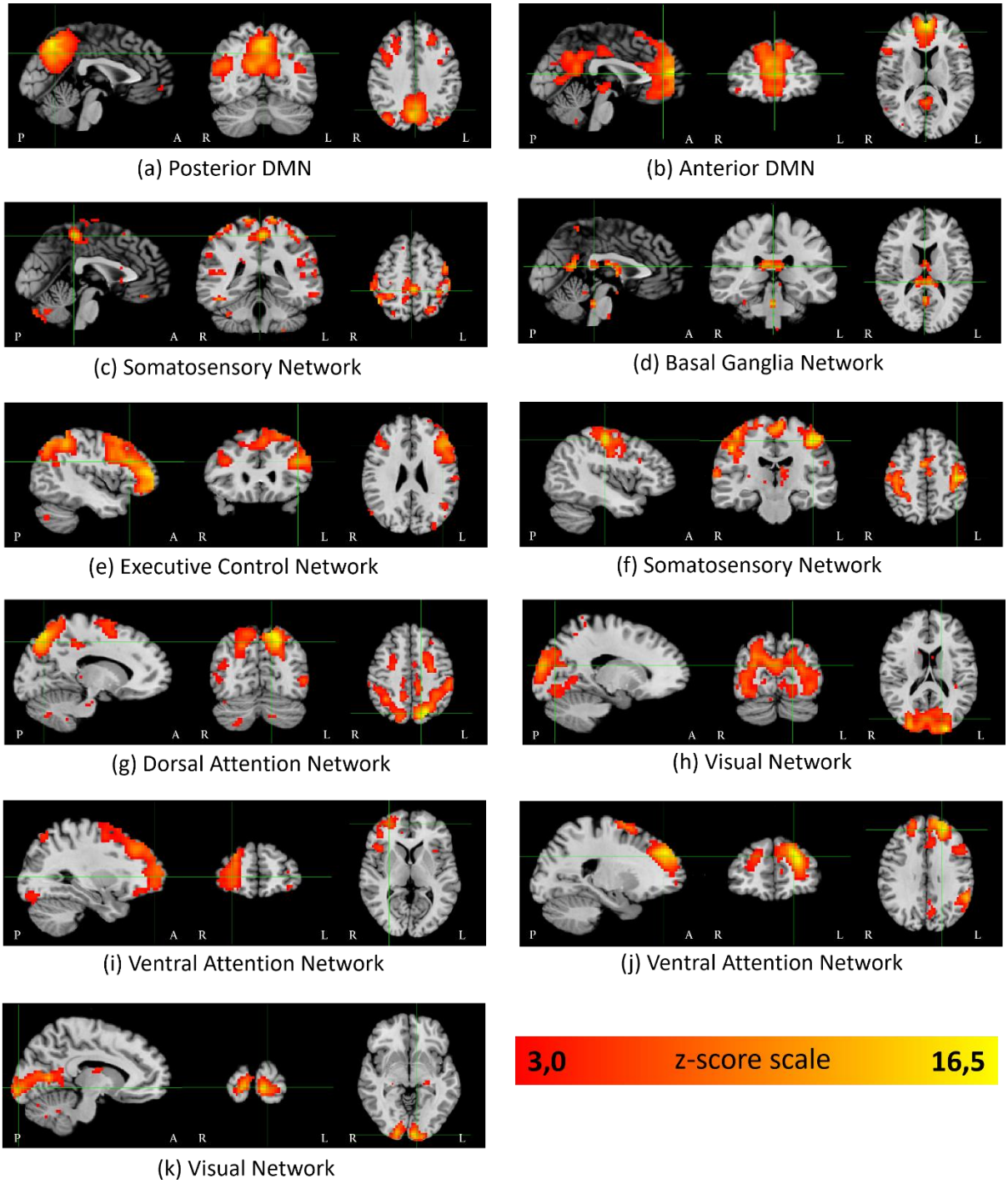

Figure 11: Resting-state networks obtained from healthy controls using MELODIC in FSL.

6.3. RSFC Differences Between Treatment Groups

Before treatment, patients in the TA+PT group demonstrated lower RSFC in two regions across two networks compared to patients in other groups. Conversely, after treatment, patients in the TA+PT group exhibited higher RSFC in five regions across three networks compared to patients in other groups.

6.3.1. Before Treatment

Compared to patients in other groups, patients in the TA+PT group before treatment illustated significantly lower RSFC in 2 distinct clusters in the precuneus within the default mode network (DMN) and the ventral attention network (Figure 12). The sizes and locations of the clusters, as well as mean Z-scores of each group are provided in Table 2. Both significant clusters overlap with each other (Figure 13).

No group difference in RSFC were observed in these clusters after treatment. Notably, patients in the TA+PT group exhibited higher RSFC in both clusters after treatment compared to their own Z-scores before treatment. The mean Z-score in the bilateral precuneus within the DMN demonstrated a weak association with the FMA.

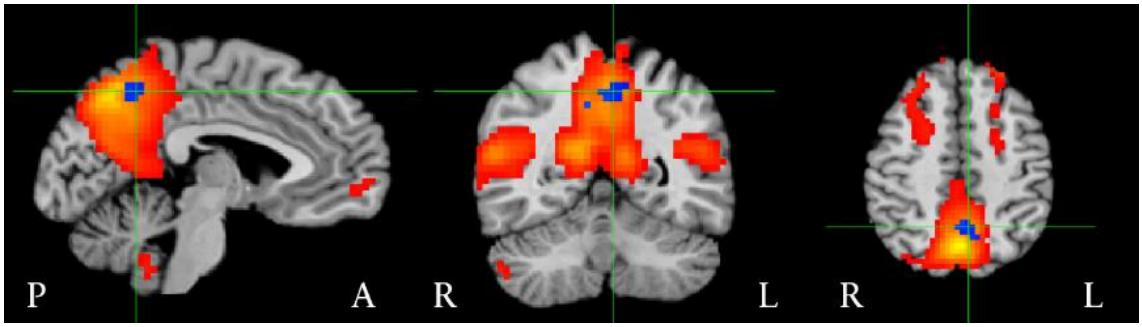

(a) Bilateral Precuneus

Default Mode Network 1

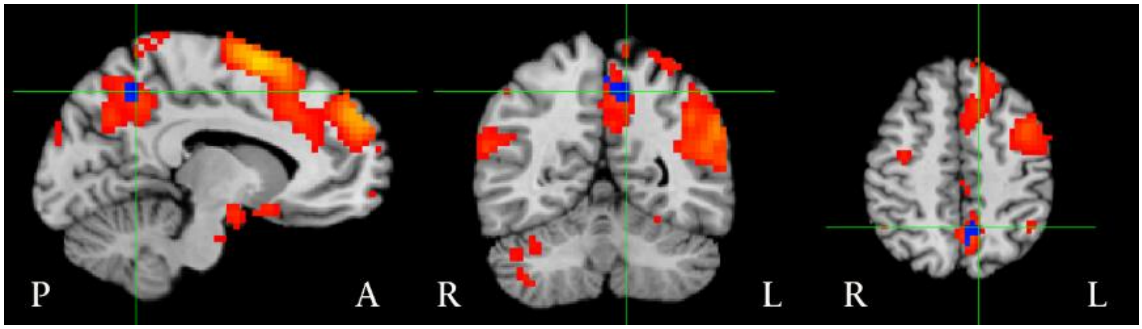

(b) L Precuneus

Ventral Attention Network

Figure 12: Each panel shows the group ICA map of a resting state network thresholded at z>3 (hot colours) and clusters where RSFC was significantly lower in patients who received TA+PT before treatment compared to others who received TA or PT+SA (in blue). Crosshairs indicate the peak coordinates.

ICA= independent component analysis. RSFC=resting state functional connectivity. TA+PT= True acupuncture and physiotherapy. TA=True acupuncture. PT+SA = Physiotherapy and sham acupuncture. L=left.

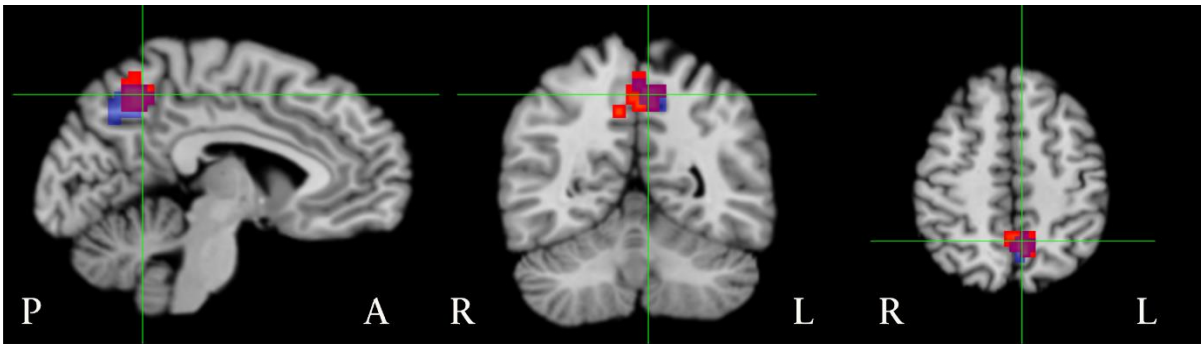

Figure 13: Panel showing the overlap of both significant precuneus clusters in the DMN (red) and the ventral attention network (blue).

Table 2: Cluster sizes and peak coordinates (in TT standard space) of regions where RSFC was lower in patients receiving TA+PT before treatment compared to others who received TA or PT+SA.

Network **Location** Peak coordinates (mm)	Cluster Size (mm^3)	Scan	Group averaged mean Z-scores within the cluster (SD) TA	 TA+PT	 SA+PT	F (p)	FMA Correlation r (p)
DMN 1							
Bilateral Precuneus	999	BT	0.82 (0.23)	0.39 (0.18)	1.15 (0.43)	10.157 (<.001)	0.29 (0.052)
-4.5, -52.5, 44.5		AT	1.02 (0.37)	1.20 (0.34)	0.95 (0.31)	1.102 (0.352)	
		t (p)	-1.313 (0.237)	-4.476 (0.007)	1.264 (0.238)		
Ventral Attention							
L Precuneus	972	BT	0.34 (0.17)	0.11 (0.05)	0.53 (0.20)	12.167 (<.001)	-0.07 (0.631)
-10.5, -52.5, 44.5		AT	0.31 (0.19)	0.42 (0.21)	0.32 (0.19)	0.629 (0.544)	
		t (p)	0.367 (0.726)	-3.244 (0.023)	2.726 (0.023)		

DMN – Default mode network, SD – Standard Deviation, BT – Before Treatment, AT – After treatment, TA – True Acupuncture, TA+PT – TA and Physiotherapy, SA+PT – Sham Acupuncture and PT, FMA – Fugl-Meyer Assessment. L=left.

6.3.2. After Treatment

Compared to patients in other groups, patients in the TA+PT group after treatment illustrated significantly higher RSFC in five regions within three networks (Figure 14), including the right (R) cingulate gyrus and R precuneus in the DMN, the left (L) orbitofrontal cortex in the executive control network, and the R inferior occipital lobe and R superolateral occipital lobe in the visual network. The sizes and locations of these significant clusters, as well as the mean Z-scores of each treatment group are indicated in Table 3. No group differences in RSFC were observed in these clusters before treatment. Notably, patients in the TA+PT group also demonstrated higher RSFC in these clusters after treatment compared to their own Z-scores before treatment. However, the mean Z-scores in these regions were not associated with FMA scores.

.

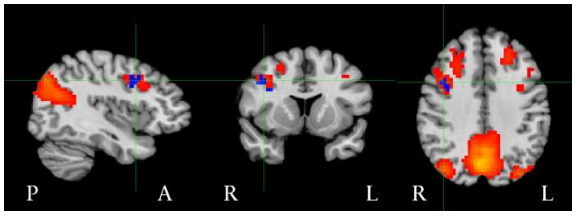

(a) R Cingulate Gyrus

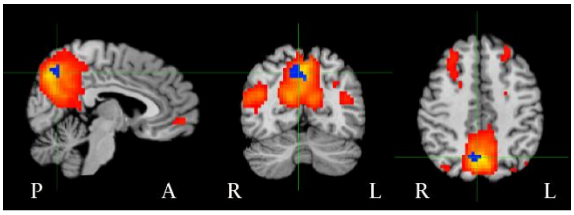

(b) R Precuneus

Default Mode Network 1

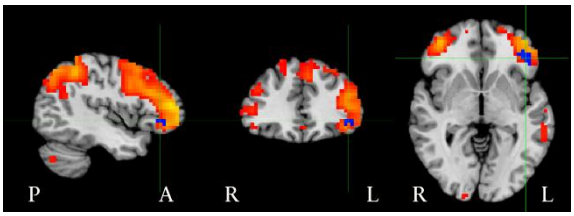

(c) L Orbitofrontal Cortex

Executive Control Network

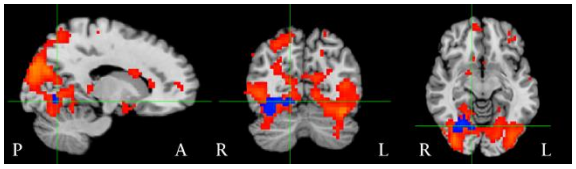

(d) R Inferior Occipital Lobe

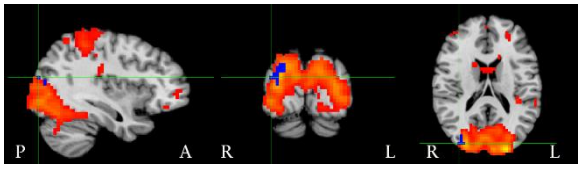

(e) R Superolateral Occipital Lobe

Visual Network

Figure 14: Each panel shows the group ICA map of a resting state network thresholded at z>3 (hot colours) and clusters where RSFC was higher after treatment in patients who received TA+PT compared to others who received TA or PT+SA (in blue). Crosshairs indicate the peak coordinates.

ICA= independent component analysis. RSFC=resting state functional connectivity. TA+PT= True acupuncture and physiotherapy. TA=True acupuncture. PT+SA = Physiotherapy and sham acupuncture. R=right. L=left.

Table 3: Cluster sizes and peak coordinates (in TT standard space) of regions where RSFC was higher after treatment in patients who received TA+PT compared to others who received TA or PT+SA.

Network **Location** Peak coordinates (mm)	Cluster Size (mm^3)	Scan	Group average mean Z-scores within the cluster (SD) TA	TA+PT	SA+PT	F (p)	FMA Correlation r (p)
DMN 1							
R Cingulate Gyrus 37.5, 7.5, 38.5	756	AT	0.22 (0.23)	0.70 (0.40)	0.13 (0.20)	8.90 (0.002)	0.234 (0.118)
		BT	0.20 (0.25)	0.10 (0.10)	0.15 (0.25)	0.296 (0.747)	
		t (p)	-0.229 (0.826)	-3.749 (0.013)	0.191 (0.853)		
R Precuneus 4.5, -61.5, 41.5	594	AT	0.79 (0.20)	1.57 (0.46)	0.83 (0.20)	15.37 (<.001)	0.040 (0.790)
		BT	1.03 (0.45)	0.75 (0.26)	1.06 (0.35)	1.535 (0.240)	
		t (p)	1.236 (0.263)	-3.639 (0.015)	1.736 (0.117)		
Executive Control							
L Orbitofrontal Cortex -40.5, 31.5, -3.5	702	AT	0.06 (0.37)	0.87 (0.19)	0.29 (0.19)	16.76 (<.001)	0.022 (0.887)
		BT	0.50 (0.35)	0.42 (0.25)	0.43 (0.32)	0.134 (0.875)	
		t (p)	1.778 (0.126)	-2.776 (0.039)	1.489 (0.171)		
Visual							
R Inferior Occipital Lobe 13.5, -64.5, -6.5	3240	AT	0.624 (0.21)	0.991 (0.52)	0.266 (0.14)	10.953 (<.001)	0.111 (0.462)
		BT	0.616 (0.39)	0.322 (0.19)	0.534 (0.37)	1.253 (0.307)	
		t (p)	-0.069 (0.947)	-2.707 (0.042)	1.969 (0.080)		
R Superolateral Occipital Lobe 34.5, -82.5, 17.5	1026	AT	0.516 (0.21)	1.547 (0.83)	0.563 (0.20)	10.979 (<.001)	0.200 (0.183)
		BT	0.492 (0.35)	0.431 (0.27)	0.790 (0.53)	1.705 (0.207)	
		t (p)	-0.262 (0.802)	-3.651 (0.015)	1.109 (0.296)		

DMN – Default mode network, SD – Standard Deviation, BT – Before Treatment, AT – After treatment, TA – True Acupuncture, TA+PT – TA and Physiotherapy, SA+PT – Sham Acupuncture and PT, FMA – Fugl-Meyer Assessment, L – Left, R – Right

6.4. RSFC Differences Within Treatment Groups

The TA group showed no significant differences in RSFC when comparing scans before and after treatment. The TA+PT group displayed higher RSFC in nine regions within four networks after treatment compared to before treatment. The SA+PT group exhibited lower RSFC in two regions within two networks after treatment compared to before treatment.

6.4.1. True Acupuncture and Physiotherapy Group

Patients in the TA+PT group demonstrated higher RSFC after treatment in nine regions within four networks compared to their own Z-scores before treatment (Figure 15), including the bilateral precuneus, R anterior calcarine sulcus, R primary motor cortex, and L angular gyrus in the first DMN, the bilateral precuneus in the second DMN, the R visual cortex, R posterior lingual gyrus and L visual cortex in the visual network, and the R posterior cingulate sulcus in the ventral attention network. The sizes and locations of these significant clusters, the mean Z-scores, as well as FMA correlations are shown in Table 4. Notably, the mean Z-scores were significantly associated with the FMA scores in the bilateral precuneus and the L angular gyrus within the first DMN, in the R visual cortex in the visual network, and in the R posterior cingulate sulcus in the ventral attention network. However, the mean Z-scores in the R anterior calcarine sulcus and R primary motor cortex in the first DMN, the bilateral precuneus in the second DMN, and the R posterior lingual gyrus and L visual cortex in the visual network demonstrated a weak correlation with the FMA.

The significant cluster found in the bilateral precuneus in the first DMN, overlaps with both significant clusters found in the precuneus showing before treatment group differences, as well as the precuneus cluster showing group differences after treatment. The significant precuneus cluster found in the second DMN does not overlap with the other four mentioned (Figure 16).

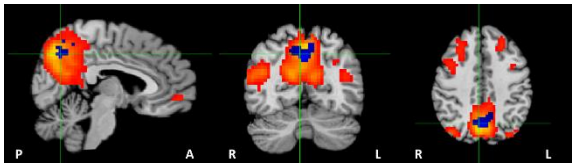

(a) Bilateral Precuneus

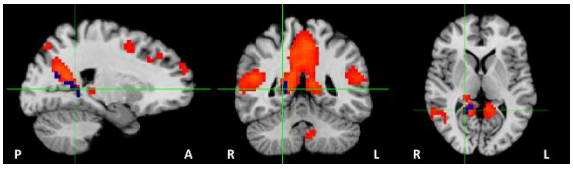

(b) R Anterior Calcarine Sulcus

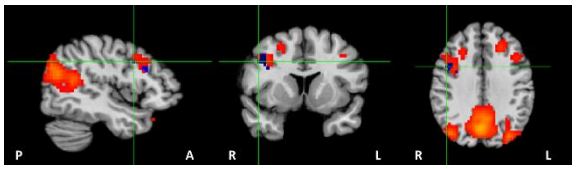

(c) R Primary Motor Cortex

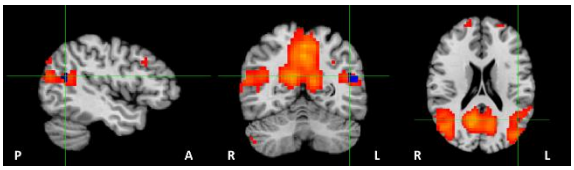

(d) L Angular Gyrus

Default Mode Network 1

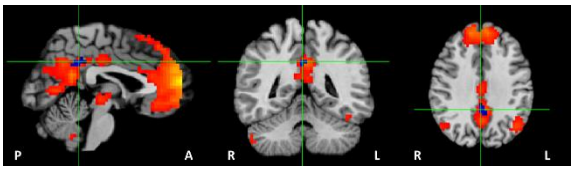

(e) Bilateral Precuneus

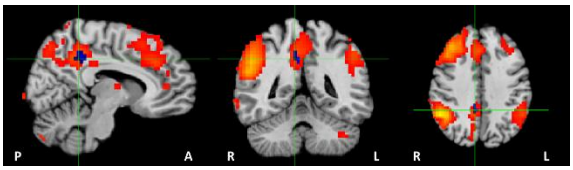

(f) R Posterior Cingulate Sulcus

Default Mode Network 2

Ventral Attention

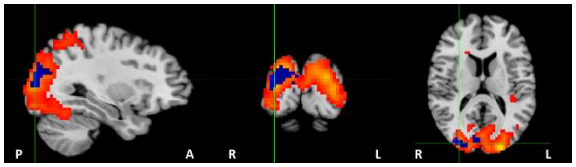

(g) R Visual Cortex

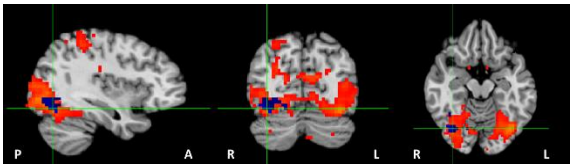

(h) R Posterior Lingual Gyrus

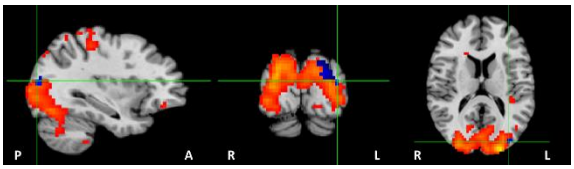

(i) L Visual Cortex

Visual Network

Figure 15: Each panel shows the group ICA map of a resting state network thresholded at z>3 (hot colours) and clusters where RSFC was higher after treatment vs before treatment in patients who received TA+PT (in blue). Crosshairs indicate the peak coordinates.

ICA= independent component analysis. RSFC=resting state functional connectivity. TA+PT= True acupuncture and physiotherapy. R=right. L=left.

Table 4: Mean Z-scores within clusters where the TA+PT treatment group had higher RSFC after treatment than before treatment.

Network **Location** Peak coordinates (mm)	Cluster Size (mm^3)		Group averaged (SD) mean Z-scores within the cluster	t (p)	FMA Correlation r(p)
DMN 1					
Bilateral Precuneus	3753	BT	0.54(0.21)	-4.561(0.006)	0.766(0.004)
4.5, -61.5, 38.5		AT	1.33(0.30)		
R Anterior Calcarine Sulcus	1782	BT	0.35(0.27)	-4.665(0.006)	0.543(0.074)
19.5, -46.5, 2.5		AT	1.26(0.52)		
R Primary Motor Cortex	1485	BT	0.03(0.07)	-3.438(0.018)	0.434(0.159)
43.5, 7.5, 32.5		AT	0.72(0.54)		
L Angular Gyrus	675	BT	0.10(0.19)	-4.899(0.004)	0.753(0.005)
-40.5, -55.5, 20.5		AT	0.73(0.39)		
DMN 2					
Bilateral Precuneus	621	BT	0.20(0.26)	-2.647(0.024)	0.448(0.144)
1.5, -43.5, 32.5		AT	0.86(0.55)		
Visual					
R Visual Cortex	3915	BT	0.37(0.18)	-3.972(0.011)	0.648(0.023)
28.5, -85.5, 14.5		AT	1.48(0.73)		
R Posterior Lingual Gyrus	3213	BT	0.18(0.20)	-2.630(0.025)	0.517(0.085)
34.5, -67.5, -12.5		AT	1.15(0.88)		
L Visual Cortex	1161	BT	0.36(0.24)	-2.739(0.041)	0.500(0.098)
-31.5, -82.5, 14.5		AT	1.38(0.98)		
Ventral Attention					
R Posterior Cingulate Sulcus	675	BT	0.13(0.22)	-3.375(0.020)	0.630(0.028)
7.5, -43.5, 35.5		AT	0.64(0.30)		

L – Left, R – Right, DMN – Default mode network, SD – Standard Deviation, BT – Before Treatment, AT – After treatment, TA+PT – True Acupuncture and Physiotherapy, FMA – Fugl-Meyer Assessment

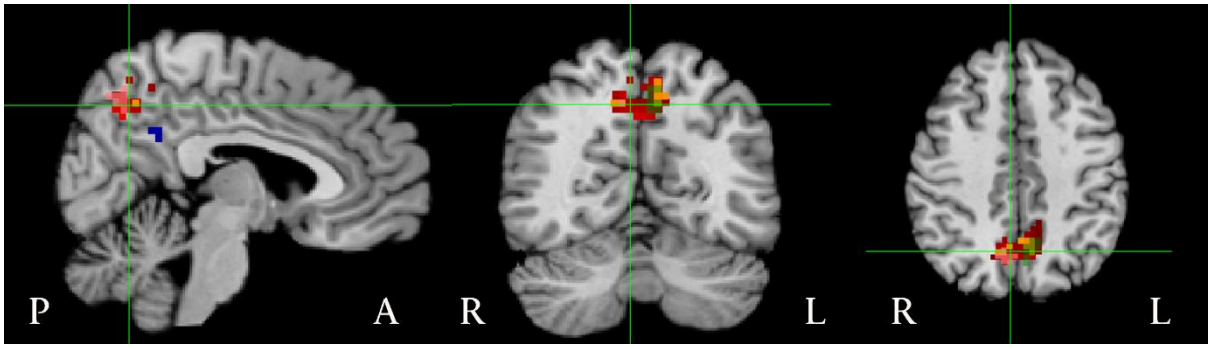

Figure 16: Overlapping of precuneus clusters. Before treatment group differences: bilateral precuneus in the first DMN (yellow) and L precuneus in the ventral attention network (green). After treatment group differences: R precuneus in first DMN (pink). Within TA+PT group differences: bilateral precuneus in first DMN (red) and bilateral precuneus in second DMN (blue).

TA+PT= True acupuncture and physiotherapy. R=right. L=left.

6.4.2. Sham Acupuncture and Physiotherapy Group

Patients in the SA+PT group demonstrated lower RSFC after treatment in two regions within two networks compared to their own Z-scores before treatment (Figure 17) including the R postcentral gyrus in the somatosensory network and the L lingual gyrus in the visual network. The sizes and locations of these significant clusters, the mean Z-scores, as well as FMA correlations are shown in Table 5. The mean Z-scores in both regions were negatively correlated with the FMA.

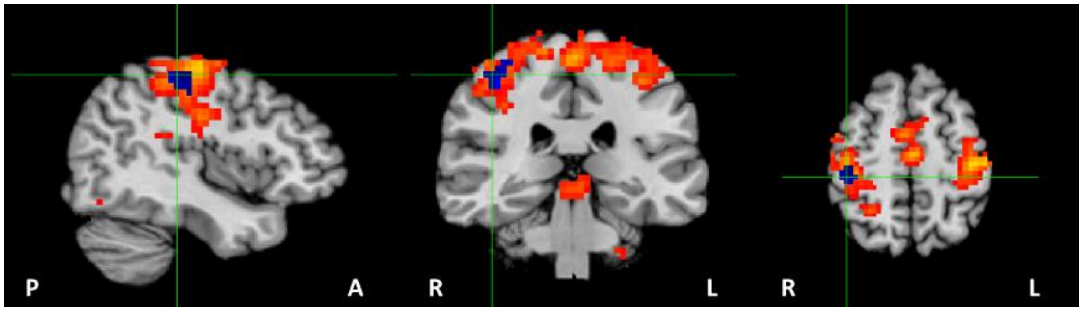

(a) R Postcentral Gyrus

Somatosensory Network

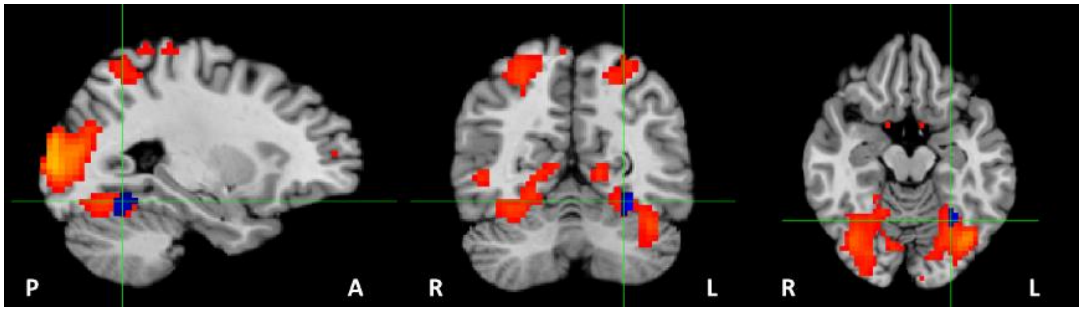

(b) L Lingual Gyrus

Visual Network

Figure 17: Each panel shows the group ICA map of a resting state network thresholded at z>3 (hot colours) and clusters where RSFC was lower after treatment vs before treatment in patients who received PT+SA. Crosshairs indicate the peak coordinates.

ICA= independent component analysis. RSFC=resting state functional connectivity. PT+SA = Physiotherapy and sham acupuncture. R=right. L=left.

Table 5: Mean Z-scores within clusters where the SA+PT treatment group had lower RSFC after treatment than before treatment.

Network **Location** Peak coordinates (mm)	Cluster Size (mm^3)		Group averaged (SD) mean Z-scores within the cluster	t (p)	FMA Correlation r(p)
Somatosensory					
R Postcentral Gyrus	1161	BT	0.98(0.44)	3.632(0.006)	-0.563(0.010)
40.5, -28.5, 50.5		AT	0.40(0.31)		
Visual					
L Lingual Gyrus	594	BT	1.02(0.86)	3.582(0.006)	-0.480(0.032)
-25.5, -55.5, -12.5		AT	-0.02(0.55)		

L – Left, R – Right, SD – Standard Deviation, BT – Before Treatment, AT – After treatment, SA+PT – Sham Acupuncture and Physiotherapy, FMA – Fugl-Meyer Assessment

6.5. Controlling for Confounders

Control variables were concerned, including sex, age, motion displacement during the MRI scan, total GM volume, and stroke side (left or right). Associations with a significance level of $P < 0.1$ were regarded as potential confounders and were subsequently included in the ANCOVA. Significant correlations are denoted by the respective superscripts.

Table 6, Table 8,

Table 10, and Table 12 indicate the Pearson correlations between the confounders and the mean RSFC in the clusters identified by the voxelwise analysis. Following control for the potential variables, the significance of these differences persisted (

Table 7, Table 9, Table 11, and Table 13).

6.5.1. Between Treatment Groups

Before Treatment:

Table 6: Correlation of each of the five control variables with the mean Z-scores in the clusters showing before treatment group differences.

Network Region	RSFC Parameters				
	Sex	Age	Motion displacement	Total GM volume	Stroke Side
DMN Bilateral Precuneus	-0.065	-0.394†	0.676***	0.224	-0.215
Ventral Attention Left Precuneus	0.089	-0.382†	0.340	0.250	-0.208

Values are Pearson r's; †P<0.10, *P<0.05, **P<0.01, ***P<0.001.

Table 7: Significance of different treatment groups to clusters in regions showing before treatment group differences while controlling for potential confounders.

Network Region	Potential confounders	Adjusted Group Significance F
DMN Bilateral Precuneus	Age, Motion displacement	13.505***
Ventral Attention Left Precuneus	Age	9.417**

Values are F with significance; †P<0.10, *P<0.05, **P<0.01, ***P<0.001.

After Treatment:

Table 8: Correlation of each of the five control variables with the mean Z-scores in the clusters showing after treatment group differences.

Network Region	RSFC Parameters				
	Sex	Age	Motion displacement	Total GM volume	Stroke Side
DMN					
Medial Cingulate Gyrus	0.352	0.122	-0.069	0.111	0.338
Precuneus	0.141	0.321	-0.273	-0.169	0.382†
Executive Control					
Orbitofrontal Cortex	0.205	0.260	-0.244	-0.067	0.219
Visual					
Inferior Occipital Lobe	0.251	0.074	0.164	-0.108	0.273
Superolateral Occipital Lobe	0.296	0.123	0.006	-0.123	0.141

Values are Pearson r's; †P<0.10, *P<0.05, **P<0.01, ***P<0.001.

Table 9: Significance of different treatment groups to clusters in regions showing after treatment group differences while controlling for potential confounders.

Network Region	Potential confounders	Adjusted Group Significance
		F
DMN		
Medial Cingulate Gyrus	None	8.897**
Precuneus	Stroke Side	11.290***
Executive Control		
Orbitofrontal Cortex	None	16.763***
Visual		
Inferior Occipital Lobe	None	10.953***
Superolateral Occipital Lobe	None	10.979***

Values are F with significance; †P<0.10, *P<0.05, **P<0.01, ***P<0.001.

6.5.2. Within-group differences

TA and PT Group:

All participants in the TA+PT group were male and hence no correlation can be calculated between sex and RSFC.

Table 10: Correlation of each of the five control variables with the mean Z-scores in the clusters showing higher RSFC after treatment than before treatment in the TA+PT group.

	RSFC Parameters				
Network Region	Sex	Age	Motion displacement	Total GM volume	Stroke Side
DMN 1					
Bilateral Precuneus	-	-0.261	0.142	0.074	-0.196
Calcarine Sulcus	-	-0.042	0.272	0.003	0.004
Primary Motor Cortex	-	0.283	0.401	-0.101	0.206
Angular Gyrus	-	-0.320	-0.006	0.001	-0.253
DMN 2					
Precuneus	-	-0.182	0.001	-0.005	0.022
Visual					
R Visual Cortex	-	-0.162	0.112	-0.210	-0.305
R Lingual Gyrus	-	-0.085	0.160	-0.160	-0.143
L Visual Cortex	-	-0.187	0.053	-0.175	-0.258
Ventral Attention					
R Cingulate Sulcus	-	-0.016	0.063	-0.081	-0.090

Values are Pearson r's; †P<0.10, *P<0.05, **P<0.01, ***P<0.001.

Table 11: Significance of different treatment scans to clusters in regions showing higher RSFC after treatment than before treatment in the TA+PT group while controlling for potential confounders.

		Treatment Scan Significance
Network Region	Potential confounders	F
P DMN		
Bilateral Precuneus	None	27.652***
Calcarine Sulcus	None	14.634**
Primary Motor Cortex	None	9.834*
Angular Gyrus	None	12.644**
A DMN		
Precuneus	None	7.007*
Visual		
R Visual Cortex	None	13.326**
R Lingual Gyrus	None	6.916*
L Visual Cortex	None	6.153*
Ventral Attention		
R Cingulate Sulcus	None	11.130**

Values are F with significance; †P<0.10, *P<0.05, **P<0.01, ***P<0.001.

SA and PT Group:

Table 12: Correlation of each of the five control variables with the mean Z-scores in the clusters showing higher RSFC before treatment than after treatment in the SA+PT group.

Network Region	RSFC Parameters				
	Sex	Age	Motion displacement	Total GM volume	Stroke Side
Somatosensory					
R Postcentral Gyrus	0.087	0.158	0.106	0.028	0.293
Visual					
Lingual Gyrus	0.356	-0.114	0.495*	0.128	0.379†

Values are Pearson r's; †P<0.10, *P<0.05, **P<0.01, ***P<0.001.

Table 13: Significance of different treatment scans to clusters in regions showing higher RSFC before treatment than after treatment in the SA+PT group while controlling for potential confounders.

Network Region	Potential confounders	Treatment Scan Significance
		F
Somatosensory		
R Postcentral Gyrus	None	11.453**
Visual		
Lingual Gyrus	Motion displacement, Stroke Side	11.915**

Values are F with significance; †P<0.10, *P<0.05, **P<0.01, ***P<0.001.

7. Discussion

This study aimed to examine the potential benefits and neural correlates in ischaemic stroke patients with unilateral limb dysfunction following three treatment arms: (1) TA, (2) TA with PT, and (3) SA with PT, during a 3-week stroke rehabilitation programme. The improvement of physical outcomes in stroke patients were evaluated using FMA. Using rs-fMRI, the effects of various treatment groups on RSFC were examined within multiple RSNs. Eleven ICs were estimated using group ICA on healthy controls and subsequently applied to the dual regression and voxelwise analyses of the stroke patients. The RSFC was assessed through Z-scores obtained from dual regression. In dual regression, two regression steps were performed to derive Z-score maps of each participant in each RSN (Beckmann & Smith, 2004). During the first step, spatial regression was performed, where predefined spatial maps representing different RSNs were used (Filippini et al., 2009). Each patient's fMRI data was regressed onto these spatial maps to obtain subject-specific time courses for each network (Beckmann & Smith, 2004). During the second regression step of dual regression, known as temporal regression, the subject-specific time courses obtained in the first step were regressed onto the original fMRI data (Beckmann & Smith, 2004; Beckmann et al., 2005). This process created subject-specific spatial maps for each network.

After the second regression step, Z-scores were calculated from the subject-specific spatial maps obtained. These Z-scores represent the number of standard deviations by which the intensity of the voxel deviates from the mean intensity across all voxels in the brain (Beckmann & Smith, 2004; Beckmann et al., 2005). Therefore, Z-scores measure the strength or amplitude of the network activity at each voxel, allowing for comparisons across subjects and studies (Smith et al., 2009).

Higher positive Z-scores in a particular region suggest increased functional connectivity or activity in that region associated with the specific network (Filippini et al., 2009; Smith et al., 2009). Conversely, lower negative Z-scores may indicate decreased connectivity or activity (Smith et al., 2009). In this study, Z-scores were used to assess the RSFC of various RSNs in each patient and treatment group.

Following the control of potential confounding variables, including sex, age, motion displacement during the MRI scan, total GM volume, and stroke side (left or right), the significance of all RSFC results persisted.

7.1. FMA Results

The FMA is a widely utilised clinical tool for the comprehensive evaluation of motor function in individuals grappling with neurological impairments, particularly after experiencing a stroke. Addressing motor impairments encompassing both upper and lower extremities, as well as balance, coordination, and sensation. The FMA offers a multifaceted examination of motor capabilities (Fugl-Meyer et al., 1975).

The interpretation of FMA scores rely on understanding its subscales and the total score, ranging from 0 (indicating complete impairment) to 100 (reflecting normal function) (Fugl-Meyer et al., 1975; Wolf et al., 2001). Essentially, a higher total FMA score indicates superior motor function, with scores nearing 100 indicating minimal impairment, while lower scores suggest more pronounced motor deficits (Wolf et al., 2001).

The FMA further dissects motor function into distinct subscales, namely Upper Extremity (UE) Motor Function, Lower Extremity (LE) Motor Function, Balance, and Sensation (Fugl-Meyer et al., 1975). This subdivision facilitates a nuanced assessment, enabling clinicians and researchers to pinpoint specific areas of motor impairment (Duncan, Propst & Nelson, 1983).

Within the clinical context, the total FMA score serves as a crucial metric, offering insights into the overall motor functionality of an individual. Notably, an increase in FMA scores over time may signify positive responses to rehabilitation interventions or natural recovery processes (Duncan, Propst & Nelson, 1983). Conversely, stagnant, or worsening scores may prompt a re-evaluation of the treatment plan, suggesting the necessity for modifications or additional assessments (Duncan, Propst & Nelson, 1983; Wolf et al., 2001). Understanding FMA scores are thus crucial in shaping how we guide rehabilitation and make decisions for people recovering from neurological issues, especially after a stroke.

In this study, significant improvements in FMA scores were seen across all three treatment groups, indicating positive responses to their respective interventions. The observed increase in FMA scores from pre-treatment to post-treatment highlights at least some level of effectiveness of the rehabilitation strategies employed within each group.

Although no statistically significant differences in FMA scores were identified between the treatment groups, the overall upward trend in FMA scores suggests that each approach made a meaningful contribution to motor function recovery. This aligns with finding from numerous studies advocating for the use of either acupuncture or physiotherapy as a post-stroke rehabilitation treatment (Rhoda, 2014; Rahayu et al., 2020; Mayo et al., 2002; Darekar et al., 2015; Zhu et al., 2021; Chen et al., 2020; Chavez et al., 2017).

In this study, only the group receiving TA with PT treatment showed a significant correlation between RSFC and FMA scores. No significant correlations were found between RSFC and

FMA scores in the other two treatment groups. This may be related to several factors. One potential consideration is the heterogeneity of lesion location and size across participants, which may influence the neural reorganisation patterns (Grefkes & Fink, 2011; Ward & Cohen, 2004). The second factor pertains the small sample size of the study, which leads to a statistical power issue. Larger samples typically improve the ability to detect meaningful correlations. Unfortunately, due to prolonged COVID-19 lockdown procedures in China, it was not feasible to recruited additional participants or transport them for scanning, resulting in a limited sample size of the study.

7.2. RSFC Differences Between Treatment Groups

7.2.1. Before Treatment

Differences in RSFC between groups before treatment were found in two regions within two networks. Specifically, these regions were the precuneus in the default mode network (DMN) and the precuneus in the Ventral Attention Network. The TA+PT group showed significantly lower RSFC before treatment. However, after treatment, there were no significant differences in Z-scores in these two regions, between the three treatment groups. This suggests that the TA+PT might have exerted a positive treatment effect on the RSFC in the precuneus within these two networks.

Lower RSFC in the precuneus within both the DMN and ventral attention network cloud imply a disturbance in the intrinsic functionality of these networks following a stroke. Given the pivotal role of precuneus as a key node in the DMN, such alterations in connectivity might signify shifts in self-referential processing or mind-wandering tendencies (Tuladhar et al., 2013).

The precuneus also plays a crucial role in numerous cognitive functions, such as episodic memory retrieval, self-processing operations, and spatial cognition (Cavanna & Trimble, 2006). Reduced RSFC in this region post-stroke could potentially be associated with impairments in these cognitive domains due to stroke (Rehme & Grefkes, 2013).

Following a stroke, the brain typically undergoes a process of neural reorganisation, where surviving regions may adopt new functional roles to compensate for damaged areas (Rehme & Grefkes, 2013). The lower RSFC observed in the precuneus could also reflect such reorganization, with alternative networks assuming tasks traditionally associated with the DMN (Buckner, Andrews-Hanna & Schacter, 2008).

7.2.2. After Treatment

Differences in RSFC between groups after treatment were found in five regions within three networks. These regions include the cingulate gyrus and the precuneus within the DMN, the orbitofrontal cortex within the executive control network, and the inferior and superolateral occipital lobe within the visual network. Remarkably, in all five of these regions, patients in the TA+PT group exhibited significantly higher RSFCs after treatment compared to individuals in the other groups. There were no significant differences in RSFC among treatment groups in these five regions before treatment, indicating that the observed differences in RSFC after treatment may be treatment-related.

The increased RSFC observed in the medial cingulate gyrus within the DMN following stroke treatment, suggests that TA with PT may have induced positive changes in neural integration and cognitive-emotional processing (Corbetta et al., 2015). The heightened connectivity in this region, implicated in cognitive control and emotional regulation (Vogt, 2005), points towards a potential improvement in these domains post-treatment. This observation alings with fMRI studies that have demonstrated acupuncture's ability to activate regions within the anti-correlated task-positive network, such as the anterior cingulate (Hui et al., 2009; Chae et al., 2013).

The disscussion regarding the increase in RSFC in the precuneus will be discussed in the next section, "RSFC Differences Within Treatment Groups", as this region forms part of the significant findings observed specificlly within the TA+PT group.

The observed increased RSFC in the orbitofrontal cortex within the executive control network following stroke treatment signifies that TA+PT may lead to a positive trajectory for cognitive recovery and emotional well-being (Rolls, 2019). The orbitofrontal cortex, a vital component of the executive control network, plays a crucial role in executive functions, decision-making, and emotional regulation (Rolls, 2019; Rolls, 2004).

The observed increase in RSFC post-treatment thus suggests that the combination of TA with PT may lead to potential improvements in higher-order executive functions, such as decision-making processes, and emotional regulation, contributing to an overall enhancement in psychological well-being (Rolls, 2004). Moreover, this increased connectivity may indicate improved integration of cognitive processes within the executive control network, fostering more efficient executive control functions (Petrides, 2005). These findings reflect the positive impact that TA with PT could potentially have on both cognitive and emotional aspects of recovery.

Greater FC increases in the executive control network could also contribute to improved attention and working memory (Blanke & Arzy, 2005). Previous studies have demonstrated

that TA can improve alertness and attention of stroke survivors (Liu et al., 2020; Liu et al., 2013).

Additionally, Increased RSFC in both the inferior and superolateral occipital lobes within the visual network following stroke treatment signifies the positive effect of TA with PT on visual processing, perception, and integration (Grill-Spector, Kourtzi & Kanwisher, 2001). These regions, integral to visual processing, play crucial roles in object recognition and spatial perception. The observed increase in RSFC post-stroke treatment suggests improved communication and coordination within the visual system, indicating potential enhancements in visual processing and perceptual functions (Grill-Spector, Kourtzi & Kanwisher, 2001; Biswal et al., 1995). Moreover, the heightened RSFC may denote improved integration of visual information across different processing regions, contributing to a more efficient and cohesive visual network function (Biswal et al., 1995). These findings reflect the positive changes that TA with PT may have on both visual processing and the integration of visual information.

7.3. RSFC Differences Within Treatment Groups

7.3.1. True Acupuncture and Physiotherapy Group

Higher RSFC post- vs pre- treatment was found in nine regions within four networks in the TA+PT group, including the bilateral precuneus, R anterior calcarine sulcus, R primary motor cortex, L angular gyrus, and bilateral precuneus within the DMN, the R visual cortex, R posterior lingual gyrus and L visual cortex within the visual network, and the R posterior cingulate sulcus within the ventral attention network.

Few studies using physiotherapy or physical therapy for stroke treatment use fMRI to assess its effects on neuroplasticity (Alcantara et al., 2018; Leonard et al., 2017). Most studies focus on the physical outcomes, such as FMA scores or other measures of physical ability and improvement. To our knowledge, no study has directly compared acupuncture with physiotherapy and assessed the differences in RSFC between these treatment modalities. This thus limits the amount of studies available for comparison or correlation with our findings.

The large cluster identified in the precuneus within the DMN overlapped with the three clusters identified in both before treatment group differences and after treatment group differences. Therefore, the cluster identified solely in the TA+PT group was hence a combination of the three clusters identified when examining between group differences.

The precuneus, a pivotal node in the DMN, plays a crucial role in various cognitive functions, such as self-awareness, episodic memory, and sensorimotor integration (Margulies et al.,

2009). The observed increase in RSFC in this region following TA with PT may indicate improved neural recovery in these domains, suggesting a potential correlation between enhanced connectivity in the precuneus and cognitive gains. Moreover, the involvement of the precuneus in sensorimotor integration suggests that increased RSFC may also reflect how TA with PT contributes to improved motor function as post-stroke treatment (Grefkes & Fink, 2011; Margulies et al., 2009).

The findings of Zhong and colleagues (2011) suggest that acupuncture has the potential to enhance the mood and cognitive functions of Alzheimer's disease patients. Additionally, they observed that acupoint GB40, which was also used during this study, activated the precuneus as a central target of this acupoint. This corresponds to our results showing increased activation in the precuneus. Similarly, Liu and colleagues (2020) reported increased FC in the precuneus of ischaemic stroke patients following scalp acupuncture treatment. They also found improvements in visual-cognitive-motor control associated with changes in the precuneus, aligning with our findings regarding the correlation between the RSFC results and increases in FMA scores. These studies collectively support the notion that acupuncture interventions, including those targeting the precuneus, may have beneficial effects on cognitive and motor functions in neurological conditions such as Alzheimer's disease and stroke.

The R anterior calcarine sulcus, known for its involvement in visual processing, exhibited increased RSFC following stroke treatment. This observation may suggest that TA with PT may lead to enhanced communication within the DMN, contributing to improved visual processing or integration of visual information (Grill-Spector, Kourtzi & Kanwisher, 2001).

Increased RSFC in the R primary motor cortex may signify how TA with PT leads to positive changes related to motor recovery. The integration of this region into the DMN post-stroke treatment could reflect enhanced coordination and communication within neural networks involved in motor functions (Grefkes & Fink, 2011). Leonard and colleagues (2017) reported increased BOLD signals in the primary motor cortex of patients with multiple sclerosis after 14 weeks of intensive physical therapy or PT. Similarly, Nierhaus and colleagues (2019) found immediate changes in RSFC in motor function brain areas of healthy participants following XNKQ acupuncture, which was also utilised in our study. These findings collectively suggest that both TA and PT can influence RSFC in motor areas, as supported by our findings.

Greater RSFC increases observed in the DMN and left angular gyrus may imply that the combination of TA and PT could lead to improved information processing, memory, self-awareness, and cognitive, language, and motor function (Seghier, 2012; Luerding et al., 2008). This aligns with studies demonstrating that acupuncture improves depression

symptoms and cognitive deficits in stroke patients, ultimately aiding in recovery (Wu et al., 2022; Hua et al., 2017; Zhang et al., 2010).

A study conducted on patients with Bell's palsy revealed that acupuncture increased RSFC in various areas of the DMN, including the precuneus and angular gyrus (He et al., 2014). Recent investigations into the DMN among individuals with conditions like Alzheimer's disease (Wu et al., 2011) and schizophrenia (Ongür et al., 2010) propose that both external and internal factors can disrupt an individual's internal balance, affecting their capacity to regulate internal experiences such as body states, feelings, and emotions. This disruption may compromise the integrity of the DMN (Buckner, Andrews-Hanna & Schacter, 2008).

In other words, alterations in the DMN may impact homeostasis and the ability to effectively regulate internal experiences such as body state, feelings, and emotions. Notably, a study observed that acupuncture induced alterations in FC specifically within the homeostatic afferent network, a phenomenon observed exclusively in functional diarrhoea patients, possibly owing to anomalies in their network functionality (Zhou et al., 2013). This somewhat corresponds with our findings, where the combination of TA and PT significantly impacted the DMN.

As suggested, studies have proposed the hypothesis that acupuncture exerts its effects through modulation of the DMN (Otti and Noll-Husson, 2012; Zhao et al., 2014; Zhang et al., 2019). This hypothesis aligns with our results, which indicates the impacts of TA with PT on RSFC in various regions within the DMN. Many studies, however, examine the effects of acupuncture on the DMN in patients with depression or Alzheimer's disease (Deng et al., 2016; Liang et al., 2014), which may yield different results compared to stroke patients. In this study, significant changes in the DMN were also not seen in the TA only group or the SA+PT group. This suggests that neither TA alone nor SA with PT has the same impact on the DMN as TA with PT. This warrants further investigation into the effect of TA combined with PT.

Greater RSFC increases in the visual network point to improved alertness, visual processing, and visual-motor control such as visually guided movements (Liu et al., 2020). The heightened connectivity observed in the L and R visual cortex may foster a more balanced and coordinated processing of visual stimuli, potentially supporting improved visual perception (Uddin, Supekar & Menon, 2010; Schaechter et al., 2006).

Increased RSFC in the R visual cortex and R posterior lingual gyrus within the Visual Network after stroke treatment may also indicate a favourable change in visual processing and integration (Grill-Spector, Kourtzi & Kanwisher, 2001). This heightened connectivity may signify improved communication within the visual network, reflecting enhanced capabilities in processing visual information. Such adaptive changes could contribute to the restoration of

visual functions and the establishment of alternative pathways to support visual processing (Carter et al., 2010).

In their investigation involving scalp acupuncture for ischaemic stroke patients, Liu and colleagues (2020) noted significant impacts on the visual network and enhancements in connectivity between regions associated with vision and motor functions. Consequently, it is reasonable to infer that the increase in RSFC seen in the visual network might be correlated with improved visual orientation processing and coordination between vision and motor functions following TA with PT (Liu et al., 2020; Zhang et al., 2016).

The R posterior cingulate sulcus is recognized as a vital component of the ventral attention network, pivotal for directing attention towards behaviourally relevant stimuli (Corbetta & Shulman, 2002). Increased RSFC in this region may imply that TA with PT potentially fosters enhanced communication within the ventral attention network, thus suggesting improvements in the brain's capacity to allocate attention to salient stimuli (He et al., 2007).

The particular stroke treatment modality utilised may have directly impacted changes in RSFC within the ventral attention network. Since PT often involves attentional training or cognitive rehabilitation, increase in connectivity in the R posterior cingulate sulcus may directly linked to the mechanisms of this intervention (Thiel, Zilles & Fink, 2004).

A study conducted by Vieira and colleagues (2017) employed physiotherapy to stimulate the lower limb in healthy subjects and utilised fMRI to identify activated brain regions. The activated areas included the precuneus, medial prefrontal cortex, and the posterior cingulate, which aligns with our findings showing increased RSFC in these regions within the DMN and ventral attention network following TA with PT.

7.3.2. Sham Acupuncture and Physiotherapy Group

In the SA+PT group, two regions within two networks exhibited lower RSFC post- vs pre-treatment. These regions were the R postcentral gyrus within the somatosensory network and the L lingual gyrus within the visual network.

The decrease in RSFC within the somatosensory network, specifically in the R postcentral gyrus following the stroke treatment may suggest nuanced changes in neural organization and sensory processing (Grefkes & Fink, 2011; Schaechter et al., 2006). This decrease in RSFC may signify that PT with SA led to a form of neural reorganisation, reflecting an adaptive response to the treatment aimed at optimising somatosensory functions (Grefkes & Fink, 2011; Wang et al., 2010). Additionally, the observed decrease in RSFC might imply functional compensation, where other regions within the somatosensory network assume a more

prominent role in sensory processing to offset alterations in the postcentral gyrus (Carter et al., 2010).

Hui and colleagues (2009) observed that using tactile stimulation as the sham condition in healthy controls induced greater sensorimotor activations compared to TA. They also concluded that this sham method did not elicit DMN stimulation to the same degree as TA, consistent with our findings where only the TA+PT group exhibited significant increases in RSFC in the DMN.

A decrease in RSFC within the visual network, particularly in the L lingual gyrus, following PT+SA treatment, may suggest a complex interplay of neural reorganisation, selective network engagement, and task-specific changes in visual processing (Carter et al., 2010; Uddin, Supekar & Menon, 2010). The diminished RSFC in the L lingual gyrus may signify neural reorganisation within the visual network, potentially driven by compensatory mechanisms as other brain regions assume a more prominent role to counterbalance changes in this region's functioning (Uddin, Supekar & Menon, 2010; Wig et al., 2014). Other studies have also indicated that visual-related brain areas were less affected by sham acupoints than when using true acupoints (Shan et al., 2014; Wu et al., 2014). Consequently, the findings observed in the SA+PT group might be attributed to neuroplasticity, as the brain attempts to adapt to changes not elicited by sham acupuncture, in contrast to alterations observed when utilizing true acupuncture in the TA with PT group.

Further research is warranted to comprehend the impact of SA on stroke patients. Some studies have found no significant differences favouring TA over SA as a treatment, and both types of acupuncture have demonstrated effects on upper limb and motor cortex function and activity after a stroke (Schaechter et al., 2007; Moffet, 2009). This is contradictory to our results, where TA with PT showed increased RSFC in various regions while SA with PT led to decreased RSFC in two regions. Huang et al. (2012) highlighted the inconsistency in studies examining the disparities between TA and SA, noting that brain responses to TA appear to be greater and more specific, which aligns with our findings. However, more research is needed to reconcile these discrepancies and provide a comprehensive understanding of the effects of SA on stroke patients.

Unfortunately, most studies examining the effect of PT only focus on its influence on motor control regions (Kuwahara, Miyawaki & Kaneko, 2022). It was hence difficult to confirm or challenging the effects of PT with SA on the regions and networks found in this study.

A lack of significant results in the SA and PT group could also potentially be attributed to the relatively short duration of the physiotherapy treatment. Participants in this study only received

3 weeks of treatment, while some studies suggest that certain patients may require up to 20 weeks of physiotherapy treatment (Kollen et al., 2009; Luke, Dodd & Brock, 2004; Paci, 2003).

8. Conclusion

This study represents a pioneering effort to investigate potential benefits of an extended (3-week) rehabilitation programme on physical outcomes and RSFC in ischaemic stroke patients with unilateral limb dysfunction. The participants were randomly assigned to one of three treatment arms, including (1) TA, (2) TA+PT, and (3) SA+PT. Following treatment, patients in all three groups presented improved FMA scores compared to themselves before treatment. However, no significant differences were observed between groups. The consistent upward trend in FMA scores suggest advancements in motor function recovery from each respective approach.

The RSFC results unveiled distinctive patterns within and across treatment groups. Notably, stroke patients following the TA+PT treatment exhibited significant increased RSFC (1) in five regions within three RSNs compared to patients in other groups after treatment and (2) in nine regions spanning four RSNs compared to themselves before treatment. The increased RSFC specifically in the precuneus, motor cortex and posterior cingulate sulcus aligns with prior studies indicating the positive effects of TA on these regions. Improvements in RSFC in these regions have also been reported on individuals following PT. Increased RSFC in the precuneus within the DMN after TA+PT suggests improved neural recovery associated with cognitive domains, sensorimotor integration, and potential motor function enhancement. Additionally, changes in RSFC within the visual network suggests improvements in alertness, visual processing, and visual-motor control.

However, patients receiving SA+PT displayed decreases in RSFC in the R postcentral gyrus within the somatosensory network and the L lingual gyrus within the visual network. This suggests nuanced neural reorganisation and compensatory mechanisms in response to the combined PT with SA approach.

Only the group receiving TA with PT treatment showed significant correlations between RSFC and FMA scores. No significant correlations were found between RSFC and FMA scores in the other two treatment groups.

This study's findings underscore the potential effectiveness of combining TA with PT in promoting positive alterations in neural connectivity, particularly in the regions crucial for cognitive, sensorimotor, and visual processing. The study contributes valuable insights into the neural mechanisms underlying various stroke rehabilitation interventions.

9. Recommendations and Limitations

During this study, only the patients in the TA with PT group displayed significant correlations between RSFC and FMA scores. However, no significant correlations emerged between RSFC changes observed in the other two treatment groups and their FMA scores. Several factors could contribute to this observed lack of correlation. One potential factor is the heterogeneity of lesion location and size across participants, which may influence the variability in neural reorganisation patterns. Importantly, consideration should be given to the sample size and statistical power of the study, as larger samples generally enhance the ability to detect meaningful correlations. Future research may benefit from deeper exploration of these factors to gain a more comprehensive understanding to complex relationship between neural activation patterns and motor recovery outcomes.

Considering the relatively brief duration of the PT treatment, which lasted for only 3 weeks, it is recommended to explore the effects of longer-term PT interventions. Future studies could focus on investigating the optimal duration of PT needed to observe substantial neural changes. This is particularly pertinent given that certain studies suggest up to 20 weeks of treatment might be necessary for certain patients to experience significant effects. Exploring varying durations of PT interventions can provide valuable insights into the time frame required for optimal neural plasticity and functional recovery, thereby informing more effective treatment protocols in clinical practice.

In this study, it was also unfortunately not possible to obtain ethics in China to have a group that received only PT (without SA), even though PT has been used as sole stroke rehabilitation treatment in many Western countries. Future studies could therefore derive valuable insights examining the effects of PT alone, without the addition of other interventions such as TA or SA. Comparing the outcomes of PT-only groups with those receiving combined interventions can shed light on the efficacy of PT in isolation and provide a clearer understanding of its role in stroke rehabilitation. Such comparative studies may offer valuable guidance for optimizing treatment strategies and tailoring rehabilitation approaches to suit varying cultural and healthcare contexts.

Given the constraints imposed by extended COVID-19 lockdown procedures, the sample size in this study was limited. To overcome this limitation and enhance statistical power, future research endeavours should strive for larger sample sizes. Doing so would bolster the ability to detect meaningful correlations between RSFC changes and physical outcomes, thereby furnishing more robust evidence regarding the effectiveness of different stroke rehabilitation interventions. By increasing the sample size, researchers can better capture the heterogeneity within the population and achieve more reliable and generalizable results. This would

contribute to advancing our understanding of the mechanisms underlying stroke recovery and inform the development of more efficacious rehabilitation strategies.

Fu and colleagues (2017) recommended that using multimodal analysis techniques should be considered for further studies. Such an approach has the potential to provide more clarity on the differences between SA and TA or PT. Subjects could also be divided into distinct groups based on similarities, such as stroke side, sex etc. to better understand the impact of these factors on treatment outcomes. Sex should particularly be considered in further research, since all participants in the TA with PT group were male, which could have affected our results. Furthermore, alternative methods for obtaining ICA maps should be explored, as the reliance solely on the healthy controls might not provide an accurate representation of RSNs to use for stroke patients. By adopting a multimodal analysis approach and refining subject stratification methods, researchers can enhance the depth and precision of their investigations, leading to more nuanced insights into the efficacy and mechanisms of various stroke rehabilitation interventions.

This study demonstrated that the stroke patients receiving TA+PT exhibited significant RSFC changes in crucial brain regions associated with cognitive domains, sensorimotor integration, and visual processing. Given these promising results, clinicians and rehabilitation specialists may contemplate integrating TA with PT as a complementary approach for individuals undergoing recovery from ischaemic stroke. By combining these modalities, practitioners can potentially enhance the rehabilitation process and facilitate improvements in various domains of functioning, ultimately contributing to better outcomes and quality of life for stroke survivors. However, further research and clinical trials are warranted to validate these findings and establish the optimal protocols for integrating TA with PT in stroke rehabilitation settings.

10. Outputs

The majority of this work has been presented at conferences and appears in the following proceedings:

2024

International conference articles:

1. Fan J., Fouché S., Lu H., Warton F., Robertson F., Wang Y., Er S., Chen J., Langerak N., Ren X., Ma X. Combrinck M., Zhang C., Meintjes E., “Effects of physiotherapy and acupuncture treatment on basal ganglia network in stroke rehabilitation”, 30th OHBM, Seoul, Korea, June 2024.
2. Fouché S., Lu H., Warton F., Robertson F, Wang Y., Er S., Chen J., Langerak N., Combrinck M., Ma X., Ren X., Meintjes E., Zhang C., Fan J., “Effects of combined physiotherapy and acupuncture treatment on RSFC in ischaemic stroke patients”, 30th OHBM, Seoul, Korea, June 2024.

2023

International conference articles:

1. Fan J., Barden F., Lu H., Fouché S., Joubert P., Wang Y., Warton F., Robertson F., Er S., Chen J., Langerak N., Ren X., Ma X., Meintjes E., Zhang C., Combrinck M., “Potential benefits of adjunctive acupuncture therapy in unilateral stroke rehabilitation”, 16th International Academic Symposium of Acupuncture and Moxibustion, Tianjin, China, November 2023. **(Invited Presentation)**
2. Fan J., Warton F., Fouché S., Lu H., Wang Y., Er S., Robertson F., Ren X., Chen J., Combrinck M., Langerak N., Ma X. Zhang C., Meintjes E., “Effect of acupuncture treatment on default mode network in ischemic stroke patients”, 1st ISMRM African Chapter, Accra, Ghana, September 2023.
3. Fouché S., Lu H., Warton F., Er S., Wang Y., Robertson F., Ren X., Chen J., Combrinck M., Langerak N., Ma X., Meintjes E., Zhang C., Fan J., “Benefits and neural correlates of acupuncture treatment on RSFC in ischemic stroke patients”, 1st ISMRM African Chapter, Accra, Ghana, September 2023.
4. Fan J., Warton F., Fouché S., Lu H., Wang Y., Er S., Robertson F., Ren X., Combrinck M., Langerak N., Ma X. Zhang C., Meintjes E., “Effect of acupuncture treatment on default mode network in ischemic stroke patients”, 29th OHBM, Montreal, Canada, July 2023.
5. Fouché S., Lu H., Warton F., Er S., Wang Y., Robertson F., Ren X., Combrinck M., Langerak N., Ma X., Meintjes E., Zhang C., Fan J., “Benefits and neural correlates of

acupuncture treatment on RSFC in ischemic stroke patients", 29th OHBM, Montreal, Canada, July 2023.

Local conference articles:

1. Fouché S., Lu H., Warton F., Er S., Wang Y., Robertson F., Ren X., Chen J., Combrinck M., Langerak N., Ma X., Meintjes E., Zhang C., Fan J., "Effects of Acupuncture Treatment on Resting-State Functional Connectivity in Stroke Patients with Unilateral Limb Dysfunction." HiP Research Symposium, Cape Town, November 2023. **(Oral Presentation)**
2. Fan J., Fouché S, Lu H., Warton F., Wang Y., Er S., Robertson F., Ren X., Chen J., Combrinck M., Langerak N., Ma X., Meintjes E., Zhang C., "Potential benefit and neurocorrelate of acupuncture treatment on default mode network" HiP Research Symposium, Cape Town, November 2023.
3. Fan J., Warton F., Fouché S., Lu H., Wang Y., Er S., Robertson F., Ren X., Combrinck M., Langerak N., Ma X. Zhang C., Meintjes E., "Effect of acupuncture treatment on default mode network in ischemic stroke patients", NI Research Day, Cape Town, March 2023.
4. Fouché S., Lu H., Warton F., Er S., Wang Y., Robertson F., Ren X., Combrinck M., Langerak N., Ma X., Meintjes E., Zhang C., Fan J., "Benefits and neural correlates of acupuncture treatment on RSFC in ischemic stroke patients", NI Research Day, Cape Town, March 2023.

References

Aertsen, A., Gerstein, G.L., Habib, M. & Palm, G. 1989. Dynamics of neuronal firing correlation: modulation of “effective connectivity”. *Journal of Neurophysiology*. 61(5):900–917. DOI: https://doi.org/10.1152/jn.1989.61.5.900.

Akinyemi, R.O., Ovbiagele, B., Adeniji, O.A., Sarfo, F.S., Abd-Allah, F., Adoukonou, T., Ogah, O.S., Naidoo, P., et al. 2021. Stroke in Africa: profile, progress, prospects and priorities. *Nature Reviews Neurology*. 17(10):634–656. DOI: https://doi.org/10.1038/s41582-021-00542-4.

Alcantara, C.C., García-Salazar, L.F., Silva-Couto, M.A., Santos, G.L., Reisman, D.S. & Russo, T.L. 2018. Post-stroke BDNF Concentration Changes Following Physical Exercise: A Systematic Review. *Frontiers in Neurology*. 9(637). DOI: https://doi.org/10.3389/fneur.2018.00637.

Almeida, S.R.M., Vicentini, J., Bonilha, L., De Campos, B.M., Casseb, R.F. & Min, L.L. 2016. Brain Connectivity and Functional Recovery in Patients With Ischemic Stroke. *Journal of Neuroimaging*. 27(1):65–70. DOI: https://doi.org/10.1111/jon.12362.

Arya, K.N., Pandian, S., Verma, R. & Garg, R.K. 2011. Movement therapy induced neural reorganization and motor recovery in stroke: A review. *Journal of Bodywork and Movement Therapies*. 15(4):528–537. DOI: https://doi.org/10.1016/j.jbmt.2011.01.023.

Bai, L., Tian, J., Zhong, C., Xue, T., You, Y., Liu, Z., Chen, P., Gong, Q., et al. 2010. Acupuncture Modulates Temporal Neural Responses in Wide Brain Networks: Evidence from fMRI Study. *Molecular Pain*. 6(1):1744–80696–73. DOI: https://doi.org/10.1186/1744-8069-6-73.

Beckmann, C.F. & Smith, S.M. 2004. Probabilistic Independent Component Analysis for Functional Magnetic Resonance Imaging. *IEEE Transactions on Medical Imaging*. 23(2):137–152. DOI: https://doi.org/10.1109/tmi.2003.822821.

Beckmann, C.F., DeLuca, M., Devlin, J.T. & Smith, S.M. 2005. Investigations into resting-state connectivity using independent component analysis. *Philosophical Transactions of the Royal Society B: Biological Sciences*. 360(1457):1001–1013. DOI: https://doi.org/10.1098/rstb.2005.1634.

Biswal, B., Zerrin Yetkin, F., Haughton, V.M. & Hyde, J.S. 1995. Functional connectivity in the motor cortex of resting human brain using echo-planar mri. *Magnetic Resonance in Medicine*. 34(4):537–541. DOI: https://doi.org/10.1002/mrm.1910340409.

Biswal, B.B., Mennes, M., Zuo, X.-N., Gohel, S., Kelly, C., Smith, S.M., Beckmann, C.F., Adelstein, J.S., et al. 2010. Toward discovery science of human brain function. *Proceedings of the National Academy of Sciences*. 107(10):4734–4739. DOI: https://doi.org/10.1073/pnas.0911855107.

Blanke, O. & Arzy, S. 2005. The Out-of-Body Experience: Disturbed Self-Processing at the Temporo-Parietal Junction. *The Neuroscientist*. 11(1):16–24. DOI: https://doi.org/10.1177/1073858404270885.

Brown, C.A., Schmitt, F.A., Smith, C.D. & Gold, B.T. 2019. Distinct patterns of default mode and executive control network circuitry contribute to present and future executive function in older adults. *NeuroImage*. 195:320–332. DOI: https://doi.org/10.1016/j.neuroimage.2019.03.073.

Buckner, R.L. & Vincent, J.L. 2007. Unrest at rest: Default activity and spontaneous network correlations. *NeuroImage*. 37(4):1091–1096. DOI: https://doi.org/10.1016/j.neuroimage.2007.01.010.

Buckner, R.L., Andrews-Hanna, J.R. & Schacter, D.L. 2008. The Brain's Default Network. *Annals of the New York Academy of Sciences*. 1124(1):1–38. DOI: https://doi.org/10.1196/annals.1440.011.

Butler, A.J. & Page, S.J. 2006. Mental Practice With Motor Imagery: Evidence for Motor Recovery and Cortical Reorganization After Stroke. *Archives of Physical Medicine and Rehabilitation*. 87(12):2–11. DOI: https://doi.org/10.1016/j.apmr.2006.08.326.

Calhoun, V.D. & Adali, T. 2006. Unmixing fMRI with independent component analysis. *IEEE Engineering in Medicine and Biology Magazine*. 25(2):79–90. DOI: https://doi.org/10.1109/memb.2006.1607672.

Calhoun, V.D., Liu, J. & Adalı, T. 2009. A review of group ICA for fMRI data and ICA for joint inference of imaging, genetic, and ERP data. *NeuroImage*. 45(1):S163–S172. DOI: https://doi.org/10.1016/j.neuroimage.2008.10.057.

Canario, E., Chen, D. & Biswal, B. 2021. A review of resting-state fMRI and its use to examine psychiatric disorders. *Psychoradiology*. 1(1):42–53. DOI: https://doi.org/10.1093/psyrad/kkab003.

Cao, B.-Q., Zhan, J., Lai, P.-H. & Tan, F. 2021. Mechanism underlying treatment of ischemic stroke using acupuncture: transmission and regulation. *Neural Regeneration Research*. 16(5):944. DOI: https://doi.org/10.4103/1673-5374.297061.

Carter, A.R., Astafiev, S.V., Lang, C.E., Connor, L.T., Rengachary, J., Strube, M.J., Pope, D.L.W., Shulman, G.L., et al. 2010. Resting state inter-hemispheric fMRI connectivity predicts performance after stroke. *Annals of Neurology*. 67(3):365–375. DOI: https://doi.org/10.1002/ana.21905.

Cavanna, A.E. & Trimble, M.R. 2006. The precuneus: a review of its functional anatomy and behavioural correlates. *Brain*. 129(3):564–583. DOI: https://doi.org/10.1093/brain/awl004.

Chae, Y., Chang, D.-S., Lee, S.-H., Jung, W.-M., Lee, I.-S., Jackson, S., Kong, J., Lee, H., et al. 2013. Inserting Needles Into the Body: A Meta-Analysis of Brain Activity Associated With Acupuncture Needle Stimulation. *The Journal of Pain*. 14(3):215–222. DOI: https://doi.org/10.1016/j.jpain.2012.11.011.

Chavez, L., Huang, S.-S., MacDonald, I., Lin, J.-G., Lee, Y.-C. & Chen, Y.-H. 2017. Mechanisms of Acupuncture Therapy in Ischemic Stroke Rehabilitation: A Literature Review of Basic Studies. *International Journal of Molecular Sciences*. 18(11):2270. DOI: https://doi.org/10.3390/ijms18112270.

Chen, J.Q., Huang, Y., Lai, X.S., Tang, C.Z., Yang, J., Chen, H., Zeng, T.J., Wu, J.X., et al. 2013. Acupuncture at Waiguan (TE5) influences activation/deactivation of functional brain areas in ischemic stroke patients and healthy people: A functional MRI study. *PubMed*. 8(3). DOI: https://doi.org/10.3969/j.issn.1673-5374.2013.03.004.

Chen, S., Cai, D., Chen, J., Yang, H. & Liu, L. 2019. Altered Brain Regional Homogeneity Following Contralateral Acupuncture at Quchi (LI 11) and Zusanli (ST 36) in Ischemic Stroke Patients with Left Hemiplegia: An fMRI Study. *Chinese Journal of Integrative Medicine*. 26(1):20–25. DOI: https://doi.org/10.1007/s11655-019-3079-6.

Chen, T., Zhang, W.W., Chu, Y.-X. & Wang, Y.-Q. 2020. Acupuncture for Pain Management: Molecular Mechanisms of Action. *The American Journal of Chinese Medicine*. 48(04):793–811. DOI: https://doi.org/10.1142/s0192415x20500408.

Chon, T.Y. & Lee, M.C. 2013. Acupuncture. *Mayo Clinic Proceedings*. 88(10):1141–1146. DOI: https://doi.org/10.1016/j.mayocp.2013.06.009.

Corbetta, M. & Shulman, G.L. 2002. Control of goal-directed and stimulus-driven attention in the brain. *Nature reviews. Neuroscience*. 3(3):201–15. DOI: https://doi.org/10.1038/nrn755.

Corbetta, M., Ramsey, L., Callejas, A., Baldassarre, A., Hacker, Carl D., Siegel, Joshua S., Astafiev, Serguei V., Rengachary, J., et al. 2015. Common Behavioral Clusters and Subcortical Anatomy in Stroke. *Neuron*. 85(5):927–941. DOI: https://doi.org/10.1016/j.neuron.2015.02.027.

Cox, R.W. 1996. AFNI: Software for Analysis and Visualization of Functional Magnetic Resonance Neuroimages. *Computers and Biomedical Research*. 29(3):162–173. DOI: https://doi.org/10.1006/cbmr.1996.0014.

Cox, R.W. & Hyde, J.S. 1997. Software tools for analysis and visualization of fMRI data. *NMR in Biomedicine*. 10(4-5):171–178. DOI: https://doi.org/10.1002/(sici)1099-1492(199706/08)10:4/5%3C171::aid-nbm453%3E3.0.co;2-l.

Cox, R.W., Chen, G., Glen, D.R., Reynolds, R.C. & Taylor, P.A. 2017. FMRI Clustering in AFNI: False-Positive Rates Redux. *Brain Connectivity*. 7(3):152–171. DOI: https://doi.org/10.1089/brain.2016.0475.

Darekar, A., McFadyen, B.J., Lamontagne, A. & Fung, J. 2015. Efficacy of virtual reality-based intervention on balance and mobility disorders post-stroke: a scoping review. *Journal of NeuroEngineering and Rehabilitation*. 12(1). DOI: https://doi.org/10.1186/s12984-015-0035-3.

Deng, D., Liao, H., Duan, G., Liu, Y., He, Q., Liu, H., Tang, L., Pang, Y., et al. 2016. Modulation of the Default Mode Network in First-Episode, Drug-Naïve Major Depressive Disorder via Acupuncture at Baihui (GV20) Acupoint. *Frontiers in Human Neuroscience*. 10:230. DOI: https://doi.org/10.3389/fnhum.2016.00230.

Devinsky, O., Morrell, M.J. & Vogt, B.A. 1995. Contributions of anterior cingulate cortex to behaviour. *Brain*. 118(1):279–306. DOI: https://doi.org/10.1093/brain/118.1.279.

Du, Y., Zhang, L., Liu, W., Rao, C., Li, B., Nan, X., Li, Z. & Jiang, H. 2020. Effect of acupuncture treatment on post-stroke cognitive impairment. *Medicine*. 99(51):e23803. DOI: https://doi.org/10.1097/md.0000000000023803.

Duncan, P.W., Propst, M. & Nelson, S.G. 1983. Reliability of the Fugl-Meyer Assessment of Sensorimotor Recovery Following Cerebrovascular Accident. *Physical Therapy*. 63(10):1606–1610. DOI: https://doi.org/10.1093/ptj/63.10.1606.

Faivre, A., Rico, A., Zaaraoui, W., Crespy, L., Reuter, F., Wybrecht, D., Soulier, E., Malikova, I., et al. 2012. Assessing brain connectivity at rest is clinically relevant in early multiple sclerosis. *Multiple Sclerosis Journal*. 18(9):1251–1258. DOI: https://doi.org/10.1177/1352458511435930.

Fan, J., Taylor, P.A., Jacobson, S.W., Molteno, C.D., Gohel, S., Biswal, B.B., Jacobson, J.L. & Meintjes, E.M. 2017. Localized reductions in resting-state functional connectivity in children with prenatal alcohol exposure. *Human Brain Mapping*. 38(10):5217–5233. DOI: https://doi.org/10.1002/hbm.23726.

Filippini, N., MacIntosh, B.J., Hough, M.G., Goodwin, G.M., Frisoni, G.B., Smith, S.M., Matthews, P.M., Beckmann, C.F., et al. 2009. Distinct patterns of brain activity in young carriers of the *APOE* -ε4 allele. *Proceedings of the National Academy of Sciences*. 106(17):7209–7214. DOI: https://doi.org/10.1073/pnas.0811879106.

Fitzgerald, J., Johnson, K., Kehoe, E., Bokde, A.L.W., Garavan, H., Gallagher, L. & McGrath, J. 2014. Disrupted Functional Connectivity in Dorsal and Ventral Attention Networks During Attention Orienting in Autism Spectrum Disorders. *Autism Research*. 8(2):136–152. DOI: https://doi.org/10.1002/aur.1430.

Fox, M.D. 2010. Clinical applications of resting state functional connectivity. *Frontiers in Systems Neuroscience*. 4(19). DOI: https://doi.org/10.3389/fnsys.2010.00019.

Fox, P.T. & Raichle, M.E. 1986. Focal physiological uncoupling of cerebral blood flow and oxidative metabolism during somatosensory stimulation in human subjects. *Proceedings of the National Academy of Sciences*. 83(4):1140–1144. DOI: https://doi.org/10.1073/pnas.83.4.1140.

Freedman, D., Pisani, R. & Purves, R. 2007. *Statistics*. New York: W.W. Norton & Company.

Fu, C.-H., Li, K.-S., Ning, Y.-Z., Tan, Z.-J., Zhang, Y., Liu, H.-W., Han, X. & Zou, Y.-H. 2017. Altered effective connectivity of resting state networks by acupuncture stimulation in stroke patients with left hemiplegia. *Medicine*. 96(47):e8897. DOI: https://doi.org/10.1097/md.0000000000008897.

Fugl-Meyer, A.R., Jaasko, L., Leyman, I., Olsson, S. & Steglind, S. 1975. The poststroke hemiplegic patient. 1. A method for evaluation of physical performance. *ScandJ Rehabil Med*. 7:13–31.

GBD Lifetime Risk of Stroke Collaborators et al. 2018. Global, Regional, and Country-Specific Lifetime Risks of Stroke, 1990 and 2016. *New England Journal of Medicine*. 379(25):2429–2437. DOI: https://doi.org/10.1056/nejmoa1804492.

Gladstone, D.J., Danells, C.J. & Black, S.E. 2002. The Fugl-Meyer Assessment of Motor Recovery after Stroke: A Critical Review of Its Measurement Properties. *Neurorehabilitation and Neural Repair*. 16(3):232–240. DOI: https://doi.org/10.1177/154596802401105171.

Gong, F., Liu, J., Song, Q., Zhong, Y., Chen, H. & Wu, J. 2022. Surgical techniques and function outcome for cingulate gyrus glioma, how we do it. *Frontiers in Oncology*. 12. DOI: https://doi.org/10.3389/fonc.2022.986387.

Graham, J.V., Eustace, C., Brock, K., Swain, E. & Irwin-Carruthers, S. 2009. The Bobath Concept in Contemporary Clinical Practice. *Topics in Stroke Rehabilitation*. 16(1):57–68. DOI: https://doi.org/10.1310/tsr1601-57.

Grefkes, C. & Fink, G.R. 2011. Reorganization of cerebral networks after stroke: new insights from neuroimaging with connectivity approaches. *Brain*. 134(5):1264–1276. DOI: https://doi.org/10.1093/brain/awr033.

Grill-Spector, K., Kourtzi, Z. & Kanwisher, N. 2001. The lateral occipital complex and its role in object recognition. *Vision Research*. 41(10-11):1409–1422. DOI: https://doi.org/10.1016/s0042-6989(01)00073-6.

Gusnard, D.A. & Raichle, M.E. 2001. Searching for a baseline: Functional imaging and the resting human brain. *Nature Reviews Neuroscience*. 2(10):685–694. DOI: https://doi.org/10.1038/35094500.

Hakon, J., Quattromani, M.J., Sjölund, C., Tomasevic, G., Carey, L., Lee, J.-M., Ruscher, K., Wieloch, T., et al. 2018. Multisensory stimulation improves functional recovery and resting-state functional connectivity in the mouse brain after stroke. *NeuroImage: Clinical*. 17:717–730. DOI: https://doi.org/10.1016/j.nicl.2017.11.022.

Han M, Zhao H, Jing X. 2017. Literature analysis of influence of different needle retaining duration on acupuncture efficacy. J Tradit Chin Med, 58(4):334–339.

Han, X., Bai, L., Sun, C., Niu, X., Ning, Y., Chen, Z., Li, Y., Li, K., et al. 2019. Acupuncture Enhances Communication between Cortices with Damaged White Matters in Poststroke Motor Impairment. *Evidence-Based Complementary and Alternative Medicine*. 2019:1–11. DOI: https://doi.org/10.1155/2019/4245753.

Hanakawa, T., Dimyan, M.A. & Hallett, M. 2008. Motor Planning, Imagery, and Execution in the Distributed Motor Network: A Time-Course Study with Functional MRI. *Cerebral Cortex*. 18(12):2775–2788. DOI: https://doi.org/10.1093/cercor/bhn036.

Hara, Y. 2015. Brain Plasticity and Rehabilitation in Stroke Patients. *Journal of Nippon Medical School*. 82(1):4–13. DOI: https://doi.org/10.1272/jnms.82.4.

Hatem, S.M., Saussez, G., della Faille, M., Prist, V., Zhang, X., Dispa, D. & Bleyenheuft, Y. 2016. Rehabilitation of Motor Function after Stroke: A Multiple Systematic Review Focused on Techniques to Stimulate Upper Extremity Recovery. *Frontiers in Human Neuroscience*. 10(442). DOI: https://doi.org/10.3389/fnhum.2016.00442.

He, B.J., Snyder, A.Z., Vincent, J.L., Epstein, A., Shulman, G.L. & Corbetta, M. 2007. Breakdown of Functional Connectivity in Frontoparietal Networks Underlies Behavioral

Deficits in Spatial Neglect. *Neuron*. 53(6):905–918. DOI: https://doi.org/10.1016/j.neuron.2007.02.013.

He, X., Zhu, Y., Li, C., Park, K., Mohamed, A.Z., Wu, H., Xu, C., Zhang, W., et al. 2014. Acupuncture-induced changes in functional connectivity of the primary somatosensory cortex varied with pathological stages of Bell's palsy. *NeuroReport*. 25(14):1162–1168. DOI: https://doi.org/10.1097/wnr.0000000000000246.

Heeger, D.J. & Ress, D. 2002. What does fMRI tell us about neuronal activity? *Nature reviews. Neuroscience*. 3(2):142–51.

Hua, J., You, X., Li, W., Song, C., Lin, X., Zhang, X., Tao, J. & Chen, L. 2017. Electroacupuncture ameliorating post-stroke cognitive impairments via inhibition of peri-infarct astroglial and microglial/macrophage P2 purinoceptors-mediated neuroinflammation and hyperplasia. *BMC Complementary and Alternative Medicine*. 17(1). DOI: https://doi.org/10.1186/s12906-017-1974-y.

Huang, W., Pach, D., Napadow, V., Park, K., Long, X., Neumann, J., Maeda, Y., Nierhaus, T., et al. 2012. Characterizing Acupuncture Stimuli Using Brain Imaging with fMRI - A Systematic Review and Meta-Analysis of the Literature. *PLoS ONE*. 7(4):e32960. DOI: https://doi.org/10.1371/journal.pone.0032960.

Huang, Y., Chen, J.-Q., Lai, X.-S., Tang, C.-Z., Yang, J.-J., Chen, H., Wu, J.-X., Xiao, H.-L., et al. 2013. Lateralisation of Cerebral Response to Active Acupuncture in Patients with Unilateral Ischaemic Stroke: An Fmri Study. *Acupuncture in Medicine*. 31(3):290–296. DOI: https://doi.org/10.1136/acupmed-2012-010299.

Huang, Y., Li, M., Li, Y., Zhang, G., Chen, J., Zhang, J., Qi, J., Lai, X., et al. 2015. Acupuncture for ischemic stroke: cerebellar activation may be a central mechanism following Deqi. *Neural Regeneration Research*. 10(12):1997. DOI: https://doi.org/10.4103/1673-5374.172318.

Hui, K.K.S., Marina, O., Claunch, J.D., Nixon, E.E., Fang, J., Liu, J., Li, M., Napadow, V., et al. 2009. Acupuncture mobilizes the brain's default mode and its anti-correlated network in healthy subjects. *Brain Research*. 1287:84–103. DOI: https://doi.org/10.1016/j.brainres.2009.06.061.

Jenkinson, M., Beckmann, C.F., Behrens, T.E.J., Woolrich, M.W. & Smith, S.M. 2012. FSL. *NeuroImage*. 62(2):782–790. DOI: https://doi.org/10.1016/j.neuroimage.2011.09.015.

Kelly, A.M.C., Uddin, L.Q., Biswal, B.B., Castellanos, F.X. & Milham, M.P. 2008. Competition between functional brain networks mediates behavioral variability. *NeuroImage*. 39(1):527–537. DOI: https://doi.org/10.1016/j.neuroimage.2007.08.008.

Kesavadas, C. 2013. Resting state functional magnetic resonance imaging: An emerging clinical tool. *Neurology India*. 61(2):103. DOI: https://doi.org/10.4103/0028-3886.111107.

Kim, S.-G. & Kamil Ugurbil. 1997. Comparison of blood oxygenattion and cerebral blood flow effect in fMRI: Estimation of relative oxygen consumption change. *Magnetic Resonance in Medicine*. 38(1):59–65. DOI: https://doi.org/10.1002/mrm.1910380110.

Kollen, B.J., Lennon, S., Lyons, B., Wheatley-Smith, L., Scheper, M., Buurke, J.H., Halfens, J., Geurts, A.C.H., et al. 2009. The effectiveness of the Bobath concept in stroke rehabilitation: what is the evidence? *Stroke*. 40(4):e89-97. DOI: https://doi.org/10.1161/STROKEAHA.108.533828.

Kuwahara, W., Miyawaki, Y. & Kaneko, F. 2022. Impact of the Upper Limb Physiotherapy on Behavioral and Brain Adaptations in Post-Stroke Patients. *Journal of robotics and mechatronics*. 34(4):718–725. DOI: https://doi.org/10.20965/jrm.2022.p0718.

Kwong, K.K., Belliveau, J.W., Chesler, D.A., Goldberg, I.E., Weisskoff, R.M., Poncelet, B.P., Kennedy, D.N., Hoppel, B.E., et al. 1992. Dynamic magnetic resonance imaging of human brain activity during primary sensory stimulation. *Proceedings of the National Academy of Sciences*. 89(12):5675–5679. DOI: https://doi.org/10.1073/pnas.89.12.5675.

Lacourse, M.G., Orr, E.L.R., Cramer, S.C. & Cohen, M.J. 2005. Brain activation during execution and motor imagery of novel and skilled sequential hand movements. *NeuroImage*. 27(3):505–519. DOI: https://doi.org/10.1016/j.neuroimage.2005.04.025.

Lee, M.H., Smyser, C.D. & Shimony, J.S. 2012. Resting-State fMRI: A Review of Methods and Clinical Applications. *American Journal of Neuroradiology*. 34(10):1866–1872. DOI: https://doi.org/10.3174/ajnr.a3263.

Leech, R., Kamourieh, S., Beckmann, C.F. & Sharp, D.J. 2011. Fractionating the Default Mode Network: Distinct Contributions of the Ventral and Dorsal Posterior Cingulate Cortex to Cognitive Control. *Journal of Neuroscience*. 31(9):3217–3224. DOI: https://doi.org/10.1523/jneurosci.5626-10.2011.

Leonard, G., Lapierre, Y., Chen, J.-K., Wardini, R., Crane, J. & Ptito, A. 2017. Noninvasive tongue stimulation combined with intensive cognitive and physical rehabilitation induces neuroplastic changes in patients with multiple sclerosis: A multimodal neuroimaging study. *Multiple Sclerosis Journal – Experimental, Translational and Clinical*. 3(1). DOI: https://doi.org/10.1177/2055217317690561.

Li, A.-H., Zhang, J.-M. & Xie, Y.-K. 2004. Human acupuncture points mapped in rats are associated with excitable muscle/skin–nerve complexes with enriched nerve endings. *Brain Research*. 1012(1-2):154–159. DOI: https://doi.org/10.1016/j.brainres.2004.04.009.

Li, G., Jack, C.R. & Yang, E.S. 2006. An fMRI study of somatosensory-implicated acupuncture points in stable somatosensory stroke patients. *Journal of Magnetic Resonance Imaging*. 24(5):1018–1024. DOI: https://doi.org/10.1002/jmri.20702.

Li, X., Morgan, P.S., Ashburner, J., Smith, J. & Rorden, C. 2016. The first step for neuroimaging data analysis: DICOM to NIfTI conversion. *Journal of Neuroscience Methods*. 264:47–56. DOI: https://doi.org/10.1016/j.jneumeth.2016.03.001.

Li, Y., Wang, Y., Zhang, H., Wu, P. & Huang, W. 2015. The Effect of Acupuncture on the Motor Function and White Matter Microstructure in Ischemic Stroke Patients. *Evidence-based Complementary and Alternative Medicine : eCAM*. 2015:164792. DOI: https://doi.org/10.1155/2015/164792.

Liang, P., Wang, Z., Qian, T. & Li, K. 2014. Acupuncture Stimulation of Taichong (Liv3) and Hegu (LI4) Modulates the Default Mode Network Activity in Alzheimer's Disease. *American Journal of Alzheimer's Disease & Other Dementiasr*. 29(8):739–748. DOI: https://doi.org/10.1177/1533317514536600.

Lin, Y.-J., Kung, Y.-Y., Kuo, W.-J., Niddam, D.M., Chou, C.-C., Cheng, C.-M., Yeh, T.-C., Hsieh, J.-C., et al. 2016. Effect of Acupuncture 'dose— on Modulation of the Default Mode Network of the Brain. *Acupuncture in Medicine*. 34(6):425–432. DOI: https://doi.org/10.1136/acupmed-2016-011071.

Liu, G., Ma, H., Hu, P., Tian, Y., Hu, S., Fan, J. & Wang, K. 2013. Effects of painful stimulation and acupuncture on attention networks in healthy subjects. *Behavioral and Brain Functions*. 9(1). DOI: https://doi.org/10.1186/1744-9081-9-23.

Liu, H., Chen, L., Zhang, G., Jiang, Y., Qu, S., Liu, S., Huang, Y. & Chen, J. 2020. Scalp Acupuncture Enhances the Functional Connectivity of Visual and Cognitive-Motor Function Network of Patients with Acute Ischemic Stroke. *Evidence-Based Complementary and Alternative Medicine*. 2020:e8836794. DOI: https://doi.org/10.1155/2020/8836794.

Lowe, M.J., Dzemidzic, M., Lurito, J.T., Mathews, V.P. & Phillips, M.D. 2000. Correlations in Low-Frequency BOLD Fluctuations Reflect Cortico-Cortical Connections. *NeuroImage*. 12(5):582–587. DOI: https://doi.org/10.1006/nimg.2000.0654.

Lu, C.-Y., Huang, H.-C., Chang, H.-H., Yang, T.-H., Chang, C.-J., Chang, S.-W. & Chen, P.-C. 2017. Acupuncture Therapy and Incidence of Depression After Stroke. *Stroke*. 48(6):1682–1684. DOI: https://doi.org/10.1161/strokeaha.117.016959.

Luerding, R., Weigand, T., Bogdahn, U. & Schmidt-Wilcke, T. 2008. Working memory performance is correlated with local brain morphology in the medial frontal and anterior

cingulate cortex in fibromyalgia patients: structural correlates of pain–cognition interaction. *Brain*. 131(12):3222–3231. DOI: https://doi.org/10.1093/brain/awn229.

Luke, C., Dodd, K.J. & Brock, K. 2004. Outcomes of the Bobath concept on upper limb recovery following stroke. *Clinical Rehabilitation*. 18(8):888–898. DOI: https://doi.org/10.1191/0269215504cr793oa.

Lv, Q., Xu, G., Pan, Y., Liu, T., Liu, X., Miao, L., Chen, X., Jiang, L., et al. 2021. Effect of Acupuncture on Neuroplasticity of Stroke Patients with Motor Dysfunction: A Meta-Analysis of fMRI Studies. *Neural Plasticity*. 2021(1):e8841720. DOI: https://doi.org/10.1155/2021/8841720.

Margulies, D.S., Vincent, J.L., Kelly, C., Lohmann, G., Uddin, L.Q., Biswal, B.B., Villringer, A., Castellanos, F.X., et al. 2009. Precuneus shares intrinsic functional architecture in humans and monkeys. *Proceedings of the National Academy of Sciences*. 106(47):20069–20074. DOI: https://doi.org/10.1073/pnas.0905314106.

Mayo, N.E., Wood-Dauphinee, S., Côté, R., Durcan, L. & Carlton, J. 2002. Activity, participation, and quality of life 6 months poststroke. *Archives of Physical Medicine and Rehabilitation*. 83(8):1035–1042. DOI: https://doi.org/10.1053/apmr.2002.33984.

McGrath, K., Cunningham, N., Moloney, E., O'Connor, M., McManus, J., Peters, C. & Lyons, D. 2018. Enhancing acute stroke services: a quality improvement project. *BMJ Open Quality*. 7(3):e000258. DOI: https://doi.org/10.1136/bmjoq-2017-000258.

McKeown, M. 2003. Independent component analysis of functional MRI: what is signal and what is noise? *Current Opinion in Neurobiology*. 13(5):620–629. DOI: https://doi.org/10.1016/j.conb.2003.09.012.

Menon, V. & Uddin, L.Q. 2010. Saliency, switching, attention and control: a network model of insula function. *Brain Structure and Function*. 214(5-6):655–667. DOI: https://doi.org/10.1007/s00429-010-0262-0.

Miller, E.K. & Cohen, J.D. 2001. An Integrative Theory of Prefrontal Cortex Function. *Annual Review of Neuroscience*. 24(1):167–202. DOI: https://doi.org/10.1146/annurev.neuro.24.1.167.

Moffet, H.H. 2009. Sham Acupuncture May Be as Efficacious as True Acupuncture: A Systematic Review of Clinical Trials. *The Journal of Alternative and Complementary Medicine*. 15(3):213–216. DOI: https://doi.org/10.1089/acm.2008.0356.

Morecraft, R.J. & van Hoesen, G.W. 1992. Cingulate input to the primary and supplementary motor cortices in the rhesus monkey: Evidence for somatotopy in areas 24c and 23c. *The*

Journal of Comparative Neurology. 322(4):471–489. DOI: https://doi.org/10.1002/cne.903220403.

Morecraft, R.J. & van Hoesen, G.W. 1993. Frontal granular cortex input to the cingulate (M3), supplementary (M2) and primary (M1) motor cortices in the rhesus monkey. *The Journal of Comparative Neurology*. 337(4):669–689. DOI: https://doi.org/10.1002/cne.903370411.

Morecraft, R.J., Stilwell-Morecraft, K.S. & Rossing, W.R. 2004. The Motor Cortex and Facial Expression: *The Neurologist*. 10(5):235–249. DOI: https://doi.org/10.1097/01.nrl.0000138734.45742.8d.

Napadow, V., Lee, J., Kim, J., Cina, S., Maeda, Y., Barbieri, R., Harris, R.E., Kettner, N., et al. 2012. Brain correlates of phasic autonomic response to acupuncture stimulation: An event-related fMRI study. *Human Brain Mapping*. 34(10):2592–2606. DOI: https://doi.org/10.1002/hbm.22091.

Ni, L. & Shi, X. 2011. Effect on neural function of Xingnao Kaiqiao and non-acupoint in treating acute cerebral infarction. *China Journal of Traditional Chinese Medicine and Pharmacy*. 26(5):891–897.

Nickerson, L.D., Smith, S.M., Öngür, D. & Beckmann, C.F. 2017. Using Dual Regression to Investigate Network Shape and Amplitude in Functional Connectivity Analyses. *Frontiers in Neuroscience*. 11:115. DOI: https://doi.org/10.3389/fnins.2017.00115.

Nierhaus, T., Chang, Y., Liu, B., Shi, X., Yi, M., Witt, C.M. & Pach, D. 2019. Somatosensory Stimulation With XNKQ Acupuncture Modulates Functional Connectivity of Motor Areas. *Frontiers in Neuroscience*. 13. DOI: https://doi.org/10.3389/fnins.2019.00147.

Ntsiea, M.V. 2019. Current stroke rehabilitation services and physiotherapy research in South Africa. *South African Journal of Physiotherapy*. 75(1). DOI: https://doi.org/10.4102/sajp.v75i1.475.

Nudo, R.J. 2007. Postinfarct cortical plasticity and behavioral recovery. *Stroke*. 38(2 Suppl):840–5. DOI: https://doi.org/10.1161/01.STR.0000247943.12887.d2.

Ogawa, S., Menon, R.S., Kim, S.-G. . & Ugurbil, K. 1998. ON THE CHARACTERISTICS OF FUNCTIONAL MAGNETIC RESONANCE IMAGING OF THE BRAIN. *Annual Review of Biophysics and Biomolecular Structure*. 27(1):447–474. DOI: https://doi.org/10.1146/annurev.biophys.27.1.447.

Ongür, D., Lundy, M., Greenhouse, I., Shinn, A.K., Menon, V., Cohen, B.M. & Renshaw, P.F. 2010. Default mode network abnormalities in bipolar disorder and schizophrenia. *Psychiatry research*. 183(1):59–68. DOI: https://doi.org/10.1016/j.pscychresns.2010.04.008.

Otti, A. & Noll-Hussong, M. 2012. Acupuncture-Induced Pain Relief and the Human Brain' s Default Mode Network – an Extended View of Central Effects of Acupuncture Analgesia. *Forschende Komplementärmedizin / Research in Complementary Medicine*. 19(4):197–201. DOI: https://doi.org/10.1159/000341928.

Owolabi, M. 2011. Taming the burgeoning stroke epidemic in Africa: stroke quadrangle to the rescue. *PubMed*. 60(4):412–21.

Pa, T., Chen, G., Glen, D.R., Rajendra Jk, Reynolds Rc & Cox Rw. 2018. FMRI processing with AFNI: Some comments and corrections on "Exploring the Impact of Analysis Software on Task fMRI Results". *bioRxiv (Cold Spring Harbor Laboratory)*. (April, 28). DOI: https://doi.org/10.1101/308643.

Paci, M. 2003. PHYSIOTHERAPY BASED ON THE BOBATH CONCEPT FOR ADULTS WITH POST-STROKE HEMIPLEGIA: A REVIEW OF EFFECTIVENESS STUDIES. *Journal of Rehabilitation Medicine*. 35(1):2–7. DOI: https://doi.org/10.1080/16501970306106.

Peng, C.-Y., Chen, Y.-C., Cui, Y., Zhao, D.-L., Jiao, Y., Tang, T.-Y., Ju, S. & Teng, G.-J. 2016. Regional Coherence Alterations Revealed by Resting-State fMRI in Post-Stroke Patients with Cognitive Dysfunction. *PLOS ONE*. 11(7):e0159574. DOI: https://doi.org/10.1371/journal.pone.0159574.

Petrides, M. 2005. Lateral prefrontal cortex: architectonic and functional organization. *Philosophical Transactions of the Royal Society B: Biological Sciences*. 360(1456):781–795. DOI: https://doi.org/10.1098/rstb.2005.1631.

Pollock, A., Baer, G., Campbell, P., Choo, P.L., Forster, A., Morris, J., Pomeroy, V.M. & Langhorne, P. 2014. Physical rehabilitation approaches for the recovery of function and mobility following stroke. *Cochrane Database of Systematic Reviews*. 4(1). DOI: https://doi.org/10.1002/14651858.cd001920.pub3.

Posner, M.I. 2008. Measuring Alertness. *Annals of the New York Academy of Sciences*. 1129(1):193–199. DOI: https://doi.org/10.1196/annals.1417.011.

Rahayu, U.B., Wibowo, S., Setyopranoto, I. & Hibatullah Romli, M. 2020. Effectiveness of physiotherapy interventions in brain plasticity, balance and functional ability in acute stroke survivors: A randomized controlled trial. *NeuroRehabilitation*. 47(4):1–8. DOI: https://doi.org/10.3233/nre-203210.

Raz, A. & Buhle, J. 2006. Typologies of attentional networks. *Nature Reviews Neuroscience*. 7(5):367–379. DOI: https://doi.org/10.1038/nrn1903.

Rehme, A.K. & Grefkes, C. 2013. Cerebral network disorders after stroke: evidence from imaging-based connectivity analyses of active and resting brain states in humans. *The Journal of Physiology*. 591(1):17–31. DOI: https://doi.org/10.1113/jphysiol.2012.243469.

Rhoda, A.J. 2014. Health-related quality of life of patients six months poststroke living in the Western Cape, South Africa. *African Journal of Disability*. 3(1). DOI: https://doi.org/10.4102/ajod.v3i1.126.

Rolls, E.T. 2004. The functions of the orbitofrontal cortex. *Brain and Cognition*. 55(1):11–29. DOI: https://doi.org/10.1016/s0278-2626(03)00277-x.

Rolls, E.T. 2019. The orbitofrontal cortex and emotion in health and disease, including depression. *Neuropsychologia*. 128:14–43. DOI: https://doi.org/10.1016/j.neuropsychologia.2017.09.021.

Schaechter, J.D., Moore, C.I., Connell, B.D., Rosen, B.R. & Dijkhuizen, R.M. 2006. Structural and functional plasticity in the somatosensory cortex of chronic stroke patients. *Brain*. 129(10):2722–2733. DOI: https://doi.org/10.1093/brain/awl214.

Schaechter, J.D., Connell, B.D., Stason, W.B., Kaptchuk, T.J., Krebs, D.E., Macklin, E.A., Schnyer, R.N., Stein, J., et al. 2007. Correlated Change in Upper Limb Function and Motor Cortex Activation After Verum and Sham Acupuncture in Patients with Chronic Stroke. *The Journal of Alternative and Complementary Medicine*. 13(5):527–532. DOI: https://doi.org/10.1089/acm.2007.6316.

Schmithorst, V.J. & Holland, S.K. 2004. Comparison of three methods for generating group statistical inferences from independent component analysis of functional magnetic resonance imaging data. *Journal of Magnetic Resonance Imaging*. 19(3):365–368. DOI: https://doi.org/10.1002/jmri.20009.

Seghier, M.L. 2012. The Angular Gyrus. *The Neuroscientist*. 19(1):43–61. DOI: https://doi.org/10.1177/1073858412440596.

Seitz, R.J., Matyas, T.A. & Carey, L.M. 2008. Neural Plasticity as a Basis for Motor Learning and Neurorehabilitation. *Brain Impairment*. 9(2):103–113. DOI: https://doi.org/10.1375/brim.9.2.103.

Shan, Y., Wang, Z., Zhao, Z., Zhang, M., Hao, S., Xu, J., Shan, B., Lu, J., et al. 2014. An fMRI Study of Neuronal Specificity in Acupuncture: The Multiacupoint Siguan and Its Sham

Point. *Evidence-Based Complementary and Alternative Medicine*. 2014:e103491. DOI: https://doi.org/10.1155/2014/103491.

Shima, K., Aya, K., Mushiake, H., Inase, M., Aizawa, H. & Tanji, J. 1991. Two movement-related foci in the primate cingulate cortex observed in signal-triggered and self-paced forelimb movements. *Journal of Neurophysiology*. 65(2):188–202. DOI: https://doi.org/10.1152/jn.1991.65.2.188.

Shi X, Li J, Yan L. 1992. Clinical observation on acupuncture in stroke treatment. Shang J Acupunct Moxib, 4(2):4–7.

Smith, S.M. 2002. Fast robust automated brain extraction. *Human Brain Mapping*. 17(3):143–155. DOI: https://doi.org/10.1002/hbm.10062.

Smith, S.M. 2012. The future of FMRI connectivity. *NeuroImage*. 62(2):1257–1266. DOI: https://doi.org/10.1016/j.neuroimage.2012.01.022.

Smith, S.M., Jenkinson, M., Woolrich, M.W., Beckmann, C.F., Behrens, T.E.J., Johansen-Berg, H., Bannister, P.R., De Luca, M., et al. 2004. Advances in functional and structural MR image analysis and implementation as FSL. *NeuroImage*. 23:S208–S219. DOI: https://doi.org/10.1016/j.neuroimage.2004.07.051.

Smith, S.M., Fox, P.T., Miller, K.L., Glahn, D.C., Fox, P.M., Mackay, C.E., Filippini, N., Watkins, K.E., et al. 2009. Correspondence of the brain's functional architecture during activation and rest. *Proceedings of the National Academy of Sciences*. 106(31):13040–13045. DOI: https://doi.org/10.1073/pnas.0905267106.

Smitha, K., Akhil Raja, K., Arun, K., Rajesh, P., Thomas, B., Kapilamoorthy, T. & Kesavadas, C. 2017. Resting state fMRI: A review on methods in resting state connectivity analysis and resting state networks. *The Neuroradiology Journal*. 30(4):305–317. DOI: https://doi.org/10.1177/1971400917697342.

Sylvester, C.M., Deanna, M., Maurizio Corbetta, Power, J.D., Schlaggar, B.L. & Luby, J.L. 2013. Resting State Functional Connectivity of the Ventral Attention Network in Children With a History of Depression or Anxiety. *Journal of the American Academy of Child and Adolescent Psychiatry*. 52(12):1326-1336.e5. DOI: https://doi.org/10.1016/j.jaac.2013.10.001.

Taylor, P.A. & Saad, Z.S. 2013. FATCAT: (An Efficient) Functional And Tractographic Connectivity Analysis Toolbox. *Brain Connectivity*. 3(5):523–535. DOI: https://doi.org/10.1089/brain.2013.0154.

Thiel, C.M., Zilles, K. & Fink, G.R. 2004. Cerebral correlates of alerting, orienting and reorienting of visuospatial attention: an event-related fMRI study. *NeuroImage*. 21(1):318–328. DOI: https://doi.org/10.1016/j.neuroimage.2003.08.044.

Tu, W.-J., Wang, L., Yan, F., Peng, B., Yang, H., Liu, M., Ji, X., Ma, L., et al. 2023. China stroke surveillance report 2021. *Military Medical Research*. 10(1). DOI: https://doi.org/10.1186/s40779-023-00463-x.

Tuladhar, A.M., Snaphaan, L., Shumskaya, E., Rijpkema, M., Fernandez, G., Norris, D.G. & de Leeuw, F.-E. 2013. Default Mode Network Connectivity in Stroke Patients. *PLoS ONE*. 8(6):e66556. DOI: https://doi.org/10.1371/journal.pone.0066556.

Uddin, L.Q., Supekar, K. & Menon, V. 2010. Typical and atypical development of functional human brain networks: insights from resting-state fMRI. *Frontiers in Systems Neuroscience*. 4. DOI: https://doi.org/10.3389/fnsys.2010.00021.

Vaughan-Graham, J., Cott, C. & Wright, F.V. 2014. The Bobath (NDT) concept in adult neurological rehabilitation: what is the state of the knowledge? A scoping review. Part I: conceptual perspectives. *Disability and Rehabilitation*. 37(20):1793–1807. DOI: https://doi.org/10.3109/09638288.2014.985802.

Veerbeek, J.M., van Wegen, E., van Peppen, R., van der Wees, P.J., Hendriks, E., Rietberg, M. & Kwakkel, G. 2014. What Is the Evidence for Physical Therapy Poststroke? A Systematic Review and Meta-Analysis. *PLoS ONE*. 9(2):e87987. DOI: https://doi.org/10.1371/journal.pone.0087987.

Vieira, A.I., Almeida, P., Canário, N., Castelo-Branco, M., Nunes, M.V. & Castro-Caldas, A. 2017. Unisensory and multisensory Self-referential stimulation of the lower limb: An exploratory fMRI study on healthy subjects. *Physiotherapy Theory and Practice*. 34(1):22–40. DOI: https://doi.org/10.1080/09593985.2017.1368758.

Viviani, R. 2013. Emotion regulation, attention to emotion, and the ventral attentional network. *Frontiers in Human Neuroscience*. 7. DOI: https://doi.org/10.3389/fnhum.2013.00746.

Vogt, B.A. 2005. Pain and emotion interactions in subregions of the cingulate gyrus. *Nature Reviews Neuroscience*. 6(7):533–544. DOI: https://doi.org/10.1038/nrn1704.

Wang, L., Yu, C., Chen, H., Qin, W., He, Y., Fan, F., Zhang, Y., Wang, M., et al. 2010. Dynamic functional reorganization of the motor execution network after stroke. *Brain*. 133(4):1224–1238. DOI: https://doi.org/10.1093/brain/awq043.

Ward, N.S. & Cohen, L.G. 2004. Mechanisms Underlying Recovery of Motor Function After Stroke. *Archives of Neurology*. 61(12). DOI: https://doi.org/10.1001/archneur.61.12.1844.

Weiss, T., Hansen, E., Beyer, L., Conradi, M.-L., Merten, F., Nichelmann, C., Rost, R. & Zippel, C. 1994. Activation processes during mental practice in stroke patients. *International Journal of Psychophysiology*. 17(1):91–100. DOI: https://doi.org/10.1016/0167-8760(94)90059-0.

Wig, G.S., Laumann, T.O., Cohen, A.T., Power, J.D., Nelson, S.M., Glasser, M.F., Miezin, F.M., Snyder, A.Z., et al. 2014. Parcellating an Individual Subject's Cortical and Subcortical Brain Structures Using Snowball Sampling of Resting-State Correlations. *Cerebral Cortex*. 24(8):2036–2054. DOI: https://doi.org/10.1093/cercor/bht056.

Winkler, A.M., Ridgway, G.R., Webster, M.A., Smith, S.M. & Nichols, T.E. 2014. Permutation inference for the general linear model. *NeuroImage*. 92:381–397. DOI: https://doi.org/10.1016/j.neuroimage.2014.01.060.

Wolf, S.L., Catlin, P.A., Ellis, M., Archer, A.L., Morgan, B. & Piacentino, A. 2001. Assessing Wolf Motor Function Test as Outcome Measure for Research in Patients After Stroke. *Stroke*. 32(7):1635–1639. DOI: https://doi.org/10.1161/01.str.32.7.1635.

Wong, N.M.L., Ma, E.P.-W. & Lee, T.M.C. 2017. The Integrity of the Corpus Callosum Mitigates the Impact of Blood Pressure on the Ventral Attention Network and Information Processing Speed in Healthy Adults. *Frontiers in Aging Neuroscience*. 9. DOI: https://doi.org/10.3389/fnagi.2017.00108.

World Health Organization. 2013. WHO traditional medicine strategy: 2014–2023. *Geneva: World Health Organization.*

Wu, C., Qu, S., Zhang, J., Chen, J., Zhang, S., Li, Z., Chen, J., Ouyang, H., et al. 2014. Correlation between the Effects of Acupuncture atTaichong(LR3) and Functional Brain Areas: A Resting-State Functional Magnetic Resonance Imaging Study Using True versus Sham Acupuncture. *Evidence-Based Complementary and Alternative Medicine*. 2014:1–7. DOI: https://doi.org/10.1155/2014/729091.

Wu, L.-K., Hung, C.-S., Kung, Y.-L., Chen, Z.-K., Lin, S.-Z., Lin, J.-G. & Ho, T.-J. 2022. Efficacy of Acupuncture Treatment for Incidence of Poststroke Comorbidities: A Systematic Review and Meta-Analysis of Nationalized Cohort Studies. *Evidence-Based Complementary and Alternative Medicine*. 2022(1):1–12. DOI: https://doi.org/10.1155/2022/3919866.

Wu, P., Zhou, Y., Liao, C., Tang, Y., Li, Y., Qiu, L., Qin, W., Zeng, F., et al. 2018. Structural Changes Induced by Acupuncture in the Recovering Brain after Ischemic Stroke. *Evidence-*

Based Complementary and Alternative Medicine. 2018:1–8. DOI: https://doi.org/10.1155/2018/5179689.

Wu, X., Li, R., Fleisher, A.S., Reiman, E.M., Guan, X., Zhang, Y., Chen, K. & Yao, L. 2011. Altered default mode network connectivity in alzheimer's disease-A resting functional MRI and bayesian network study. *Human Brain Mapping*. 32(11):1868–1881. DOI: https://doi.org/10.1002/hbm.21153.

Xie, C., Luo, Y., Pang, Y., Gao, X., Li, M., Wen, H. & Chen Rui-fang. 2014. [Effect of electroacupuncture on CD 34+ endothelial progenitor cell counts in bone marrow and peripheral blood in focal cerebral ischemia/reperfusion rats]. *PubMed*. 39(6):437–42.

Xu, J., Pei, J., Fu, Q., Wang, L.-Y., Zhan, Y.-J. & Tao, L. 2020. Earlier Acupuncture Enhancing Long-Term Effects on Motor Dysfunction in Acute Ischemic Stroke: Retrospective Cohort Study. *The American Journal of Chinese Medicine*. 48(08):1787–1802. DOI: https://doi.org/10.1142/s0192415x20500895.

Zago, L., Pesenti, M., Mellet, E., Crivello, F., Mazoyer, B. & Tzourio-Mazoyer, N. 2001. Neural Correlates of Simple and Complex Mental Calculation. *NeuroImage*. 13(2):314–327. DOI: https://doi.org/10.1006/nimg.2000.0697.

Zhang, Y. 2021. Interpretation of acupoint location in traditional Chinese medicine teaching: Implications for acupuncture in research and clinical practice. *The Anatomical Record*. 304(11):2372–2380. DOI: https://doi.org/10.1002/ar.24618.

Zhang, W., Wang, J., Fan, L., Zhang, Y., Fox, P.T., Eickhoff, S.B., Yu, C. & Jiang, T. 2016. Functional organization of the fusiform gyrus revealed with connectivity profiles. *Human Brain Mapping*. 37(8):3003–3016. DOI: https://doi.org/10.1002/hbm.23222.

Zhang, Y., Li, K., Ren, Y., Cui, F., Xie, Z., Shin, J.-Y., Tan, Z., Tang, L., et al. 2014. Acupuncture Modulates the Functional Connectivity of the Default Mode Network in Stroke Patients. *Evidence-Based Complementary and Alternative Medicine*. 2014:1–7. DOI: https://doi.org/10.1155/2014/765413.

Zhang, Y., Zhang, H., Nierhaus, T., Pach, D., Witt, C.M. & Yi, M. 2019. Default Mode Network as a Neural Substrate of Acupuncture: Evidence, Challenges and Strategy. *Frontiers in Neuroscience*. 13(100). DOI: https://doi.org/10.3389/fnins.2019.00100.

Zhang, Y., Chen, Q., Wang, Q., Ding, S., Li, S., Chen, S., Lin, X., Li, C., et al. 2020. Role of Parameter Setting in Electroacupuncture: Current Scenario and Future Prospects. *Chinese Journal of Integrative Medicine*. (July, 20). DOI: https://doi.org/10.1007/s11655-020-3269-2.

Zhang, Z.-J., Chen, H.-Y., Yip, K., Ng, R. & Wong, V.T. 2010. The effectiveness and safety of acupuncture therapy in depressive disorders: Systematic review and meta-analysis. *Journal of Affective Disorders*. 124(1-2):9–21. DOI: https://doi.org/10.1016/j.jad.2009.07.005.

Zhao, L., Liu, J., Zhang, F., Dong, X., Peng, Y., Qin, W., Wu, F., Li, Y., et al. 2014. Effects of Long-Term Acupuncture Treatment on Resting-State Brain Activity in Migraine Patients: A Randomized Controlled Trial on Active Acupoints and Inactive Acupoints. *PLoS ONE*. 9(6):e99538. DOI: https://doi.org/10.1371/journal.pone.0099538.

Zheng, F., Cao, P., Zhou, J., Li, C. & Norris, J. 2020. Study on Neurologic and Cognitive Dysfunction in Breast Cancer Patients Undergoing Chemotherapy with Resting State fMRI. *World Neurosurgery*. 149. DOI: https://doi.org/10.1016/j.wneu.2020.10.088.

Zhong, C., Bai, L., Dai, R., Xue, T., Wang, H., Feng, Y., Liu, Z., You, Y., et al. 2011. Modulatory effects of acupuncture on resting-state networks: A functional MRI study combining independent component analysis and multivariate granger causality analysis. *Journal of Magnetic Resonance Imaging*. 35(3):572–581. DOI: https://doi.org/10.1002/jmri.22887.

Zhou, S.-Y., Zeng, F., Liu, J., Zheng, H., Huang, W., Liu, T., Chen, D.-S., Qin, W., et al. 2013. Influence of Acupuncture Stimulation on Cerebral Network in Functional Diarrhea. *Evidence-based complementary and alternative medicine*. 2013:1–9. DOI: https://doi.org/10.1155/2013/975769.

Zhu, J., Li, J., Yang, L. & Liu, S. 2021. Acupuncture, from the ancient to the current. *The Anatomical Record*. 304(11):2365–2371. DOI: https://doi.org/10.1002/ar.24625.

Appendix A

This appendix contains codes used during pre-processing of the rs-fMRI data.

Pre-processing Codes

1. afni-proc.py

The following afni-proc.py code was used during pre-processing:

```
#!/bin/tcsh

set here = $PWD

set namelist = `ls -d *`

foreach pref ($namelist)
    cd $here/$pref
#   echo "I am here now: $PWD"
#   echo $pref


## input data sets
set rest_set = "${pref}_rest.nii.gz"
set anat_set = "${pref}_T1.nii.gz"

# output file prefix
set sub_name = "${pref}_proc"
#!!! MAYBE MAKE RPI FIRST TO BE SURE?

afni_proc.py \
    -subj_id ${sub_name}                                                \
                -dsets ${rest_set}                                          \
                -copy_anat ${anat_set}                                          \
                -blocks despike tshift align tlrc volreg blur mask regress     \
                -tcat_remove_first_trs 4                                        \
          -align_opts_aea -cost lpc+ZZ -giant_move                  \
                -volreg_align_e2a                                           \
                -volreg_tlrc_warp                                           \
          -tlrc_base /home/sone/researchdata_mri/UserFolders/Sone/NewData/Cut_Volumes/
          TT_N27_RPI_111.nii.gz                                         \
          -tlrc_NL_warp                         \
                -blur_size 6.0                                              \
                -mask_apply epi                                             \
                -mask_segment_anat yes                                      \
                -regress_bandpass 0.01 0.1                                  \
                -regress_apply_mot_types demean deriv                       \
                -regress_ROI WMe CSFe                                   \
                -regress_RSFC                                               \
                -regress_run_clustsim no                                    \
                -regress_est_blur_errts

tcsh -xef proc.${sub_name} |& tee output.proc.${sub_name}

cd "$sub_name".results

3dcopy RSFC_LFF_rall_$sub_name+tlrc. RSFC_LFF_rall_$sub_name.nii.gz

end


echo "\n\tDONE.\n"

```

2. Motion testing codes

The following two codes were used to assess the motion of each participant during the MRI scan:

```
#!/bin/tcsh -xef
### Run from Documents


##Goes through all subjects, showing their motion graphs and tells which should be included or excluded  (based on choice of inputs)

##NB: F_flag_motion.py must be in the same folder as the data to be processed.



###################################
#### INPUTS
###################################
    set thresh = 3
    set min_TR = 158
    set min_partial = 130
###################################



###################################
 #### VARIABLES
###################################
     set script =  /home/sone/researchdata_mri/UserFolders/Sone/NewData/Cut_Volumes/A1
      set input = /home/sone/researchdata_mri/UserFolders/Sone/NewData/Cut_Volumes/A1
###################################




     set A = 0   ##count for full recovery
     set B = 0   ##count for partial recovery

     set sub_1 = ()
     set min_1 = ()
     set max_1 = ()
     set index_1 = ()
     set TR_1 = ()

     set sub_2 = ()
     set min_2 = ()
     set max_2 = ()
     set index_2 = ()
     set TR_2 = ()

 #1) GET SUBJECT LIST
     cd $input
     set sub_list = `ls -d *`
     set sub_count = ${#sub_list}

#2) HEADING FOR TEXTFILE
        echo "SCRIPT TO CHECK ALL THE SUBJECTS WITH MOTION ABOVE LIMIT TO SEE IF ANY CAN BE RECOVERED"      >> MOTION_OK.txt
       echo ""
                     >> MOTION_OK.txt
       echo "THRESHOLD = $thresh mm"
                                                                                >>
       MOTION_OK.txt
       echo "MIN TRS that need to be below THRESHOLD limit = $min_TR"
                                            >> MOTION_OK.txt
       echo "MIN TRS that need to be below THRESHOLD limit for PARTIAL RECOVERY = $min_partial"            >> MOTION_OK.txt
       echo "_____________________________________________"                >>
       MOTION_OK.txt
      printf "%-10s %-10s %-10s %-10s %-10s %-10s %-10s %-10s\n" 'SUBJECT' '# OLD' '# NEW' 'INDEX' 'min old' 'max old' 'min new' 'max new' >> MOTION_OK.txt

#3) FOR LOOP: DO MOTION CALCULATIONS
    foreach sub ($sub_list)
       cd $input
       set  volreg_file = $input/${sub}/${sub}_proc.results/dfile_rall.1D
```

```
64
65      #INPUTS: python script
66      set out = `python zF_flag_motion.py -i $volreg_file -s $sub -t $thresh -n $min_TR`
67
68  echo hello
69      echo $out[0] > out.${sub}.txt
70      echo $out[1] >> out.${sub}.txt
71      echo $out[2] >> out.${sub}.txt
72      echo $out[3] >> out.${sub}.txt
73      echo $out[4] >> out.${sub}.txt
74
75      #IF STATEMENT: determine if it can be recovered
76
77      ## FULL RECOVERY
78        if (($out[1] >= $min_TR) || ($out[4] >= $min_TR)) then   ## FULL RECOVERY
          (11111111)
79
80          ## NEW INDEX
81          if ($out[4] > $out[1]) then                ## if new TR > old TR
82              set sub_1 = ($sub_1:q $sub)
83              set min_1 = ($min_1:q $out[5])         ## min = new min
84              set max_1 = ($max_1:q $out[6])         ## max = new max
85              set index_1 = ($index_1:q $out[7])     ## Index = new index
86              set TR_1 = ($TR_1:q $out[4])           ## num TR  = new num of TR
87              @ A++
88          else    ## OLD INDEX
89              set sub_1 = ($sub_1:q $sub)
90              set min_1 = ($min_1:q $out[2])         ## min = old min
91              set max_1 = ($max_1:q $out[3])         ## max = old max
92              set index_1 = ($index_1:q '2')           ## Index = old index
93              set TR_1 = ($TR_1:q $out[1])           ## num TR  = old num of TR
94              @ A++
95          endif
96
97        else if (($out[1] >= $min_partial) || ($out[4] >= $min_partial)) then  ##
          PARTIAL RECOVERY (2222222)
98
99          ## NEW INDEX
100         if ($out[4] > $out[1]) then                ## if new TR > old TR
101             set sub_2 = ($sub_2:q $sub)
102             set min_2 = ($min_2:q $out[5])         ## min = new min
103             set max_2 = ($max_2:q $out[6])         ## max = new max
104             set index_2 = ($index_2:q $out[7])     ## Index = new index
105             set TR_2 = ($TR_2:q $out[4])           ## num TR  = new num of TR
106             @ B++
107         else    ## OLD INDEX
108             set sub_2 = ($sub_2:q $sub)
109             set min_2 = ($min_2:q $out[2])         ## min = old min
110             set max_2 = ($max_2:q $out[3])         ## max = old max
111             set index_2 = ($index_2:q '2')           ## Index = old index
112             set TR_2 = ($TR_2:q $out[1])           ## num TR  = old num of TR
113             @ B++
114         endif
115
116      else echo "none"
117      endif   ## end recovery if statement
118
119     #TEXT FILE
120        cd $input
121        printf "%-10s %-10d %-10d %-10d %-10d %-10d %-10d %-10d\n" $sub $out[1] $out[4]
           $out[7] $out[2] $out[3] $out[5] $out[6]  >> MOTION_OK.txt
122     end  ##end for loop
123
124 #4) TEXT FILE
125      cd $input
126      echo "_____"
                                                >> MOTION_OK.txt
127      echo "NUMBER OF TOTAL SUBJECTS FOUND IN ELIMINATED MOTION FOLDER (INPUT):
         $sub_count"  >> MOTION_OK.txt
128      echo "      "                       >> MOTION_OK.txt
129
130      echo "FULL RECOVERY INFO: ($A subjects)       " >> MOTION_OK.txt
131      echo "     Subject: $sub_1"           >> MOTION_OK.txt
```

```
132         echo "     Min:     $min_1"           >> MOTION_OK.txt
133         echo "     Max:     $max_1"           >> MOTION_OK.txt
134         echo "     Index:   $index_1"         >> MOTION_OK.txt
135         echo "     TR:      $TR_1"            >> MOTION_OK.txt
136
137         echo "      "                        >> MOTION_OK.txt
138         echo "PARTIAL RECOVERY INFO: ($B subjects)      " >> MOTION_OK.txt
139         echo "     Subject: $sub_2"          >> MOTION_OK.txt
140         echo "     Min:     $min_2"          >> MOTION_OK.txt
141         echo "     Max:     $max_2"          >> MOTION_OK.txt
142         echo "     Index:   $index_2"        >> MOTION_OK.txt
143         echo "     TR:      $TR_2"           >> MOTION_OK.txt
144
145         notepad++ MOTION_OK.txt
146
147
148
```

```
#!/usr/bin/python3

# Simple Python program to give useful information about volreg output
# files from afni_proc.py.
#
# The user inputs:
#    -i "the volreg file"
#    -s "a subject identity"
#    -t "a numerical threshold for motion"
#    -n "a minimum number of time points for having sub-threshold motion"
# and then the output is simply a line of three numbers:
#    [Max. consec. non-motion points] [min brik index] [max brik index]
# and that's that.
#
# Version 1.0, Feb, 2014.
# written:  PA Taylor and J Toich, UCT.
#
# run from command line using, for example:
# $ python flag_motion -i INFILE -s SUBJ -t THRESH -n N_PTS
#


import numpy as np
import matplotlib.pyplot as plt
import getopt, sys

Ncol = 6

whichcol = ['Tx','Ty','Tz','Rx','Ry','Rz']


def main(argv):
    '''Basic reading in of commandline options.'''
    help_line = 'flag_motion.py -i INFILE -s SUBJECT -t THR_MOT -n N_POINTS'
    file1 = ''
    sub_name = ''
    THRESH = -1
    min_consec = -1
    try:
        opts, args = getopt.getopt(argv,"hi:s:t:n:",["infile=","subname=",
                                                     "thresh=","npoints="])
    except getopt.GetoptError:
        print (help_line)
        sys.exit(2)
    for opt, arg in opts:
        if opt == '-h':
            print (help_line)
            sys.exit()
        elif opt in ("-i", "--infile"):
            file1 = arg
        elif opt in ("-s", "--subname"):
            sub_name = arg
        elif opt in ("-t", "--thresh"):
            THRESH = float(arg)
        elif opt in ("-n", "--npoints"):
            min_consec = int(arg)

    if (file1 == '') or (sub_name == '' ) or \
         (THRESH == -1) or (min_consec == -1):
        print ("**ERROR with one of the inputs")
        sys.exit()

    return file1, sub_name, THRESH, min_consec



def search_bads( Y, THRESH ):
    N, Ncol = np.shape(Y)
    Z = np.zeros(N)            # binarized set, flag bad motion

    bads = [-1]
    for i in range(N):
```

```
            for j in range( Ncol ):
                if abs(Y[i][j]) > THRESH and Z[i]==0:
                    Z[i] = 1
                    bads.append(i)
        bads.append(N)

        max_diff, bad1, bad2 = longest_nonbadness( bads )

        return Z, max_diff, bad1, bad2

    def longest_nonbadness( bads ):
        N = bads[-1] # because we stored the value in previous use

        bads_diff = np.zeros(len(bads)-1,dtype='int')
        max_diff = -1
        bad1 = 0
        bad2 = N - 1
        for i in range(len(bads)-1):
            bads_diff[i] = bads[i+1] - bads[i] - 1
            if bads_diff[i] > max_diff :
                max_diff = bads_diff[i]
                bad1 = bads[i]+1
                bad2 = bads[i+1]-1

        if max_diff == -1 :
            max_diff = N

        return max_diff, bad1, bad2




    ###########################################################################

    if __name__=="__main__":
        np.set_printoptions(linewidth=200)

        file1, sub_name, THRESH, min_consec = main(sys.argv[1:])

        # read in 6 colume file
        fff = open(file1,'r')
        x = fff.readlines()
        fff.close()

        N = len(x)

        # go through each time point, convert to floats, binarize based
        # on thresh
        Y = np.zeros( ( N, Ncol )) # stores integrated motion with current ref

        for i in range(N):
            Y[i,:] = np.array(x[i].split(),dtype=np.float32)

        # get binarized badness and list of bad intervals
        Z, max_diff, bad1, bad2 = search_bads( Y, THRESH )

        NEW_BASE = 0
        if max_diff >= min_consec:
            title1 = "YIPPEE! Usable. Max number of points: %d  [%d, %d]" % \
             ( max_diff, bad1, bad2 )
            make_col = 'green'
        else:
            title1 = "BOOO! Not usable. Max number of points: %d  [%d, %d]" % \
             ( max_diff, bad1, bad2 )
            make_col = 'red'
            NEW_BASE = 1

        reftobeat = -1
        if NEW_BASE:

            maxtobeat = max_diff
```

```
145
146         X = np.zeros( ( N, Ncol )) # stores different motion, find better ref?
147         for i in range(1,N):
148             for j in range( Ncol ):
149                 X[i][j] = Y[i][j] - Y[i-1][j]
150
151         for k in range(N):
152             V_temp = np.zeros( ( N, Ncol )) # simulated integrated motion
153
154             for j in range( Ncol ):
155                 for i in range(k+1,N):
156                     V_temp[i][j] = V_temp[i-1][j]+X[i][j]
157                 for i in range(k-1,0-1,-1):
158                     V_temp[i][j] = V_temp[i+1][j]-X[i+1][j]
159
160             # give this synthetic one the treatment
161             VZ_temp, Vmax_diff_temp, Vbad1_temp, Vbad2_temp = search_bads( V_temp,
                THRESH )
162
163             #print Vmax_diff_temp,  maxtobeat
164             if Vmax_diff_temp > maxtobeat:
165                 #print "YAY"
166                 maxtobeat = Vmax_diff_temp
167                 reftobeat = k
168                 VZ, Vmax_diff, Vbad1, Vbad2 = VZ_temp, Vmax_diff_temp, Vbad1_temp,
                    Vbad2_temp
169                 V = V_temp
170
171
172     if not(reftobeat ==-1):
173         #print "NEW REFBRICK CHAMP", reftobeat
174         print (max_diff, bad1, bad2, Vmax_diff, Vbad1, Vbad2, reftobeat)
175         if Vmax_diff >= min_consec:
176             Vtitle1 = "WELL, TRY new ref=%d. Max number of points: %d  [%d, %d]" % \
177               ( reftobeat, Vmax_diff, Vbad1, Vbad2 )
178             Vmake_col = 'green'
179         else:
180             Vtitle1 = "BOOO! Still Unusable. Max number of points: %d  [%d, %d]" % \
181               ( Vmax_diff, Vbad1, Vbad2 )
182             Vmake_col = 'red'
183     else:
184         #print "Couldn't do better than original. Sorry."
185         VZ, Vmax_diff, Vbad1, Vbad2 = Z, max_diff, bad1, bad2
186
187         print (max_diff, bad1, bad2, -1, -1, -1, -1)
188
189     ################################# PLOTTING ############################
190
191     figg = plt.figure("SUBJECT: "+sub_name,figsize=(15,8))
192
193     # ------------------> binary motion plot <------------------ #
194     subb = plt.subplot(221)
195     plt.title(title1)
196     subb.axhline(color='gray')
197     #for k in range( Ncol ):
198     subb.plot( Z, color=make_col,lw=2 )
199     goodie = np.arange(bad1, bad2+1)
200     subb.plot(goodie ,0.5*np.ones(len(goodie)), \
201                   color='k', marker='*', mew=0 )
202     plt.ylabel('Binarized')
203     plt.ylim([-0.1,1.1])
204     plt.xlim([0,N])
205
206     abscissa = list(np.arange(0,N,25))
207     if not(abscissa[-1] == N-1) :
208         abscissa.append(N-1)
209     plt.xticks( abscissa )
210
211     #box = subb.get_position()
212     #subb.set_position([box.x0, box.y0 , \
213     #                       box.x0+box.width*0.9, box.height])
214
```

```
215       # ------------------> Actual motion plot <------------------ #
216       view_thr_up = 0
217       view_thr_down = 0
218       subb3 = plt.subplot(223)
219       subb3.axhline(color='gray')
220       for k in range( Ncol ):
221           subb3.plot(Y[:,k], lw=1.5, label=whichcol[k] )
222           if Y[:,k].max() > THRESH:
223               view_thr_up = 1
224           if Y[:,k].min() < -THRESH :
225               view_thr_down = 1
226       if view_thr_up:
227           subb3.plot(np.arange(N),THRESH*np.ones(N), \
228                      'k--', lw=1.5)
229       if view_thr_down:
230           subb3.plot(np.arange(N),-THRESH*np.ones(N), \
231                      'k--', lw=1.5)
232
233       plt.xlim([0,N])
234       plt.ylabel('Float Mot.')
235       abscissa = list(np.arange(0,N,25))
236       if not(abscissa[-1] == N-1) :
237           abscissa.append(N-1)
238       plt.xticks( abscissa )
239
240       box3 = subb3.get_position()
241       sqz = 0.1
242       #subb3.set_position([box3.x0, box3.y0 + box3.height*sqz*1.0, \
243        #                   box3.x0+box.width*0.9, box3.height * 1.0*(1 - sqz)])
244       ncols = Ncol #if (Ncol < 4 ) else 3
245       subb3.legend(loc='upper center', ncol=ncols, borderpad=0.2, \
246                    bbox_to_anchor = (.5, -1.*sqz), fontsize=11)
247
248
249           # ------------------> binary motion plot <------------------ #
250       if not(reftobeat ==-1):
251           subb2 = plt.subplot(222)
252           plt.title(Vtitle1)
253           subb2.axhline(color='gray')
254           #for k in range( Ncol ):
255           subb2.plot( VZ, color=Vmake_col,lw=2 )
256           Vgoodie = np.arange(Vbad1, Vbad2+1)
257           subb2.plot(Vgoodie ,0.5*np.ones(len(Vgoodie)), \
258                      color='k', marker='*', mew=0 )
259           plt.ylabel('BinarizedV')
260           plt.ylim([-0.1,1.1])
261           plt.xlim([0,N])
262
263           abscissa = list(np.arange(0,N,25))
264           if not(abscissa[-1] == N-1) :
265               abscissa.append(N-1)
266           plt.xticks( abscissa )
267
268           box2 = subb2.get_position()
269           #subb2.set_position([box2.x0, box2.y0 , \
270           #                    box2.x0+box2.width*0.9, box2.height])
271
272           # ------------------> Actual motion plot of copy <------------------ #
273           view_thr_up = 0
274           view_thr_down = 0
275           subb4 = plt.subplot(224)
276           subb4.axhline(color='gray')
277           for k in range( Ncol ):
278               subb4.plot(V[:,k], lw=1.5, label=whichcol[k] )
279               if V[:,k].max() > THRESH:
280                   view_thr_up = 1
281               if V[:,k].min() < -THRESH :
282                   view_thr_down = 1
283           if view_thr_up:
284               subb4.plot(np.arange(N),THRESH*np.ones(N), \
285                          'k--', lw=1.5)
286           if view_thr_down:
```

```
287             subb4.plot(np.arange(N),-THRESH*np.ones(N), \
288                        'k--', lw=1.5)
289
290         plt.xlim([0,N])
291         plt.ylabel('Float Mot.')
292         abscissa = list(np.arange(0,N,25))
293         if not(abscissa[-1] == N-1) :
294             abscissa.append(N-1)
295         plt.xticks( abscissa )
296
297         #box = subb4.get_position()
298         #sqz = 0.1
299         #subb4.set_position([box.x0, box.y0 + box.height*sqz*1.0, \
300         #                    box.x0+box.width*0.9, box.height * 1.0*(1 - sqz)])
301         #ncols = Ncol #if (Ncol < 4 ) else 3
302         #plt.legend(loc='upper center', ncol=ncols, borderpad=0.2, \
303         #               bbox_to_anchor = (.5, -1.*sqz), fontsize=11)
304
305
306     # ------------------> save and show the plot <------------------ #
307     name_out = "zcheck_motion_fig"
308     plt.savefig(name_out+'_'+sub_name+'.pdf')
309     plt.savefig(name_out+'_'+sub_name+'.png')
310
311     #plt.ion()
312     #plt.show()
313
```

Appendix B

This appendix contains codes that were used during the data analysis of the rs-fMRI data.

1. MELODIC-FSL Code

The following code was used during ICA:

```
melodic -i RSFC_LFF_rall_MRKY-JK01-004_proc.nii_masked.nii.gz,RSFC_LFF_rall_MRKY-JK02-
004_proc.nii_masked.nii.gz,RSFC_LFF_rall_MRKY-JK03-
004_proc.nii_masked.nii.gz,RSFC_LFF_rall_MRKY-JK04-
004_proc.nii_masked.nii.gz,RSFC_LFF_rall_MRKY-JK05-
004_proc.nii_masked.nii.gz,RSFC_LFF_rall_MRKY-JK07-
004_proc.nii_masked.nii.gz,RSFC_LFF_rall_MRKY-JK08-
004_proc.nii_masked.nii.gz,RSFC_LFF_rall_MRKY-JK09-
004_proc.nii_masked.nii.gz,RSFC_LFF_rall_MRKY-JK10-004_proc.nii_masked.nii.gz -o
Melodic_Results_CT -d 20
```

2. Dual regression Codes

The following codes were used during dual regression:

2.1. After treatment scans

```
dual_regression melodic_IC.nii.gz 1 GLM_Groups/GLM_Groups23.mat GLM_Groups/GLM_Groups23.con
0 DualRegressionCT_AT_Groups RSFC_LFF_rall_MRKY107-2_proc.nii_masked.nii.gz
RSFC_LFF_rall_MRKY108-2_proc.nii_masked.nii.gz RSFC_LFF_rall_MRKY109-
2_proc.nii_masked.nii.gz RSFC_LFF_rall_MRKY110-2_proc.nii_masked.nii.gz
RSFC_LFF_rall_MRKY111-2_proc.nii_masked.nii.gz RSFC_LFF_rall_MRKY112-
2_proc.nii_masked.nii.gz RSFC_LFF_rall_MRKY113-2_proc.nii_masked.nii.gz
RSFC_LFF_rall_MRKY115-2_proc.nii_masked.nii.gz RSFC_LFF_rall_MRKY116-
2_proc.nii_masked.nii.gz RSFC_LFF_rall_MRKY117-2_proc.nii_masked.nii.gz
RSFC_LFF_rall_MRKY118-2_proc.nii_masked.nii.gz RSFC_LFF_rall_MRKY119-
2_proc.nii_masked.nii.gz RSFC_LFF_rall_MRKY120-2_proc.nii_masked.nii.gz
RSFC_LFF_rall_MRKY122-2_proc.nii_masked.nii.gz RSFC_LFF_rall_MRKY123-
2_proc.nii_masked.nii.gz RSFC_LFF_rall_MRKY124-2_proc.nii_masked.nii.gz
RSFC_LFF_rall_MRKY125-2_proc.nii_masked.nii.gz RSFC_LFF_rall_MRKY126-
2_proc.nii_masked.nii.gz RSFC_LFF_rall_MRKY127-2_proc.nii_masked.nii.gz
RSFC_LFF_rall_MRKY128-2_proc.nii_masked.nii.gz RSFC_LFF_rall_MRKY129-
2_proc.nii_masked.nii.gz RSFC_LFF_rall_MRKY130-2_proc.nii_masked.nii.gz
RSFC_LFF_rall_MRKY131-2_proc.nii_masked.nii.gz
```

2.2. Before treatment scans:

```
dual_regression melodic_IC.nii.gz 1 GLM23.mat GLM23.con 0 DualRegression_BT
Masked_RSFC/RSFC_LFF_rall_MRKY107-1_proc.nii_masked.nii.gz
Masked_RSFC/RSFC_LFF_rall_MRKY108-1_proc.nii_masked.nii.gz
Masked_RSFC/RSFC_LFF_rall_MRKY109-1_proc.nii_masked.nii.gz
Masked_RSFC/RSFC_LFF_rall_MRKY110-1_proc.nii_masked.nii.gz
Masked_RSFC/RSFC_LFF_rall_MRKY111-1_proc.nii_masked.nii.gz
Masked_RSFC/RSFC_LFF_rall_MRKY112-1_proc.nii_masked.nii.gz
Masked_RSFC/RSFC_LFF_rall_MRKY113-1_proc.nii_masked.nii.gz
Masked_RSFC/RSFC_LFF_rall_MRKY115-1_proc.nii_masked.nii.gz
Masked_RSFC/RSFC_LFF_rall_MRKY116-1_proc.nii_masked.nii.gz
Masked_RSFC/RSFC_LFF_rall_MRKY117-1_proc.nii_masked.nii.gz
Masked_RSFC/RSFC_LFF_rall_MRKY118-1_proc.nii_masked.nii.gz
Masked_RSFC/RSFC_LFF_rall_MRKY119-1_proc.nii_masked.nii.gz
Masked_RSFC/RSFC_LFF_rall_MRKY120-1_proc.nii_masked.nii.gz
Masked_RSFC/RSFC_LFF_rall_MRKY122-1_proc.nii_masked.nii.gz
Masked_RSFC/RSFC_LFF_rall_MRKY123-1_proc.nii_masked.nii.gz
Masked_RSFC/RSFC_LFF_rall_MRKY124-1_proc.nii_masked.nii.gz
Masked_RSFC/RSFC_LFF_rall_MRKY125-1_proc.nii_masked.nii.gz
Masked_RSFC/RSFC_LFF_rall_MRKY126-1_proc.nii_masked.nii.gz
Masked_RSFC/RSFC_LFF_rall_MRKY127-1_proc.nii_masked.nii.gz
Masked_RSFC/RSFC_LFF_rall_MRKY128-1_proc.nii_masked.nii.gz
```

```
Masked_RSFC/RSFC_LFF_rall_MRKY129-1_proc.nii_masked.nii.gz
Masked_RSFC/RSFC_LFF_rall_MRKY130-1_proc.nii_masked.nii.gz
Masked_RSFC/RSFC_LFF_rall_MRKY131-1_proc.nii_masked.nii.gz
```

2.3. Healthy Controls

```
dual_regression ../Melodic_Results_CT/melodic_IC.nii.gz 1 ../GLM_Groups/GLM_CT_9.mat
../GLM_Groups/GLM_CT_9.con 0 ../DualRegression_CT RSFC_LFF_rall_MRKY-JK01-
004_proc.nii_masked.nii.gz RSFC_LFF_rall_MRKY-JK02-004_proc.nii_masked.nii.gz
RSFC_LFF_rall_MRKY-JK03-004_proc.nii_masked.nii.gz RSFC_LFF_rall_MRKY-JK04-
004_proc.nii_masked.nii.gz RSFC_LFF_rall_MRKY-JK05-004_proc.nii_masked.nii.gz
RSFC_LFF_rall_MRKY-JK07-004_proc.nii_masked.nii.gz RSFC_LFF_rall_MRKY-JK08-
004_proc.nii_masked.nii.gz RSFC_LFF_rall_MRKY-JK09-004_proc.nii_masked.nii.gz
RSFC_LFF_rall_MRKY-JK10-004_proc.nii_masked.nii.gz
```

2.4. Before and after treatment scans combined

```
dual_regression Melodic_Results_CT/melodic_IC.nii.gz 1 GLM_46/GLM.mat GLM_46/GLM.con 0
DualRegression_BAT Masked_RSFC/RSFC_LFF_rall_MRKY107-1_proc.nii_masked.nii.gz
Masked_RSFC/RSFC_LFF_rall_MRKY107-2_proc.nii_masked.nii.gz
Masked_RSFC/RSFC_LFF_rall_MRKY108-1_proc.nii_masked.nii.gz
Masked_RSFC/RSFC_LFF_rall_MRKY108-2_proc.nii_masked.nii.gz
Masked_RSFC/RSFC_LFF_rall_MRKY109-1_proc.nii_masked.nii.gz
Masked_RSFC/RSFC_LFF_rall_MRKY109-2_proc.nii_masked.nii.gz
Masked_RSFC/RSFC_LFF_rall_MRKY110-1_proc.nii_masked.nii.gz
Masked_RSFC/RSFC_LFF_rall_MRKY110-2_proc.nii_masked.nii.gz
Masked_RSFC/RSFC_LFF_rall_MRKY111-1_proc.nii_masked.nii.gz
Masked_RSFC/RSFC_LFF_rall_MRKY111-2_proc.nii_masked.nii.gz
Masked_RSFC/RSFC_LFF_rall_MRKY112-1_proc.nii_masked.nii.gz
Masked_RSFC/RSFC_LFF_rall_MRKY112-2_proc.nii_masked.nii.gz
Masked_RSFC/RSFC_LFF_rall_MRKY113-1_proc.nii_masked.nii.gz
Masked_RSFC/RSFC_LFF_rall_MRKY113-2_proc.nii_masked.nii.gz
Masked_RSFC/RSFC_LFF_rall_MRKY115-1_proc.nii_masked.nii.gz
Masked_RSFC/RSFC_LFF_rall_MRKY115-2_proc.nii_masked.nii.gz
Masked_RSFC/RSFC_LFF_rall_MRKY116-1_proc.nii_masked.nii.gz
Masked_RSFC/RSFC_LFF_rall_MRKY116-2_proc.nii_masked.nii.gz
Masked_RSFC/RSFC_LFF_rall_MRKY117-1_proc.nii_masked.nii.gz
Masked_RSFC/RSFC_LFF_rall_MRKY117-2_proc.nii_masked.nii.gz
Masked_RSFC/RSFC_LFF_rall_MRKY118-1_proc.nii_masked.nii.gz
Masked_RSFC/RSFC_LFF_rall_MRKY118-2_proc.nii_masked.nii.gz
Masked_RSFC/RSFC_LFF_rall_MRKY119-1_proc.nii_masked.nii.gz
Masked_RSFC/RSFC_LFF_rall_MRKY119-2_proc.nii_masked.nii.gz
Masked_RSFC/RSFC_LFF_rall_MRKY120-1_proc.nii_masked.nii.gz
Masked_RSFC/RSFC_LFF_rall_MRKY120-2_proc.nii_masked.nii.gz
Masked_RSFC/RSFC_LFF_rall_MRKY122-1_proc.nii_masked.nii.gz
Masked_RSFC/RSFC_LFF_rall_MRKY122-2_proc.nii_masked.nii.gz
Masked_RSFC/RSFC_LFF_rall_MRKY123-1_proc.nii_masked.nii.gz
Masked_RSFC/RSFC_LFF_rall_MRKY123-2_proc.nii_masked.nii.gz
Masked_RSFC/RSFC_LFF_rall_MRKY124-1_proc.nii_masked.nii.gz
Masked_RSFC/RSFC_LFF_rall_MRKY124-2_proc.nii_masked.nii.gz
Masked_RSFC/RSFC_LFF_rall_MRKY125-1_proc.nii_masked.nii.gz
Masked_RSFC/RSFC_LFF_rall_MRKY125-2_proc.nii_masked.nii.gz
Masked_RSFC/RSFC_LFF_rall_MRKY126-1_proc.nii_masked.nii.gz
Masked_RSFC/RSFC_LFF_rall_MRKY126-2_proc.nii_masked.nii.gz
Masked_RSFC/RSFC_LFF_rall_MRKY127-1_proc.nii_masked.nii.gz
Masked_RSFC/RSFC_LFF_rall_MRKY127-2_proc.nii_masked.nii.gz
Masked_RSFC/RSFC_LFF_rall_MRKY128-1_proc.nii_masked.nii.gz
Masked_RSFC/RSFC_LFF_rall_MRKY128-2_proc.nii_masked.nii.gz
Masked_RSFC/RSFC_LFF_rall_MRKY129-1_proc.nii_masked.nii.gz
Masked_RSFC/RSFC_LFF_rall_MRKY129-2_proc.nii_masked.nii.gz
Masked_RSFC/RSFC_LFF_rall_MRKY130-1_proc.nii_masked.nii.gz
Masked_RSFC/RSFC_LFF_rall_MRKY130-2_proc.nii_masked.nii.gz
Masked_RSFC/RSFC_LFF_rall_MRKY131-1_proc.nii_masked.nii.gz
Masked_RSFC/RSFC_LFF_rall_MRKY131-2_proc.nii_masked.nii.gz
```

2.5. FSLmaths code

The following FSLmaths code was used to apply the binary IC masks to the corresponding dual regression outcome.

```
#!/bin/bash

# Set the directory where the files are located
DR_input_directory="/home/sone/researchdata_mri/UserFolders/Sone/NewData/Cut_Volumes/RSFC_All/DualRegression_BAT"
M_input_directory="/home/sone/researchdata_mri/UserFolders/Sone/NewData/Cut_Volumes/RSFC_All/Melodic_Results_CT"

# Loop through the 4-digit numbers
for number in {0000..0019}; do
    # Create arrays to store filenames with the current number
    dr_files=()
    melodic_files=()

    # Loop through the files in the directory
    for file in "$DR_input_directory"/dr_stage2_ic"${number}".nii.gz; do
        if [ -f "$file" ]; then
            dr_files+=("$file")
        fi
    done

    for file in "$M_input_directory"/melodic_IC_bin"${number}".nii.gz; do
        if [ -f "$file" ]; then
            melodic_files+=("$file")
        fi
    done

    # Check if there are at least one "dr" file and one "melodic" file with the same number
    if [ "${#dr_files[@]}" -ge 1 ] && [ "${#melodic_files[@]}" -ge 1 ]; then
        # Perform the multiplication using fslmaths
        result_file="${DR_input_directory}/DR_masked_${number}.nii.gz"
        fslmaths "${dr_files[0]}" -mul "${melodic_files[0]}" "$result_file"

        echo "Multiplied files with $number and saved result as $result_file"
    else
        echo "Not enough files found for $number"
    fi
done
```

3. FSL Randomise Codes

The following codes were used during the three randomise runs:

A. Between group differences

```
#!/bin/bash

#Melodic binary masks directory:
M_input_directory=
"/home/sone/researchdata_mri/UserFolders/Sone/NewData/Cut_Volumes/RSFC_All/Melodic_Results_CT"

# Loop through the numbers from 00 to 19
for i in {00..19}; do
    # Generate the input file name (e.g., DR_masked_0000.nii.gz)
    input_file="DR_masked_$(printf "%04d" $i).nii.gz"

    # Generate the output folder name (e.g., BT_All_00)
    output_folder="AT_F_Test_$(printf "%02d" $i)"

    melodic_file="${M_input_directory}/melodic_IC_bin$(printf "%04d" $i).nii.gz"

    # Run the randomise command
    randomise -i "${input_file}" -o "${output_folder}" -d F_Test.mat -t F_Test.con -f F_Test.fts
     -m "${melodic_file}" -n 5000 -T --quiet --uncorrp
done
```

B. Within group differences

```
#!/bin/bash

M_input_directory="/home/sone/researchdata_mri/UserFolders/Sone/NewData/Cut_Volumes/RSFC_All/Melodic_Results_CT"
DR_input_directory="/home/sone/researchdata_mri/UserFolders/Sone/NewData/Cut_Volumes/RSFC_All/DualRegression_BAT"
output_directory="/home/sone/researchdata_mri/UserFolders/Sone/NewData/Cut_Volumes/RSFC_All/DualRegression_BAT_Ttests"

# Loop through the numbers from 00 to 19
for i in {00..19}; do
    # Generate the input file name (e.g., DR_masked_0000.nii.gz)
    input_file="${DR_input_directory}/DR_masked_$(printf "%04d" $i).nii.gz"

    # Generate the output folder name (e.g., BT_All_00)
    output_folder="${output_directory}/BAT_T_Test_$(printf "%02d" $i)"

    melodic_file="${M_input_directory}/melodic_IC_bin$(printf "%04d" $i).nii.gz"

    # Run the randomise command
    randomise -i "${input_file}" -o "${output_folder}" -d GLM_46_T/GLM_46_T.mat -t GLM_46_T/GLM_46_T.con -m "${melodic_file}" -n 5000 -x --quiet --uncorrp
done
```

4. FSL Cluster

```
#!/bin/bash

# Loop through the numbers from 00 to 19
for i in {00..19}; do
    # Generate the input file name (e.g., BAT_All_00_vox_corrp_tstat1.nii.gz)
    input_file_1="BAT_T_Test_$(printf "%02d" $i)_vox_p_tstat1.nii.gz"
    input_file_2="BAT_T_Test_$(printf "%02d" $i)_vox_p_tstat2.nii.gz"
    input_file_3="BAT_T_Test_$(printf "%02d" $i)_vox_p_tstat3.nii.gz"
    input_file_4="BAT_T_Test_$(printf "%02d" $i)_vox_p_tstat4.nii.gz"
    input_file_5="BAT_T_Test_$(printf "%02d" $i)_vox_p_tstat5.nii.gz"
    input_file_6="BAT_T_Test_$(printf "%02d" $i)_vox_p_tstat6.nii.gz"

    # Generate the output file name (e.g., BAT_All_00)
    output_file_1="T_Test_1_$(printf "%02d" $i)_BAT_99.txt"
    output_file_2="T_Test_2_$(printf "%02d" $i)_BAT_99.txt"
    output_file_3="T_Test_3_$(printf "%02d" $i)_BAT_99.txt"
    output_file_4="T_Test_4_$(printf "%02d" $i)_BAT_99.txt"
    output_file_5="T_Test_5_$(printf "%02d" $i)_BAT_99.txt"
    output_file_6="T_Test_6_$(printf "%02d" $i)_BAT_99.txt"


    # Run the cluster command
    fsl-cluster -i "${input_file_1}" -t 0.99 -o tstat1_cluster_index_$(printf "%02d" $i)_99 --osize=tstat1_cluster_size_$(printf "%02d" $i)_99 > "${output_file_1}" --mm
    fsl-cluster -i "${input_file_2}" -t 0.99 -o tstat2_cluster_index_$(printf "%02d" $i)_99 --osize=tstat2_cluster_size_$(printf "%02d" $i)_99 > "${output_file_2}" --mm
    fsl-cluster -i "${input_file_3}" -t 0.99 -o tstat3_cluster_index_$(printf "%02d" $i)_99 --osize=tstat3_cluster_size_$(printf "%02d" $i)_99 > "${output_file_3}" --mm
    fsl-cluster -i "${input_file_4}" -t 0.99 -o tstat4_cluster_index_$(printf "%02d" $i)_99 --osize=tstat4_cluster_size_$(printf "%02d" $i)_99 > "${output_file_4}" --mm
    fsl-cluster -i "${input_file_5}" -t 0.99 -o tstat5_cluster_index_$(printf "%02d" $i)_99 --osize=tstat5_cluster_size_$(printf "%02d" $i)_99 > "${output_file_5}" --mm
    fsl-cluster -i "${input_file_6}" -t 0.99 -o tstat6_cluster_index_$(printf "%02d" $i)_99 --osize=tstat6_cluster_size_$(printf "%02d" $i)_99 > "${output_file_6}" --mm
done
```

Appendix C

Extracting Z-score values

The following MATLAB code was used to extract the mean Z-scores values for each cluster for each respective participant or scan:

```
close all
clear
clc


TT=[0 1 2 3 4 5 6 7 8 9 10 11 12 13 14 15 16 17 18 19 20 21 22 23 24 25 26 27 28 29 30 31
32 33 34 35 36 37 38 39 40 41 42 43 44 45];


for v1=1:46

name1='/home/sone/researchdata_mri/UserFolders/Sone/NewData/Cut_Volumes/RSFC_All/DualRegres
sion_BAT_Ttests/Clusters/tstat5_cluster_10_21/' ;% change the directory;
 name2='vol000';
 name3='vol00';


v = sprintf('%s%s%d.nii',name1,name2,TT(v1))


 uu=exist(v)


 if (uu~=2)


  v = sprintf('%s%s%d.nii',name1,name3,TT(v1))
   uu=exist(v)
 end


k=spm_vol(v);
im=spm_read_vols(k); % which givesyou your 3d volume to play with


G1=nonzeros(im(:));


yy=mean(G1);


Re(2,v1)=yy;
Re(1,v1)=TT(v1);


 clear name1 name2 name3 G1 k im;
end


Re=Re';
```